A STUDY ON HEAT TRANSFER ASPECTS ON UNDERGROUND HEATING OF AIRPORT APRONS AND RUNWAYS

A THESIS SUBMITTED TO
THE GRADUATE SCHOOL OF NATURAL AND APPLIED SCIENCES
OF
THE MIDDLE EAST TECHNICAL UNIVERSITY

BY

AHMET YÜCE ALPAN

IN PARTIAL FULFILMENT OF THE REQUIREMENTS FOR THE DEGREE OF

MASTER OF SCIENCE

IN

THE DEPARTMENT OF MECHANICAL ENGINEERING

DECEMBER 2001

Approval of the Graduate School of Natural And Applied Sciences

Prof. Dr.Tayfur ÖZTÜRK
Director

I certify that this thesis satisfies all the requirements as a thesis for the degree of Master of Science.

Prof. Dr. Eres SÖYLEMEZ
Head of Department

This is to certify that we have read this thesis and that in our opinion it is fully adequate in scope and quality, as a thesis for the degree of Master of Science

Assoc. Prof. Dr. Cemil YAMALI
Supervisor

Examining Committee Members

Prof. Dr. Kahraman ALBAYRAK

Prof. Dr. Ercan ATAER

Asst. Prof. Dr. Tahsin ÇETİNKAYA

Asst. Prof. Dr. İlker TARI

Assoc. Prof. Dr. Cemil YAMALI

ABSTRACT

A STUDY ON HEAT TRANSFER ASPECTS ON UNDERGROUND HEATING OF AIRPORTS APRONS AND RUNWAYS

ALPAN, Ahmet Yüce

M.S., Department Of Mechanical Engineering

Supervisor: Assoc. Prof. Dr. Cemil Yamalı

December 2001, 209 pages

In this study, underground heating of airport apron and runway surfaces by means of embedded hot fluid pipes, was investigated using a theoretical approach which is based on a mathematical modeling. The apron heating system was modeled from cross-sectional & top views for convective and radiative boundary condition at the apron surface. Three-dimensional transient temperature distribution and heat transfer rates are evaluated for various geometric and heat transfer parameters. Using these results, relations between some of the important system parameters are investigated.

Keywords: Underground heating, buried pipe, snow melting

ÖZ

HAVA ALANI PİSTLERİNİN YER ALTINDAN ISITILMASININ
ISI TRANSFERİ AÇISINDAN İNCELENMESİ ÜZERİNE BİR ÇALIŞMA

ALPAN, Ahmet Yüce

Yüksek Lisans, Makina Mühendisliği Bölümü

Tez Yöneticisi: Doç. Dr.Cemil Yamalı

Aralık 2001, 209 Sayfa

Bu çalışmada, havaalanı pistlerinin gömülü sıcak akışkan boruları ile ısıtılması, matematiksel modelleme ile teorik açıdan incelenmiştir. Pistin ısıtılması, taşınımsal ve ışınımsal sınır şartları göz önüne alınarak kesit görünümü ve üstten görünüm kullanılarak modellenmiştir. Üç boyutlu ve zamana bağlı sıcaklık dağılımı ve ısı transfer değerleri çeşitli geometrik ve ısı transfer değişkenleri için hesaplanmıştır.Bu çalışmalar sonucunda, bazı önemli sistem parametreleri arasındaki ilişkiler incelenmiştir.

Anahtar kelimeler: Yeraltından ısıtma, gömülü boru, kar erimesi

To the memories of Prof. Dr. Birol YÜCEL, my mother & Mr. Şerif ÇİM

ACKNOWLEDGEMENTS

I express sincere appreciation to Assoc. Prof. Dr Cemil Yamalı for his guidance and insight throughout the research. Thanks go to the other faculty members, Prof. Dr. Hafit Yüncü, Prof. Dr. Birol Yücel and Prof. Dr. Yalçın Göğüş for their previous suggestions and comments. I also acknowledge to General Manager of TÜMAŞ company, Mr. Çetin ATUK for his special help and other TÜMAŞ personnel. To my wife, Ferhan, I offer sincere thanks for her unshakable faith in me. To my father Nejat ALPAN (Ms. Mechanical Engineer, ITÜ – 1954) for his special support.

TABLE OF CONTENTS

LIST OF TABLES

LIST OF FIGURES

LIST OF SYMBOLS

A^*	First non-dimensional coefficient, Eqn. (3.24)	-
$A_{SOLID-2}$	Outer surface area of solid above the pipe (Lz_2 L)	m^2
$A_{SOLID-2}{}^*$	Non-dimensional outer surface area of solid above the pipe (lz_2 l)	-
B^*	Second non-dimensional coefficient , Eqn. (3.24)	-
Bi_∞	Biot number for atmosphere (h_∞ R/k)	-
Bi_m	Biot number for pipe (h_m R/k)	
C	Distance where the temperature reaches to the ground temperature T_b	m
c	Non-dimensional value of C (C/R)	-
C^*	Third non-dimensional coefficient , Eqn. (4.20)	-
c_p	Specific heat of solid	J/kg K
c_{pw}	Specific heat of fluid	J/kg K
D	Pipe diameter	m
dx	Value of increment in x^*	-
dy	Value of increment in y^*	-
dz	Value of increment in z^*	-
Fo	Incremental Fourier Number based on solid parameters ($\alpha\ \Delta t/R^2$)	-
Fo_w	Incremental Fourier Number based on fluid parameters ($\alpha_w\ \Delta t/R^2$)	-
h	Non-dimensional burial depth of pipe (H/R)	-
H	Burial depth of pipe	m

h_∞	Combined heat transfer coefficient	W/m^2K
h_m	Heat transfer coefficient for pipe	W/m^2K
I_L	Latent heat for melting of snow	J/kg
I_L^*	Non-dimensional latent heat for melting of snow, Eqn. (4.37)	-
k	Thermal conductivity of solid	W/mK
K_i	Nodal coefficient for neighboring node at $-z^*$ direction , Eqn. (3.12)	-
k_w	Thermal conductivity of fluid	W/mK
K_{xm1}	Nodal coefficient for neighboring node at $-x^*$ direction , Eqn. (3.12)	-
K_{xp1}	Nodal coefficient for neighboring node at $+x^*$ direction , Eqn. (3.12)	-
K_{ym1}	Nodal coefficient for neighboring node at $-y^*$ direction , Eqn. (3.12)	-
K_{yp1}	Nodal coefficient for neighboring node at $+y^*$ direction , Eqn. (3.12)	-
K_{zm1}	Nodal coefficient for neighboring node at $-z^*$ direction , Eqn. (3.12)	-
K_{zp1}	Nodal coefficient for neighboring node at $+z^*$ direction , Eqn. (3.12)	-
L	Pipe spacing	m
l	Non-dimensional pipe spacing (L/R)	-
Lz_1	Length of Solid-1 in z direction	m
lz_1	Length of Solid-1 in z^* direction	-
Lz_2	Length of Solid-2 in z direction	m
lz_2	Length of Solid-2 in z^* direction	-
m	Mass flow rate in the pipe	kg/s
m_S	Mass of snow	kg

Nu_R	Nusselt Number ($h_m R/k_w$)	-
nx	Total number of nodes in x^* direction	-
ny	Total number of nodes in y^* direction	-
nz_1	Number of nodes in z^* direction of Solid-1	-
nz_2	Number of nodes in z^* direction of Solid-2	-
nztotal	Total number of nodes in z^* direction	-
Pr	Prandtl Number	
Q_{DOWN}	Heat transfer rate to ground for any node at base plane	W
Q_{DOWN}^*	Non-dimensional value of Q_{DOWN}, Eqn. (4.11)	-
$Q_{DOWNSUM}^*$	Total non-dimensional heat transfer rate to ground , Eqn. (4.12)	-
Q_{LOAD}	Heating load	J
Q_{LOAD}^*	Non-dimensional heating load, Eqn (4.37)	-
Q_{LOSS}^*	Heat loss rate (Section 4.3)	-
Q_{SIDES}	Heat transfer rate to first side plane for any node at first side plane	W
Q_{SIDES}^*	Non-dimensional value of Q_{SIDES} , Eqn. (4.15)	-
$Q_{SIDESSUM}^*$	Total non-dimensional heat transfer rate to atmosphere , Eqn. (4.16)	-
Q_{TOTAL}^*	Total heat transfer rate , Eqn. (4.24)	-
Q_{UP}	Heat transfer rate to atmosphere for any node at outer surface	W
Q_{UP}^*	Non-dimensional value of Q_{UP} , Eqn. (4.7)	-
Q_{UPSUM}^*	Total non-dimensional heat transfer rate to atmosphere, Eqn. (4.8)	-
Q_{USED}^*	Used heat transfer rate (Section 4.3)	
$Q_{USEDCUM}$	Cumulative heat transfer , Eqn.(4.26)	J
$Q_{USEDCUM}^*$	Non-dimensional form of cumulative heat transfer, Eqn.(4.34).	

R	Pipe Radius	m
r	Radial direction defined from point of origin (x and y coordinates are zero)	m
r'	Radial direction defined from point with x coordinate is L & y coordinate is zero)	m
r'^*	Non-dimensional value of r' (r'/R)	-
r^*	Non-dimensional value of r (r/R)	-
Re_D	Reynolds Number ($4\ m/\pi D\mu$)	
S_m	Sum of nodal coefficients , Eqn. (3.14))	-
S_{xm1}	Shape factor for neighboring node at -x direction	m or m^2
S_{xm1}^*	Non-dimensional shape factor for neighboring node at $-x^*$ direction	-
S_{xp1}	Shape factor for neighboring node at +x direction	m or m^2
S_{xp1}^*	Non-dimensional shape factor for neighboring node at $+x^*$ direction	-
S_{ym1}	Shape factor for neighboring node at -y direction	m or m^2
S_{ym1}^*	Non-dimensional shape factor for neighboring node at $-y^*$ direction	-
S_{yp1}	Shape factor for neighboring node at +y direction	m or m^2
S_{yp1}^*	Non-dimensional shape factor for neighboring node at $+y^*$ direction	-
S_{zm1}	Shape factor for neighboring node at -z direction	m or m^2
S_{zm1}^*	Non-dimensional shape factors for neighboring node at $-z^*$ direction	-
S_{zp1}	Shape factor for neighboring node at +z direction	m or m^2

S_{zp1}^{*}	Non-dimensional shape factor for neighboring node at $+z^{*}$ direction	-
t	Time	s
T_{∞}	Atmospheric temperature	°C
t^{*}	Non-dimensional time ($\alpha t/R^2$)	-
T_b	Ground temperature	°C
T_C	Critical surface temperature, Section 5.3.1	°C
T_{CL}	Limit of critical surface temperature	°C
Timestep	Number of increment in t^{*}	-
T_m	Fluid temperature	°C
T_{mi}	Supply fluid temperature	°C
T_{mo}	Fluid temperature at the exit of the pipe	°C
T_S	Surface temperature considered for Objective-1	°C
t_S^{*}	Thickness of snow or ice on $A_{SOLID-2}^{*}$	-
t_{SR}^{*}	Reference snow or ice thickness on $A_{SOLID-2}^{*}$	-
t_{SM}	Melted snow thickness	m
t_{SM}^{*}	Dimensionless melted snow thickness (t_{SM}/R)	-
$T_{X+1,y,z}^{P+1}$	Temperature value of neighboring node at +x direction at t+Δt	°C
$T_{x,Y+1,z}^{P+1}$	Temperature value of neighboring node at +y direction at t+Δt	°C
$T_{x,y,Z+1}^{P+1}$	Temperature value of neighboring node at +z direction at t+Δt	°C
$T_{x,y,Z-1}^{P+1}$	Temperature value of neighboring node at -z direction at t+Δt	°C
$T_{x,y,z}^{P}$	Temperature for pointer node (or center node) of any prismatic nodal element at any time t	°C
$T_{x,y,z}^{P+1}$	Temperature for pointer node (or center node) of any prismatic nodal element at any time t+Δt	°C

$T_{x,Y-1.z}^{P+1}$	Temperature value of neighboring node at -y direction at t+Δt	°C
$T_{X-1.y.z}^{P+1}$	Temperature value of neighboring node at -x direction at t+Δt	°C
V^*	Nodal volume, Eqn. (3.11)	-
x	Coordinate index value along x^* coordinate direction (Section 3.4.3)	-
x^*	Non-dimensional coordinate value	-
y	Coordinate index value along y^* coordinate direction (Section 3.4.3)	-
y^*	Non-dimensional coordinate value	-
z	Coordinate index value along z^* coordinate direction (Section 3.4.3)	-
z^*	Non-dimensional coordinate value	-

Greek Letters

σ	Stefan-Boltzman Constant	W/m^2K^4
ϵ	Emissivity, Eqn. (3.1)	-
θ	Non-dimensional temperature $((T-T_\infty)/(T_b-T_\infty))$	-
α	Thermal diffusivity of solid	m^2/s
η	Efficiency , Eqn. (4.26)	-
μ	Dynamic viscosity of fluid	Pa s
ρ	Density of solid	kg/m^3
ρ_S	Density of snow	kg/m^3
θ_∞	Dimensionless atmospheric temperature	-
θ_b	Non-dimensional base temperature	-
θ_C	Critical surface temperature, Section 5.3.1	-

θ_{CL}	Limit of critical surface temperature	-
θ_i	Supply fluid temperature	-
θ_{mo}	Non-dimensional exit fluid temperature	-
θ_S	Non-dimensional surface temperature	-
ρ_S	Density of snow	kg/m^3
Δt	Time increment	s
α_w	Thermal diffusivity of fluid	m^2/s
ρ_w	Density of fluid	kg/m^3
$\theta_{x,y,Z+1}^{P+1}$	Non-dimensional temperature value of neighboring node at $+z^*$ direction at t^*+Fo	-
$\theta_{x,y,z}^{P}$	Non-dimensional temperature for pointer node (or center node) of any prismatic nodal element at any time t^*	-
$\theta_{x,y,z}^{P+1}$	Non-dimensional temperature for pointer node (or center node) of any prismatic nodal element at any time t^*+Fo	-
$\theta_{x,Y+1,z}^{P+1}$	Non-dimensional temperature value of neighboring node at $+y^*$ direction at t^*+Fo	-
$\theta_{X+1,y,z}^{P+1}$	Non-dimensional temperature value of neighboring node at $+x^*$ direction at t^*+Fo	-
$\theta_{x,y,Z-1}^{P+1}$	Non-dimensional temperature value of neighboring node at $-z^*$ direction at t^*+Fo	-
$\theta_{x,Y-1,z}^{P+1}$	Non-dimensional temperature value of neighboring node at $-y^*$ direction at t^*+Fo	-
$\theta_{X-1,y,z}^{P+1}$	Non-dimensional temperature value of neighboring node at $-x^*$ direction at t^*+Fo	-

CHAPTER 1

INTRODUCTION

In cold climatic conditions, some problems arise as a result of the weather conditions in winter. Due to the snowfall and ice formation on the highways, airport aprons, public building entrances, footpaths and such similar places, life becomes harder.

Bad winter conditions mostly affect the traffic on the highways. Many accidents occurs because of the slipping of vehicles on the road. Such accidents result in dead or injury of the people. Beside these, transportation is interrupted for a long period

Similar to airport aprons, in urbanized regions footpaths and public building entrances are affected by heavy winter conditions. For example, walking of the people becomes difficult and uncomfortable. Psychological health is also disturbed besides the time delays. Moreover, residential driveways are needed to be kept free of snow and ice.

There are convenient methods to overcome the problem explained up to this point. These are based on manual, mechanical or chemical preventing of ice and removing of snow. For instance, in order to protect the apron surface of an airport, urea or other type of chemical solutions are usually used. Similarly, heavy duty machines or manpower are employed to remove the snow and scrape the ice layers. Such methods can not be used while the snow is actually falling. Also, it is known that the application of chemicals causes some small cracks on the surface. The mechanical and manual methods are not enough to remove the ice layer unless it is softened. The concrete or asphalt surfaces can be damaged if the ice layer is forced to be removed.

In this manner, underground heating of the necessary and important surfaces is an alternative to the convenient methods. Underground heating is performed by the embedded electrical coils or embedded hot water pipes. Such systems are much effective than the others, if they are properly designed and installed.

Underground heating systems can widely be applied in Turkey. First of all in the mountain passes, like Zigana, Kuzgunkiran or the ramps such as near Ulukışla, this system provides beneficial results from transportation point of view. Also for the airports located in East or Central Anatolia, underground heating system can be helpful to keep regular flight schedule. In Southeast Anatolia, it is very difficult to communicate with the rural areas. Mostly, the helicopters are used to overcome the problem. However, it is usually impossible to find a favorable place for landing. Small heliports can be constructed together with underground heating system for landing of the helicopters.

CHAPTER 2

LITERATURE SURVEY

2.1 AIRPORT APRON and PAVEMENT SURFACE CROSS-SECTION

Airfield structural pavement of the runways , taxiways and special areas (holding areas) are designed to provide yearlong continues flight operation. Modern airfield pavement is a sandwich structure. Various materials are used for its construction. Three main structural layers of different purposes are shown in the Fig. 2.1.

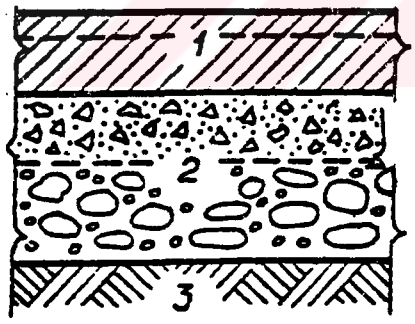

Figure 2.1 Airfield pavement structural layers:

1) Pavement

2) Structural Foundation

3) Ground Foundation

1. The Pavement: Proper upper layer made of the strongest materials as it takes the airplane load and is subjected to the environmental factors. The pavement sometimes may include two or more uniform layers which differ by compound components, reinforcement, physico-mechanical characteristics. For example the pavement may include three hard asphalt-concrete layers: the upper thin layer is made of the strongest fine grained asphalt concrete, middle and lower layers are made respectively thicker and coarse grained asphalt concrete with lower strength. As another example the pavement consists of two layers. Upper layer made of reinforce concrete while the lower layer made of plain concrete. The material used for pavement gives the name of the airfield pavement. In the first case airfield pavement is called asphalt-concrete, in the second case reinforced two ply with concrete upper layer.

2. The Structural Foundation: It is the lower layer (or layers) that together with the pavement provides airplane vertical load transmission to the bedding. The structural foundation is made of grained mineral materials such as chips, gravel, sand etc. with or without astringent treatment (bitumen, cement, lime or others).The structural foundation may include layers that provide drainage waterproofing, antisilting, thermal insulation and other special and structural layers.

3) Ground Foundation: It is the upper cover of virgin soil or filled up ground planned and stabilized in a proper way before structural foundation being constructed. Overall airplane load , the pavement layers load and structural foundation load are transmitted to the ground foundation. The ground foundation thickness is equal to the depth of compressive stress distribution caused by the ground load (active ground zone thickness). Depending on different airplane loads, it may vary from 2 to 6 m. Within the limit of active zone, the ground foundation may be of uniform

composition or may include some ground layers with different types and qualities. Ground foundation is sometimes called natural pavement foundation.

2.2 CONVENTIONAL SNOW REMOVAL & ICE CONTROL FOR AIRPORT APRONS AND RUNWAYS

Removal of the various contaminants may be accomplished by one or more methods, by using one or more machines of the same type or by the combination of a train or family of machines, some of which will perform a dual role. Generally, removal of the most critical contaminants of snow, slush and ice may be accomplished by mechanical, chemical or thermal action and may be conducted as a high-speed operation on "live" runways, or at more conventional speeds in less priority areas where heavy, deep accumulations of snow have built up.

The following sections will consider the various mechanical, chemical and thermal methods, equipment and materials used, for the removal of snow, slush and ice.

2.2.1 MECHANICAL METHODS

The operation should commence as soon as the snow begins to accumulate on the surface. The machinery employed for the first operation in this procedure depends upon the equipment available, the type of snow, whether wet or dry, and the direction and strength of the wind. Normally, the ATS unit staff will designate the runway to be cleared based upon the meteorological forecast for conditions after the passage of the storm.

The metal underbody of snow ploughs or blowers should have a minimum clearance of 4 cm from the pavement surface. The use of vehicles with tire chains, high speed snow drags and underbody metal scrapers should be forbidden. Runway sweepers

should be utilized first and during as much of the snow removal activity as possible. Snow ploughs and blowers should supplement the sweeper operation only when the sweeper can not efficiently remove the accumulation.

Aprons used for aircraft parking, loading or servicing must usually be ploughed one way because of abutting and haul the snow to a dump area from these restricted locations. The snow is wind-rower and loaded into trucks by snowblowers or loader vehicles. At many airports snow removal from areas such as access roads, servicing areas, etc. may be cleared by contract resources.

2.2.2 JET AIR BLAST AND FLAME HEATING

In some military airports turbine engine exhaust blast and flame throwing torches has proven to be a novel method of snow disposal. However, this method of melting accumulated snow is extremely slow, involves very high fuel consumption and heat losses, and may lead to pavement damage through careless application of the heat.

2.2.3 CHEMICAL METHODS AND MATERIALS USED

Extreme caution must be exercised in the use of chemicals for removing snow or ice from the movement area or an area adjacent to it, as many chemicals are highly corrosive to metals or have other harmful effects upon materials used in the manufacture of aircraft. Wherever a chemical intended for use in snow or ice removal may come in contact with aircraft, a through analysis of the chemical should be conducted to ensure that it will not have a deleterious effect on aircraft components. The use of calcium or sodium chlorides on the movement area is not approved.

Further, chemicals should be used with caution in order not to create slippery conditions at sub-freezing temperatures. The melting process may result in any icy

surface covered by water. In this case the danger of aquaplaning will exist in addition to the braking action in itself being poor. It is to be noted that water on ice constitutes one of the most slippery surfaces that exist. If the icy surface to be cleared is dry, creation of a slippery surface can be avoided by using chemicals in the form of pellets. The pellets, when spread on a icy surface, will penetrate the ice and after some time loosen the ice from the paved surface. The ice may then be removed mechanically and slippery conditions due to water will be avoided.

This material has gained wide acceptance because of its effectiveness both as an anti-icer and as a de-icer. It has effectively reduced the usage of sand at airports generally while totally displacing it at airports in moderate climates. Its use to date has not indicated any deleterious side-effect on aircraft components, airport structures or to the surrounding ecology.

It is used as a de-icer to melt ice formations or as an anti-icer to prevent or retard the formation of ice covering. Although urea possesses de-icing qualities, it is considered to be essentially an anti-icer. It is most effective when the pavement is wet and a freezing temperature is forecast, or when rain is forecast and the pavement temperature is below freezing. The action of urea in lowering the freezing point of water allows time for the removal of water by sweeping to prevent the formation of ice on the pavement. When used as a de-icer, as much snow and surface ice as possible should first be removed by conventional means. To facilities the removal of ice by the use of urea, the ambient temperature should be higher than -3 ° C. If extreme low temperature conditions occur after the application of urea, the surface may become slushy; immediate removal by sweeping is necessary. Because of appreciable material cost, equipment calibration and application should be precisely controlled. When used as an anti-icer, a spreading rate of 20 gr/m^2 should be sufficient.

Sodium chloride may be used to melt ice from roads and sidewalks, spreading it sparingly by hand or vehicle spreader. It is effective to about -12 ° C but is highly corrosive to metals and detrimental to portland cement concrete and vegetation. It should not be used on or in the vicinity of the movement area.

Calcium chloride may be used to melt snow or ice. It is very similar to salt except that it is effective to about -18 ° C and is more corrosive than sodium chloride. Both salts may be mixed with an abrasive material to increase the anti-skid effectiveness on snow or ice. The same restrictions against use on or in the vicinity of the movement area apply to calcium chloride. Steel bristled sweepers may be applied to the surfaces to assist in the dispersal of melt water after the snow or ice has liquefied.

2.3. FACTORS OF SNOWFALL AS BASIS FOR DESIGN

2.3.1. LOW AIR TEMPERATURES WITH SNOW

One important condition which must be allowed for is the possibility of a very rapid drop in temperature which may take place soon after a heavy snow storm. Furthermore, such a drop in temperature may be accompanied by a very strong wind. These conditions, when occurring simultaneously, place a tremendous load on the system, and if the surface has not been completely cleared of snow and moisture before such a change in the weather, ice will form and create a dangerous condition.

The question is often raised as to whether a heavy fall of snow will coincide with a very low air temperature, and if this can be predicted. The U. S. Weather Bureau states that the forecaster requires data from a large surrounding area, including the upper air, for several hours before making a reasonably accurate forecast of snow, and that the temperature of the surface will determine whether snow and sleet remain unmelted on the surface.

Therefore, since the advent of a snow storm appears to be rather unpredictable, it is advisable, with important installations, to maintain a moderate heat in the pipes during periods when snow is possible. This preliminary heat may be turned on manually when the local Weather Bureau forecasts calls for precipitation with a possibility of snow, or when the temperature is falling rapidly and freezing rain may occur. If, for any reason, this precaution is considered undesirable, then provision can be made to start the system automatically as snow actually begins to fall.

It is pointed out that snow will fall at any temperature below 0 °C but as the air temperature falls, the amount of water vapor the air can hold decreases also and, consequently, the rate at which snow can be precipitated is comparatively small for very low temperatures. Thus, it is not usually necessary to allow for very low temperature losses with a heavy rate of precipitation.

A surplus of boiler capacity will help matters under all conditions, but when the air temperature drops very low, and the wind velocity is high, the loss of heat from the exposed surface directly above the pipes is so rapid, because of low air temperature and high air velocity, that unless the pipes are placed fairly close together the heat transmitted by the embedded pipes is dissipated within a few centimeters of the pipes, even though the circulating liquid can be maintained at a relatively high temperature. In other words, the heat loss from the surface of the road or driveway directly above the pipes, is so rapid compared with the conduction of the heat transversely, that there are strips of bare surface above the pipes and a formation of ice and snow between the pipes. Such a condition is shown in Fig. 2.2, taken when the air temperature dropped very rapidly to near -18°C after several inches of snow had fallen. The embedded pipes had melted some of the snow, but before the melting could be completed, the near -18°C temperature, and a strong wind changed the melted snow into ice. This

could prove positively dangerous if it occurred on the runway of an airport, or the surface of a footpath.

2.3.2 DENSITY OF SNOW

One other point to remember is that the weight of snow per centimeter of depth varies considerably according to the air temperature. This means that with the temperature near 0 °C (freezing point), it requires more heat for melting centimeter of snowfall than with temperatures near -20°C. On the other hand, the heat loss to the air from any surface already exposed will be considerably greater at the lower temperatures, especially if a high wind is blowing.

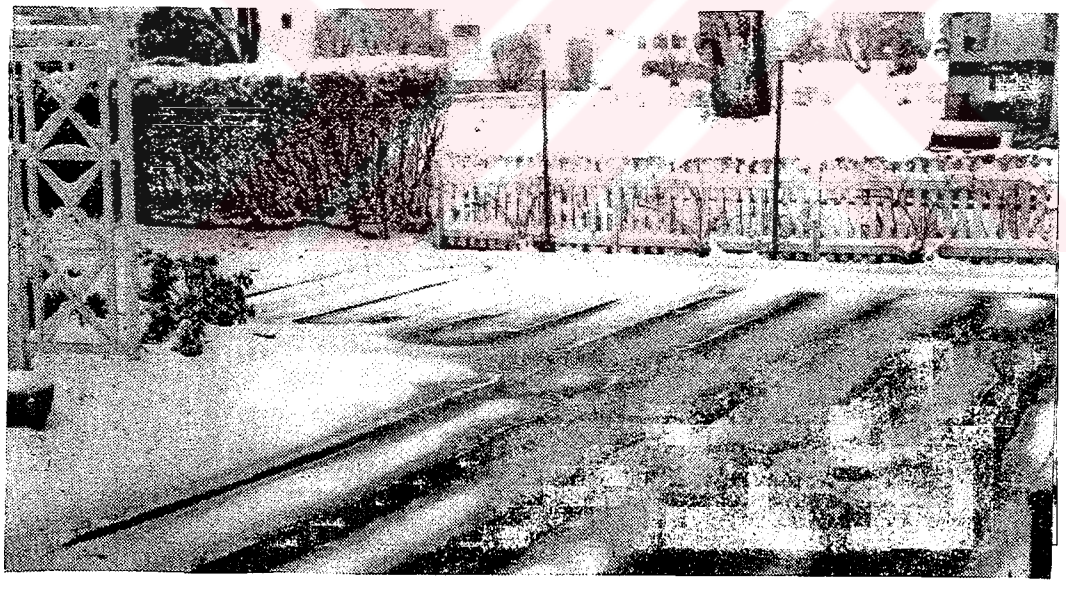

Figure 2.2. Partially melted snow frozen after melting due to sudden drop in outside temperature

Attempts to classify snow densities according to surface air temperatures, was not successful in establishing any definite relation between surface air temperatures and the density of falling snow.

When calculating the maximum load which a snow melting system may have to deal with, it is not always safe to assume an average snowfall if it is desired to keep the area free of snow at all times. According to some recorded observations, a heavy snowfall often starts slowly and builds up in intensity after a few hours duration. The peak intensity of snowfall, which often take place several hours after the start of a heavy fall, can, in some cases, defeat the whole object of a snow melting system if not taken into consideration in providing sufficient capacity to deal with the worse conditions. Many systems calculated on the basis of average rate of precipitation fail to give satisfaction on exceptional occasions, mainly because the pipes are spaced too far apart and the boiler or heater power is inadequate for the extra load.

When the rate of snowfall becomes too intense for the power of the system, snow begins to accumulate over the surface and tunnels are formed, which, if the pipes are spaced wide apart, do not usually disappear until some considerable time after the snowfall ceases, unless the tunnels are broken down manually. This may, of course, defeat the object of a snow melting system, which for many applications should be capable of dealing with all weather conditions.

These questions become more serious when dealing with such installations as airport runways, parking areas, and any spaces used for commercial purposes, where the accumulation of snow and ice will mean a loss in revenue, and to the contractor, a loss in prestige.

2.3.3 EFFECT OF SURFACE COLOR ON MELTING

In any case, for asphalt driveways, it is always advisable to space the pipes not more than 30 centimeters apart if it is desired to keep the surface free of all snow and ice, regardless of the maximum snowfall anticipated. With black asphalt surfaces, considerable advantage can be obtained from the sun, providing the surface is located in a sunny position and with this object in mind, a considerable saving can be effected, both in the installation and operating costs.

Snow reflects over 90 % of the sun's energy, whereas black asphalt absorbs practically 100 % of the energy received. This is the reason why snow covering the whole area of any unheated surface takes much longer to melt than when part of the snow has been cleared away by shoveling, by a snow plow, or a snow melting system. This is true for practically all kinds of surfaces, whether it is a concrete pavement, a macadamized road, or a dirt road. It is, however, very much more pronounced when the surface is rough and black as with asphalt.

The energy reaching the earth in the sun's rays is absorbed by surfaces in relation to their emissivity, and since the emissivity of black surfaces is usually high, the heat absorbed by these bare surfaces is quickly conducted to the adjoining surfaces and melts the snow resting on adjoining surfaces. This effect of the sun's energy is clearly demonstrated on snow piled up by a snow plow. On roadways where no gravel or cinders have been placed on the surface prior to the snow storm, the snow piled up is usually quite clean and white, and because of this, it remains for days even in bright sunshine.

2.4 PROPER WORKING FLUID

Steam, was first used in the pipes as the heating medium with the inlet at point X (Fig.2.3) and steam traps installed at the lowest point Y to keep the pipes free of condensate. When operating with steam, the two pipes were working in parallel instead of a continuous coil as in Fig.2.3. The method of using steam as a heating medium proved satisfactory until, to effect some emergency repairs to the steam boiler, the steam had to be shut off during a very cold spell.

During the shut down, the temperature of the embedded pipes fell below 0° C with the result that when steam was turned on again, ice collected in the pipes as the condense became frozen, thereby causing a complete block and two split pipes.

Because of bad experiences with steam it is recommended a good antifreeze liquid as the most reliable heating medium to use. Furthermore, since with steam it is imperative to keep the heat in the system throughout the winter months, steam heat often means a considerable waste of fuel. It is, of course, a decided advantage to keep a mild heat on the system during periods of possible precipitation, regardless of the heating medium used, but the temperature can be modulated more easily and more economically controlled with an antifreeze solution than with steam, since the former can be circulated at any moderate temperature. With steam, however, it is necessary to operate at practically full power throughout the season if expensive troubles are to be avoided.

2.5. A SAMPLE SET UP FOR SNOW MELTING

The layout was illustrated in Fig.2.3 wrought iron pipes installed in the upper part of a layer of broken stones, and with concrete slabs 10 cm thick forming the finished path. The slabs were made removable so that inspection of the pipes could be made at any time without destroying the concrete, and the object of placing the pipes in the broken stone rather than in the concrete was to provide more freedom for expansion.

The footpath being over 46 m long, it was necessary that the expansion of the pipes be given serious consideration. To deal with the expansion of the concrete slabs, an expansion joint of asphalted material was formed around each slab, and since the average size of the slabs was only 2 m x 1,5 m these joints provided adequate relief for any reasonable change in slab temperature during the tests.

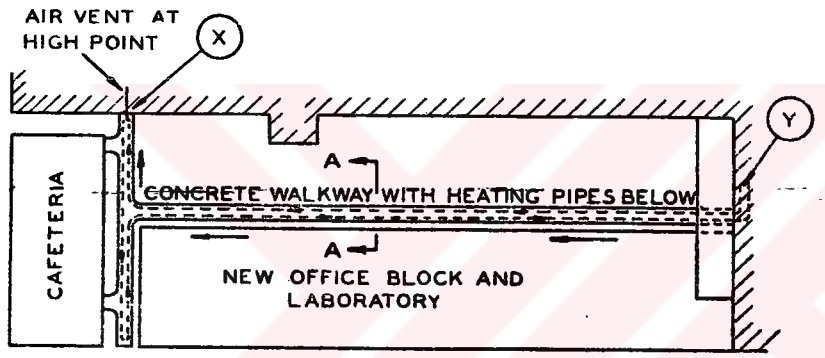

Figure 2.3. Footpath with heating coils below

In Fig. 2.3, the broken lines indicated the position of the pipes under the concrete footpath, and in Fig.2.4 a cross-section of the footpath shows how the pipes are placed in the broken stone in relation to the concrete slabs.

Fig.2.5 illustrates the hook-up of heater, controls and circulating pump, with a large expansion tank E provided to take up the expansion of the antifreeze solution. Since the co-efficient of cubical expansion for antifreeze is somewhat greater than for water,

and because the cost of antifreeze is usually high, it is advisable to have ample storage capacity to prevent loss of the liquid due to over expansion.

A flow meter at M recorded the amount of circulating liquid, and the temperature differential was registered by the thermometers at A and B. A measure of the

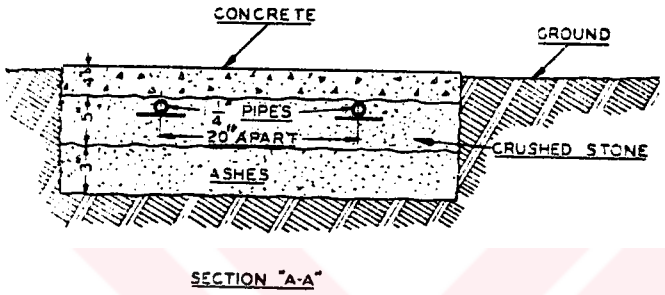

Figure. 2.4 Section A-A of Figure 2.3

condensate leaving the heater H was used as a check against the heat output as calculated by the meter reading at M, and the temperature differential between A and B. With the arrangements as shown, the manually operated modulating steam valve R, with a locked restricted control valve S inserted in the bypass connection, enables a moderate temperature to be maintained at times when snow is predicted, or when ice formation is possible due to freezing rain, which usually takes place at temperatures -1 to 0°C.

The thermostat T with steam control valve Y, automatically controls the temperature of the liquid when under normal working conditions the system is put into full operation immediately snow actually begins to fall. It is customary to set the valve S

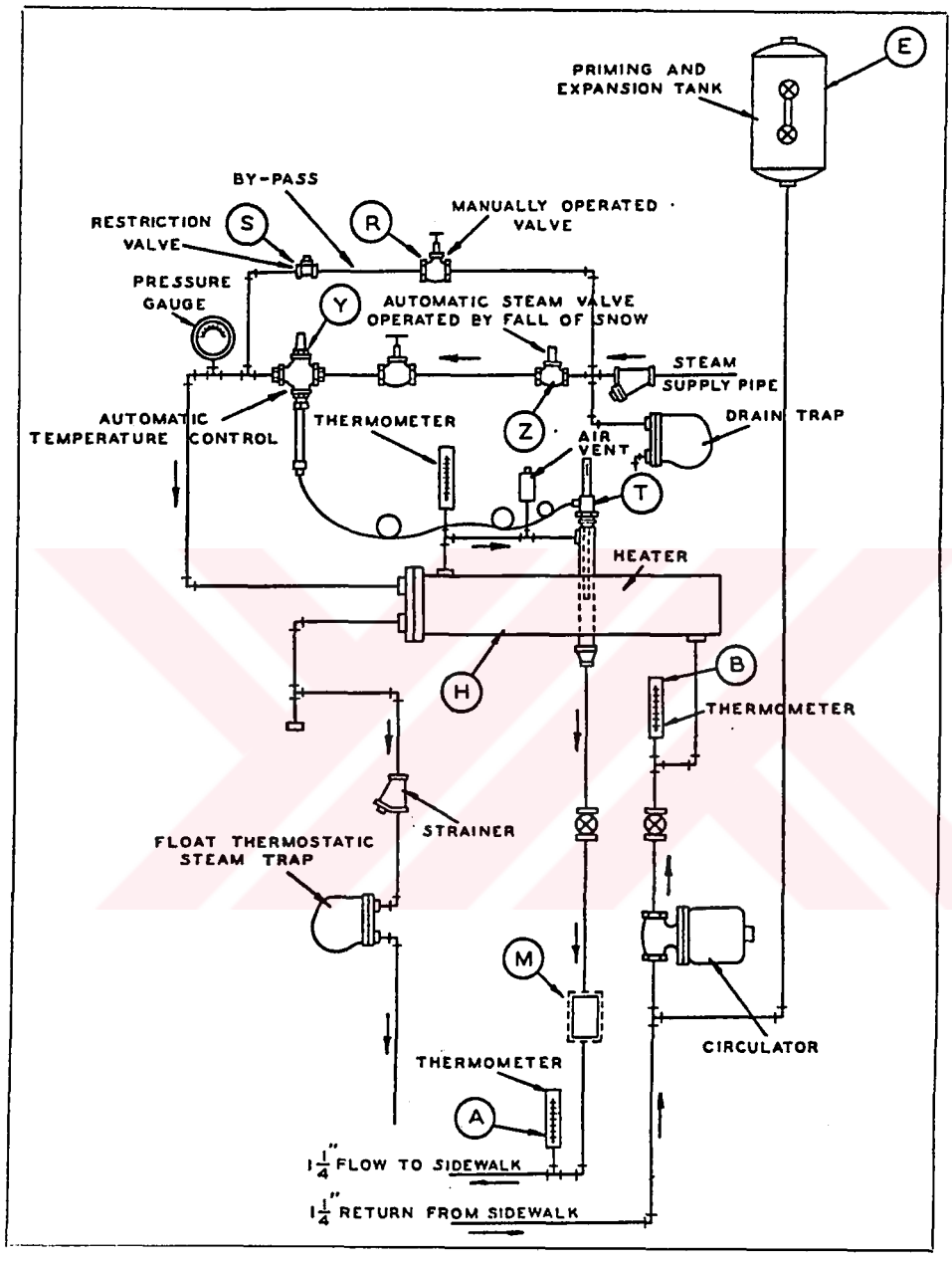

Figure 2.5. Heating equipment with controls and meters

so that the circulating water is maintained at a temperature of approximately 32° C, A temperature usually sufficient to prevent the formation of ice caused only by freezing rain.

A temperature of 32°C is not sufficient , however, to prevent ice formation which often takes place after a snow storm due to very low air temperatures and a high wind, and is recommended only to keep the ground just above freezing temperature prior to a storm. For actual snow melting , the regulator valve Y, in this case, controls the temperature of the circulating liquid at 72 to 82 °C.

Fig. 2.6 illustrates a foreshortened plan of the footpath with letters and numbers indicating the surface spots where some of the temperatures were recorded. The letters indicate spots on the surface where temperature were recorded directly above the embedded pipes, and the numbers indicate surface spots between the pipes. In addition to these surface temperatures, a series of temperatures were taken of the exposed earth surface some distance from the footpath for comparison with the surface temperature of the heated surface.A tabulation of the surface temperatures under various conditions appears in Table 2.1, and it will be observed that the temperature of the exposed earth followed very closely the temperature of the air. Where not indicated otherwise, the temperatures were taken when the surface was dry. Fig.2.6 is the key to the point locations.

It was observed on all tests covering a very wide range of air temperatures, that during actual snowfall, the surface temperature dropped to an average of +1 to +2 ° C, but rapidly increased to +3 or +4 ° C within a few minutes after snow ceased, even though the surface was still wet. Gradually the surface became dry and warmer as the heat from the pipes evaporated the moisture. This process invariably produces considerable vapor which can often be seen rising from the surface as the moisture is evaporated. It will be noted from the third and fourth horizontal rows, respectively, of

Table 2.1, that there was a considerable difference between wet and dry surface temperatures.

Table 2.1 Surface temperatures for sample setup

OUTSIDE AIR TEMP. °C	PT. A °C	PT. B °C	PT. C °C	PT. D °C	PT. E °C	PT. F °C	PT. J °C	PT. K °C	AVER. °C
1	16	14	13	12	9	11	13	13	12
-2	13	12	11	10	5	8	12	11	10
0 dry surface	15	13	12	11	9	10	12	12	11
0 wet surface	2	2	1	1	1	1	2	2	1
-18	0	-1	-2	-2	-3	-2	2	3	-1

OUTSIDE AIR TEMP. °C	PT. 1 °C	PT. 2 °C	PT 3 °C	PT. 4 °C	PT. 5 °C	AVERAGE °C
1	14	13	11	9	10	11
-2	11	8	7	6	5	8
0 dry surface	13	12	9	9	9	11
0 wet surface	1	1	1	1	1	1
-18	-2	-3	-3	-4	-4	-3

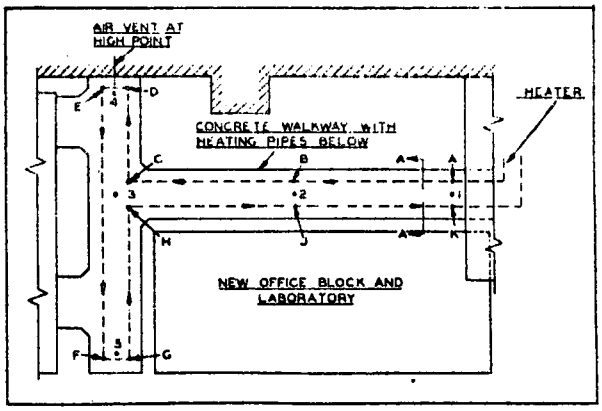

Figure 2.6. Key to locations of points where surface temperatures were taken

The lower surface temperatures recorded when snow was actually falling is due, of course, to the rapid dissipation of heat used to melt the snow. In other words, these lower and consistent surface temperatures are because of the latent heat of fusion of snow which is equal to 349 kJ/kg. These consistent surface temperatures when snow is being melted provided a reliable basis for calculation. The relatively lower surface temperature when wet as compared with the surface temperature when dry is due to the evaporation from a wet surface. The latent heat of the moisture quickly absorbs the heat being transmitted through the concrete and reduces the surface temperature accordingly.

2.6 THE HEAT DISTRIBUTION OF SYSTEM

During fair weather tests with little movement of air temperature of -18°C, approximately 55.1 % of the heat transmitted by the heating pipes to the footpath was found to be given off by the surface of the concrete and 44.9 % absorbed by the earth. Under similar conditions, but with an outside air temperature of 0° C , the heat given off from the surface of the heated concrete was reduced to about 46.3 % with 53.7 % transmitted to the earth. The amount of heat given off from the pipes did, however, vary according to the atmospheric conditions prevailing at the time and, therefore, these ratios changed considerably when snow was actually falling on the surface. The

conditions which exist when snow is falling are due to the fact that the concrete cools more rapidly as snow is being melted and the heat is dissipated more easily from the surface of the concrete.

Under such conditions, it was found that when melting snow approximately 70 % of the heat transmitted by the embedded pipes was usefully employed in melting the snow, and about 8 to 10 % was given off to the atmosphere. The remaining 20 to 22 % was lost downwards to the earth.

The nature and condition of the soil below the pipes naturally affects the loss downwards, as also will the thickness and nature of the material above the pipes. In point of fact, the ratio of the heat traveling in each direction will, in every case, be affected by the conductance of the material above and around the pipes and by the condition of the soil below the pipes. If the surrounding medium is wet due to previous rain, or because of melted snow, its conductivity will be increased considerably, thus making the path easier for heat to travel sideways and downwards. In the same manner, any change in the conductivity due to moisture in the material above the pipes will affect not only the heat traveling in an upward direction, but also change the ratio of the heat traveling in other directions. Furthermore, it was found on some tests that the rate at which snow was falling, together with ambient air temperature and movement, considerably affected the two major factors in the heat equation. The conditions with the lower temperature water will invariably allow the surface to be maintained above freezing point if the air temperature is not too low, and usually is sufficient to take care of any slight snow which may fall before the system attains the full operating temperature, providing the heat is put on full power immediately snow commences to fall.

2.7 CALCULATING THE HEAT REQUIRED

To make calculations on the heat required for a reliable snow melting system, it is necessary first to decide what maximum rate of snowfall it is intended to meet. We should allow sufficient power for 8 cm per hour, with perhaps additional reserve in boiler power to meet extreme conditions of temperature and snow drifts, which occasionally occur.

The rate of heat emission from the pipes seems to depend more on the conductivity of the medium surrounding the pipes and the temperature gradient in all directions than on the relation between the temperature of the liquid and the air temperature. This also appears to be true in all radiant heat installations, and seems to be the reason why calculations based on the relation between air temperature and water temperature are so often unreliable and unsatisfactory.

Evaporation can provide a very serious setback for the system if not taken into consideration, especially near the end of a storm. If 2mm of water only is left on the surface, and this has to be evaporated to prevent its freezing, it requires 11.36 kJ per sq. m to dry the surface. The danger is that if the surface is not dry and the air temperature suddenly drops to considerably below 0 °C, ice may be formed which often proves more dangerous than a layer of snow.

With asphalt driveways, the recommended maximum mean temperature of the liquid shall not exceed 70 ° C and, in some cases, it may be necessary to operate at an even lower mean temperature. In either case, it leaves the upper surface of the driveway in a very disintegrated state, thereby ruining its appearance and reducing its life.

The boiler capacity needed is based on the

1) Area of the snow melting surface times the total heat load per unit area.

2) Heat loss to downwards and to sides.

3) Boiler pick up allowance to prevent too much lag after snow falls till the system begins to melt the snow.

A margin of 50% of the sum of (1) and (2) might be allowed for (3)in the absence of specific information. More accurately to calculate the pick-up load (3) it is necessary to determine:

a) The heat necessary to heat up the piping

b) The heat necessary to heat up the solution of water and antifreeze.

c) The heat necessary to heat up the surface material (asphalt, concrete etc.)

d) The heat necessary to heat up the gravel below and the adjacent soil.

2.8 PIPE FRICTION AND PUMP SELECTION

The frictional resistance of the piping in large snow melting installations may be of major importance and, therefore, should receive careful consideration. In connection with calculations of pipe friction, it is necessary to consider the viscosity and density of the antifreeze and also its specific heat. The specific heat of antifreeze is usually less than that of water, and ,therefore, a greater volume has to be circulated to obtain the equivalent amount of heat, unless a greater temperature differential is allowed.

It is necessary to calculate the friction for designing the pump. First, determine the critical circuit which creates the greatest frictional resistance. However, it is always a good practice to check on the resistance set up in each circuit because the more correctly the system is balanced, the more efficient will be the melting of the snow.

If the coils are arranged in parallel it is only necessary to calculate the resistance of the connecting mains and the largest coil, or the coil which will set up the greatest

resistance, to obtain the total resistance of the system. If the design is such that the largest coil is closer to the pump, then it may be necessary to calculate the resistance of each coil, or each set of coils, before calculating the resistance in each section of the main.

According to the required liquid flow and the frictional resistance created the pump is selected from the manufacturers data. While selecting the pump extra resistance of the antifreeze solution at the low temperature must be taken into consideration.

2.9 EXPANSION OF ANTIFREEZE SOLUTION AND PIPING

Since it is very important to prevent any loss of the antifreeze, or even the introduction of any fresh water into a snow melting system once the system is started, care must be taken to provide sufficient storage capacity to take care of the maximum amount of the expansion which will occur at the highest temperature the liquid will reach.

In order to calculate the amount of expansion for the antifreeze liquid, first of all the amount of liquid in the coil piping,, the main piping and the boiler or heater must be known.

The lowest temperature assumed will depend on the location, but for average conditions it may be safe to allow for an average temperature of the antifreeze of -17°C. On the other hand, in locations where the outside temperature goes very low, it will be safer to use a low temperature approaching that of the minimum temperature reached. For the greatest expansion, take into consideration the possibility of a higher temperature than actually needed for melting the snow, and to be safe , allow for an additional 10-15 °C.

Generally speaking, it is considered a good practice to allow for a tank with a reserve capacity at least three times the space required for antifreeze expansion. The tank should have ample capacity to allow several inches depth of the antifreeze solution in the tank when the contents of the system is at its lowest possible temperature .

If the pipes are very long and too much expansion has to be absorbed in the concrete or other rigid material. It is likely to produce hardening stresses in the metal and thereby cause it to become brittle. This may result in the tubes developing fractures, or undue expansion may set up strains where branch connections are embedded in the concrete, and if these forces are very severe they may cause some connections to shear off where the junctions are welded. These tubes may not develop immediately, and since the strains are set up only when the heat is either turned on or off, it is something a hydraulic test will not reveal. If such weaknesses exist, they may be revealed only after a few years.

It is suggested by some pipe manufactures that the concrete be poured while the system is in operation, with the water in the pipes circulating at the highest working temperature. While this method insures that the pipes are made to expand the limit for ordinary working conditions while the concrete or plaster is in a plastic state, it does not effect a real remedy. After the heat has been turned off, the pipes will again become cold and similar stresses will be set up when the metal contracts. This may also cause shearing or hardening during the process of cooling and heating as the weather conditions change.

If, for the purpose of forming an actual space between the concrete and the pipe, instead of maintaining a constant high temperature during the pouring and setting of the concrete, the temperature of the water is allowed to change over fairly wide limits, then a little more freedom for the pipes to expand will be provided. However, in doing this, the heat transmission may somewhat impaired. An air space formed

between the pipe and the concrete will act as an insulator and interrupt the continuity of heat conduction between the pipe and the concrete. Consequently, in the interest of getting the greatest efficiency from embedded pipes, this practice is not recommended.

It is sometimes erroneously stated that if the coefficient of expansion of the pipe is equal to that of the surrounding material, no relative expansion will exist and no strains will be set up in the metal of the pipe. If pipes are embedded in a concrete pavement, for instance, there may at times be a considerable difference between the temperature of the pipe and the average temperature of the concrete. For instance, the liquid circulating in the pipe coils may be as high as 65 or 70 °C, and if high pressure-high temperature water is used, the pipes may reach a temperature above 150 °C, whereas, the average temperature of the concrete when the heat is turned on may be considerably lower. This should be given serious consideration, if long grid coils are contemplated, because it can lead to considerable trouble.

The introduction of expansion joints is very important due to the expansion of the heated concrete during cold weather. For this purpose, it is recommended Flexible, a waterproof type of insulating board, although other types of material can be used if found satisfactory.

The advantage of this board is that there is practically no extrusion of the material under compression and it will immediately re-expand when released from the compression due to the expansion of the concrete slabs. It seems apparent from the use of this board that there is no disintegration of the material and no uneven surfaces caused at the joints.

2.10 ANTI-FREEZE SOLUTIONS AND THEIR USE AS WORKING LIQUID

Basic types of antifreeze can be listed as follows:

1. Methyl alcohol (methanol)
2. Ethyl alcohol (ethanol)
3. Isopropyl (isopropanol)
4. Ethylene glycol
5. Propylene glycol
6. Salt-base
7. Glycerin-base
8. Petroleum-base

Most of the antifreeze solutions are of the glycol family and are considered to be non-corrosive since many of the reliable manufacturers of antifreeze solutions include an inhibitor. This is something which should be confirmed before using, and it is important to insure that the inhibitor used does not break down at the highest temperature reached in the boiler. It must be remembered that the whereas an antifreeze solution may be used in an automobile cooling system for a period of 6 months or so at a time, and a car may be replaced with a new one every few years, a snow melting system should be expected to last for 20 or 30 years without any expensive repairs.

Wherever possible, a heat exchanger should be used so that the anti-freeze does not come in contact with high temperature surfaces. However, this often adds considerably to he cost of the installation unless an existing hot water boiler, with ample margin of power or a good supply of system, is already available, in which case a heat exchanger is the correct thing to use.

Table 2.2. Flash and fire points of aqueous ethylene glycol solutions at atmospheric pressure

GLYCOL PERCENTAGE BY WEIGHT	FLASH POINT °C	FIRE POINT °C
100	118	121
95	127	132
90	133	138
85	--	--

Broadly speaking, the requirements of a good antifreeze solution may be considered as follows :

1. It should prevent freezing of the solution at the lowest temperature to which any part of the system will be exposed. In this respect, it may be considered that pipes buried below the surface will be somewhat warmer than the air above, depending on the depth of the pipes and the nature of the soil. If the pipe coils are embedded in a concrete slab which is supported above and clear of the earth, then, if the system is not in use for some time, it may be possible for some parts of the pipes and contents to reach the temperature of the surrounding air. Then again, even though all the pipe coils are buried in the earth, if some small part of the circuit is left exposed to the air, it must be considered that the antifreeze in this part may reach air temperature and solidify if the air temperature drops below the freezing point of the antifreeze.

2. It must not attack any of the materials used under any conditions. This also applies to the packing used in valves and pump glands.

3. It must be chemically stable under conditions of operation since decomposition products of an unstable antifreeze may be highly corrosive, or they may be too volatile.

4. The viscosity should not increase seriously at either high or low temperatures. A large increase in viscosity will mean more load on the pump, making a larger circulator imperative, or it will reduce the circulating velocity throughout the system.

5. The specific heat and heat conductivity should be as high as possible. Otherwise, there will be a large temperature differential across the system and also to the walls of the embedded pipes.

6. The boiling point should not be much less than water, and should follow the characteristics of water as closely as possible.

7. It should have a low coefficient of expansion to prevent overflow losses.

8. It should be non-toxic and certainly non-flammable.

9. It should not produce an unpleasant odor, although this may be considered as a minor requirement.

While it is generally conceded that no practical solution will satisfy all these requirements, there are solutions which will meet most of the important requirements. These include the ethylene and propylene glycol's, and to some extent solutions of the simple alcohol's (methyl, ethyl and isopropyl). Many other substances may be

used, but it is advisable to use only those solutions which have satisfactory withstood a prolonged test for the points mentioned above.

It has been found that a good brand of ethylene glycol gives very good results, but it is always advisable to check the condition of the solution at intervals to determine whether the effectiveness of the inhibitor is being impaired with use. This can be done by nothing the appearance of the solution and if this has a brown or rusty color the solution should be drained and a fresh filling made; and, secondly titrating with a standard acid solution for loss of reserve alkalinity. Even though a good brand of antifreeze is selected, it is advisable to take all reasonable precautions against trouble.

The "freezing point " of an antifreeze solution is defined as the temperature at which the first ice crystals form. Antifreeze solutions, however, do not usually become solid at their freezing points, but simply develop into a mush state. This condition, while not being as dangerous as the solid state in causing fracture of the pipes, will stop the circulation if the temperature drops a few degrees below its freezing point, and put the system out of commission until the weather becomes milder, or until heat is applied locally to change its state back to liquid again.

By using the freezing point as a determining factor for the solution, a slight margin of safety is available for emergency, especially since the temperature of the solution in the embedded pipes will be somewhat above the lowest air temperature.

2.11 AUTOMATIC CONTROLS FOR START-UP

It is a good practice to maintain a circulation of medium temperature water or antifreeze in the coils during the periods when snow is predicted, and to switch on the full heat immediately precipitation commences. There are some cases where it is not considered possible to maintain a continuous flow of heat, even at low temperatures.

While such a decision is often prompted by the cost of operation, it may be because the only available heat is required for other purposes. However, regardless as to whether preliminary heat is applied before the snow storm commences or not, it is very important that the full heat be turned on immediately snow commences to fall. That is, of course, an operation which may be accomplished manually if someone is available at the time to turn on the heat, but since snow storms are so unpredictable and often start during the night, or during the absence of the caretaker, it is an advantage to have an automatic starter for important installations.

2.12 REVIEW OF SOME PREVIOUS WORK

M. Chung, R. Hangel [8] investigated the problem of heat transfer from a pipe buried in a semi-infinite medium with constant wall temperature. Plane surface is exposed to fluid flow. Using a conformal mapping, the original semi-infinite physical domain is transformed into a finite rectangular domain. The panel efficiency and maximum surface temperatures are presented in terms of Biot Number.

G.P. Zhang, S. Weinbaum [9-10] presented a steady-state approximate solution for the three-dimensional melting or freezing around a fluid-carrying pipe buried in asemi-infinite phase change medium (PCM).

A. Negiz and A. Hastaoglu, A. Heidemann [11] analyzed the transient heat transfer problem of solidification of stationary liquid around a buried pipe. The system is cooled from a horizontal flat top surface. The solution is obtained using a string-intersected boundary formulation and a three level alternating direction implicit finite difference method.

Facas, N [12] presented numerical solutions for the natural convection heat transfer from a pipe with two baffles attached along its surface beneath a semi-infinite

saturated porous medium. The surface of medium is assumed to be permeable. A simple correlation for Nusselt Number as a function of Rayleigh Number, pipe burial depth and baffle length.

Ali M, Latif M and S.Weinbaum [13] explored the use of boundary-integral equation method (BIEM) for multidimensional problems with a moving phase change interface. Quasi-steady heat conduction is assuned in both the thawed and frozen zones.

Dayan and Herbaum [14] investigated two-dimensional steady temperature distribution in soil around a network of subsurface horizontal warm water pipes.

Haim H. Bau, [15-16] presented two-dimensional analytical solution for heat losses from a buried pipe. Turbulent and laminar flow are analyzed separately. In turbulent flow case, uniform heat transfer coefficient at the pipe surface is assumed and expression for a shape factor is determined. In laminar flow case linear temperature variations along the pipe axis is considered.

Moya [17] performed an experimental analysis of heat and moisture transfer around a heated cylinder surrounded by an unsaturated soil. The main motivation for this work is its application for high-voltage electrical power distribution in urban areas which, in general, makes the use of underground cables.

Gauthier and Lacroix [18] conducted a numerical study for the thermal behavior of soil heat exchanger-storage systems (SHESS) aimed at reducing the energy consumption of greenhouses. These systems consist of buried pipes circulating air for storing and removing heat from the soil. Results indicate that the total amount of energy stored or recovered daily per volume decreases exponentially with the pipe center-center distance and pipe length.

Mei [19] derived a new ground coil model, which based on energy balance rather than the traditional line source theory. The results indicated that for winter coil operation, the new model predicted the coil liquid exit temperature less than 2°C maximum deviation from the measured values, with an average deviation less than 1°C. For summer operation, all models under-predicted the measured soil temperatures because the effect of thermal backfill material was not included in the models.

Negiz and Hastaoglu [20] presented a model for heat transfer from a fluid in laminar flow inside a buried horizontal pipe. The problem is modeled as a transient three-dimensional process in cylindirical geometry.

CHAPTER 3

HEAT TRANSFER MODELING OF THE SYSTEM

In this chapter, the general approach to the problem solution will be explained.

3.1 THE GEOMETRY OF SYSTEM

The basic reason for designing the underground heating (or snow melting) system is to heat up the apron surface. For this reason buried pipe coils are used. As it is seen in the Figure 3.1, heating fluid flows in opposite direction in neighboring pipes in order to obtain more uniform temperature in the solid.

In other words cross-flow is assumed. This structure is composed of symmetric regions. The meaning of "Guide Line For Symmetry" will be explained later in this chapter.

3.2 GENERAL REMARKS AND ASSUMPTIONS

Heat is transferred from the heating fluid in the pipe to the ground by convection, conducted from solid to the surface and convected to the atmosphere. Also, the effect of radiation heat transfer from surface to atmosphere, must be taken into consideration.

The following assumptions have to be mentioned:

1) The underground heating system is considered as three dimensional and unsteady.

2) Convective and radiative heat transfer were accounted by a combined heat transfer coefficient. At the surface boundary the following expressions can be written.

$$-k\frac{\partial T}{\partial y} = h_0(T-T_\infty) + \sigma\epsilon(T^4 - T_\infty^4)$$

$$= h_0(T-T_\infty) + \sigma\epsilon(T^3 + T T_\infty^2 + T_\infty T^2 + T_\infty^3)(T-T_\infty) \qquad (3.1)$$

From the Eqn. 3.1 the equivalent *radiative* heat transfer coefficient , h_r , can be written as:

$$h_r = \sigma\epsilon(T^3 + T T_\infty^2 + T_\infty T^2 + T_\infty^3) \qquad (3.2)$$

As it is seen the radiative heat transfer coefficient is actually temperature dependent. But for design of underground heating system, maximum amount of radiative heat transfer coefficient is assumed throughout the procedure. In extreme cases following values are used.

T_∞= -3 °C = 270 K

T = +7 °C = 280 K (Temperature at the surface)

$\epsilon = 1$

$\sigma = 5.669 \times 10^{-8}$ W/m^{2}K^4

Therefore from Eqn. (3.2),

$h_r = 4.7$ W/m^{2}K

3) A perfect contact was assumed between coil pipes and surrounding solid.

4) Constant temperature at a certain depth C.

5) Negligible pipe thickness and pipe thermal resistance and uniform properties.

6) For modeling purpose the effect of collectors, elbows etc. are neglected.

7) Initially, outer surface of the solid in atmospheric temperature and solid temperature is linearly increasing up to a base temperature at depth C.

8) Initially temperature of the liquid is equal to neighboring solid temperature, inside the pipe.

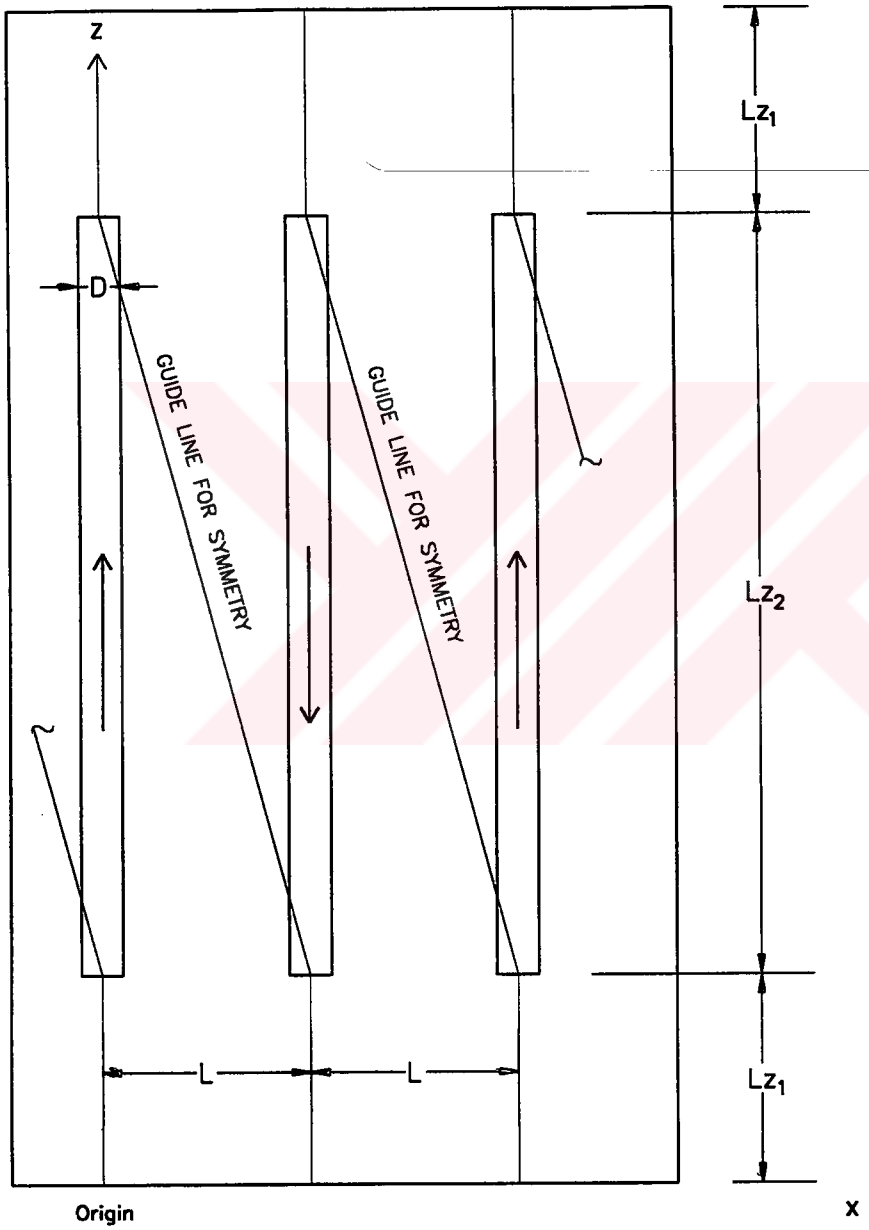

Figure 3.1. Top view of the piping model with basic dimensions.

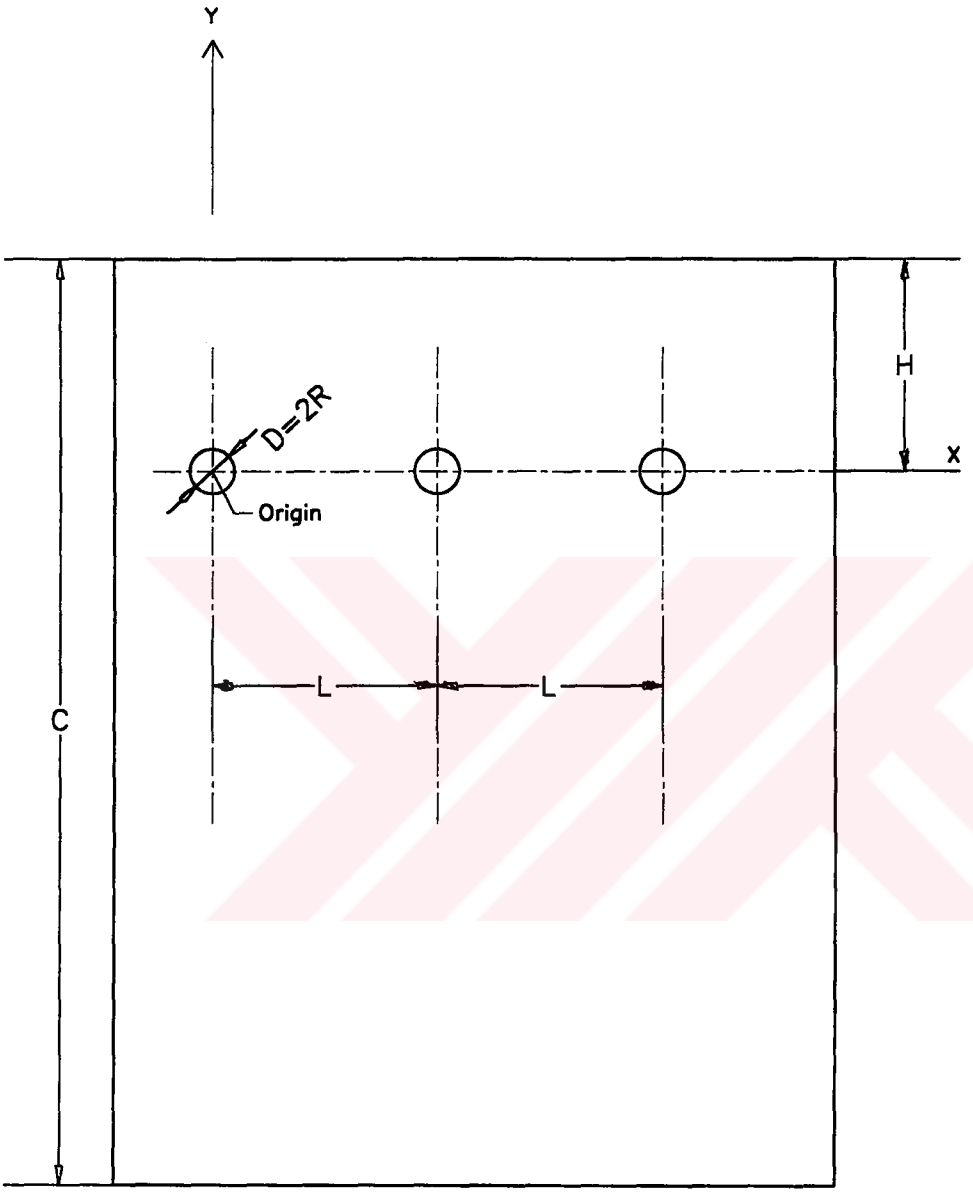

C: Distance where the temperature reaches to the ground temperature

Figure 3.2. Piping cross-section with basic dimensions.

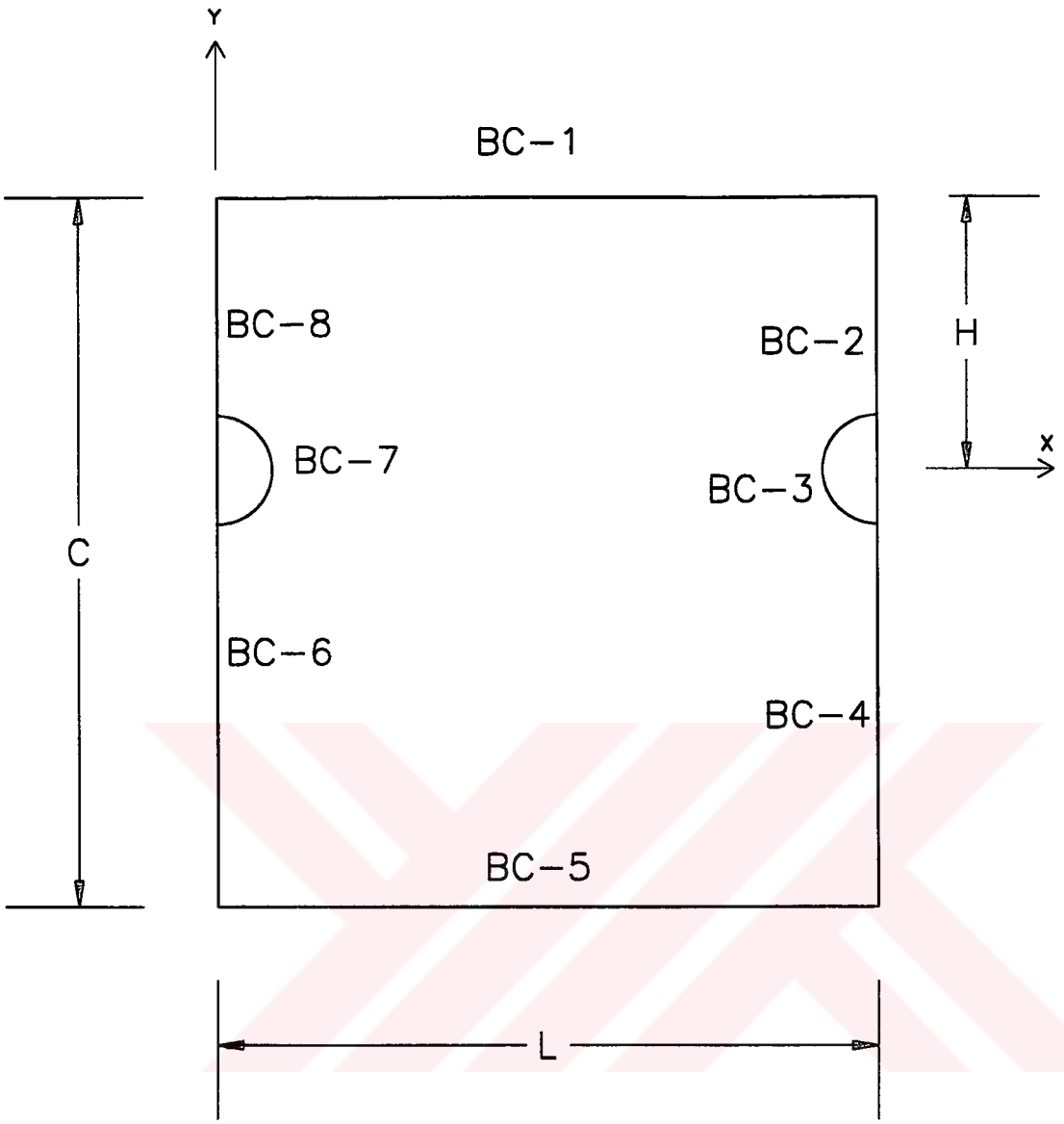

Figure 3.3. The solution domain of heat conduction problem with the boundary conditions.

9) The pipe and surrounding soil is treated as a control volume. As the system is started the liquid with temperature T_i enters to the control volume, so that the surrounding solid and the outer surface is heated. Two objectives of the system are:

Objective - 1: To melt the snow or ice on the surface (if exists).

Objective - 2: If there is no snow or ice, to keep the surface temperature above a certain level.

Therefore for Objective - 1, outer surface temperature is constant. For Objective - 2 there is a convective boundary condition having combined convective and radiative heat transfer coefficients as stated in the beginning of this section.

10) The solid side of the control volume is divided into two. Solid-1 is for the entrance solid without pipe. Solid-2 contains pipe inside.

3.3. FORMULATION OF PROBLEM

The governing differential equation in Cartesian coordinates can be written as:

$$\frac{\partial^2 T}{\partial x^2} + \frac{\partial^2 T}{\partial y^2} + \frac{\partial^2 T}{\partial z^2} = \frac{1}{\alpha}\frac{\partial T}{\partial t} \qquad (3.3)$$

The boundary conditions are listed for T = T(x,y,z,t), as follows

BC-1:

For Objective - 1:

At y = H $\qquad T = T_s$

For Objective - 2:

At y = H $\qquad -k\frac{\partial T}{\partial y} = h_\infty (T - T_\infty)$

where h_∞ is the combined convective and radiative heat transfer coefficient.

BC-2:

For $y > R$

At $x = L$ $\qquad \dfrac{\partial T}{\partial x} = 0$

BC-3:

For $-R < y < R$

At $r' = R$ (or $(x - L)^2 + y^2 = R^2$) $\qquad -k\dfrac{\partial T}{\partial r'} = h_i (T_{mo} - T)$

where T_{mo} is fluid temperature at the exit of the pipe.

BC-4:

For $y < -R$

At $x = L$ $\qquad \dfrac{\partial T}{\partial x} = 0$

BC-5:

At $y = -(C - H)$ $\qquad T = T_b$

where T_b is ground temperature

BC-6:

For $y < -R$

At $x = 0$ $\qquad \dfrac{\partial T}{\partial x} = 0$

BC-7:

For $-R < y < R$

At $r = R$ (or $x^2 + y^2 = R^2$) $$-k\frac{\partial T}{\partial r} = h_i(T_m - T)$$

BC-8:

For $y > R$

At $x = 0$ $$\frac{\partial T}{\partial x} = 0$$

BC-9:

For Objective - 1:

At $z = 0$ $$T(x, y, 0, t) = T_S + (T_b - T_S)\frac{H - y}{C}$$

where T_S is temperature at the surface

For Objective - 2:

At $z = 0$ $$T(x, y, 0, t) = T_\infty + (T_b - T_\infty)\frac{H - y}{C}$$

where T_∞ is the atmospheric temperature.

Initial Condition

For Objective - 1:

For the initial temperature distribution in the solid region and in the pipe, it is assumed that the surface temperature is equal to, T_S , and linearly increasing up to base temperature, T_b at depth C. Therefore,

For the node in solid and in the pipe:

$$T(x,y,z,0) = T_S + (T_b - T_S)\frac{H - y}{C}$$

For Objective - 2:

For the initial temperature distribution in the solid region and in the pipe, it is assumed that the surface temperature is equal to the outside temperature ,T_∞ , and linearly increasing up to base temperature, T_b at depth C. Therefore,

For the node in the solid and in the pipe:

$$T(x,y,z,0) = T_\infty + (T_b - T_\infty)\frac{H - y}{C}$$

In order to keep the approach more general, the following non-dimensional parameters are applied.

$$x^* = \frac{x}{R} \qquad y^* = \frac{y}{R} \qquad r^* = \frac{r}{R} \qquad z^* = \frac{z}{R} \qquad t^* = \frac{\alpha t}{R^2}$$

(3.4a)

$$\theta = \frac{T - T_\infty}{T_b - T_\infty} \qquad (3.4b)$$

The non-dimensional differential equation then can be written as:

$$\frac{\partial^2\theta}{\partial x^{*2}} + \frac{\partial^2\theta}{\partial y^{*2}} + \frac{\partial^2\theta}{\partial z^{*2}} = \frac{\partial\theta}{\partial t^*} \qquad (3.5)$$

Also, the boundary conditions and initial condition take the following non-dimensional form:

BC-1:
For Objective - 1:

$$\text{At } y^* = h = \frac{H}{R} \qquad \theta = \theta_S$$

For Objective - 2:

$$\text{At } y^* = h = \frac{H}{R} \qquad \frac{\partial\theta}{\partial y^*} + Bi_\infty\theta = 0$$

where Bi_∞ is Biot number defined between solid surface and atmosphere.

$$Bi_\infty = \frac{h_\infty R}{k}$$

k: thermal conductivity of solid.

BC-2:

For $y^* > 1$

$$\text{At } x^* = l = \frac{L}{R} \qquad \frac{\partial\theta}{\partial x^*} = 0$$

BC-3:

For $-1 < y^* < 1$

$$\text{At } r'^* = 1 \ (\text{or } (x^* - l)^2 + y^{*2} = 1) \qquad \frac{\partial\theta}{\partial r'^*} + Bi_m(\theta - \theta_{mo}) = 0$$

where Bi_m is Biot number defined between solid surface and fluid in the pipe.

BC-4:

For $y^* < -1$

$$\text{At } x^* = l = \frac{L}{R} \qquad \frac{\partial\theta}{\partial x^*} = 0$$

BC-5:

At $y^* = -(c - h) = -\left(\frac{C}{R} - \frac{H}{R}\right)$ $\theta_b = 1$

BC-6:

For $y^* < -1$

At $x^* = l = \frac{L}{R}$ $\frac{\partial \theta}{\partial x^*} = 0$

BC-7:

At $r^* = 1$ (or $x^{*2} + y^{*2} = 1$) for $-1 < y^* < 1$

$$\frac{\partial \theta}{\partial r^*} + Bi_m (\theta - \theta_m) = 0$$

BC-8:

For $y^* > 1$

At $x^* = l = \frac{L}{R}$ $\frac{\partial \theta}{\partial x^*} = 0$

BC-9:

For Objective - 1:

At $z^* = 0$ $\theta(x^*, y^*, 0, t^*) = \theta_S + (1 - \theta_S)\frac{h - y^*}{c}$

where θ_S is non-dimensional temperature defined as Eqn. (3.4b) at the surface.

For Objective - 2:

$$\text{At} \qquad z^* = 0 \quad \theta(x^*, y^*, 0, t^*) = \frac{h - y^*}{c}$$

Initial Condition

For Objective - 1:

$$\theta(x^*,y^*,z^*,0) = \theta_S + (1 - \theta_S)\frac{h - y^*}{c}$$

For Objective - 2:

$$\theta(x^*, y^*, 0, t^*) = \frac{h - y^*}{c}$$

It is important to recall that h, c and l are non-dimensional geometrical parameters defined with respect to pipe radius R, as in the Eqn. (3.4a)

3.4 APPROACH FOR THE SOLUTION

The conduction problem described above is too complicated for an analytical treatment, a numerical method is needed to find the temperature distribution. In this study, Finite Difference Method is used for obtaining the solution. In Fig. 3.4a, the discrete sized structure of a sample geometry is illustrated on $x^* - y^*$ plane.

In Fig. 3.4b the discrete sized structure of a geometry is illustrated on $x^* - z^*$ plane.

While writing and solving the three dimensional unsteady equations, the implicit method [6] is selected. The computer program listed in the Appendix-C is used to derive and solve the nodal equations, and the non-dimensional temperature distribution is obtained.

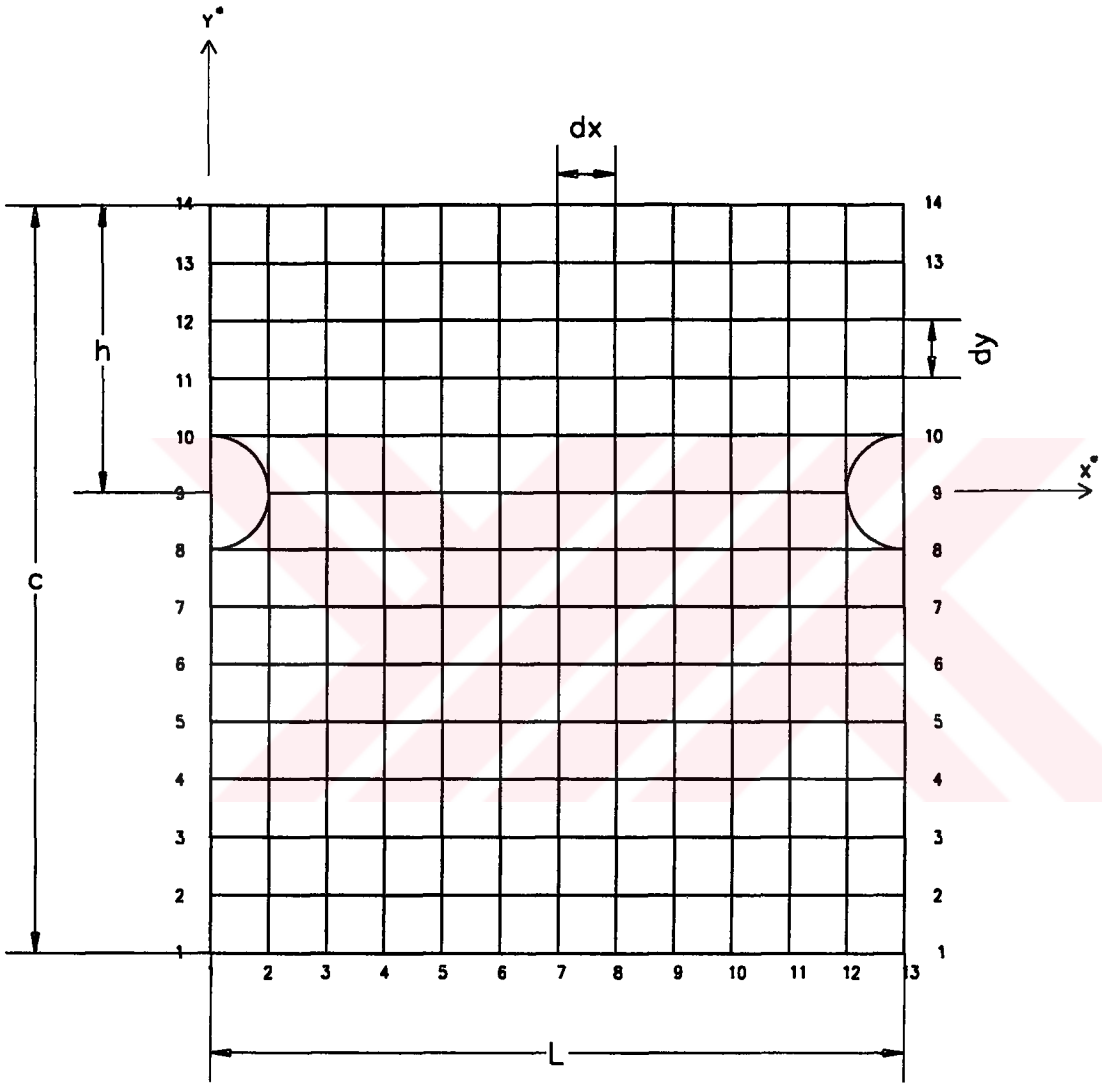

Figure3.4a. Gridding for finite difference for l = 12, h = 5, c = 13 on $x^* y^*$ plane.

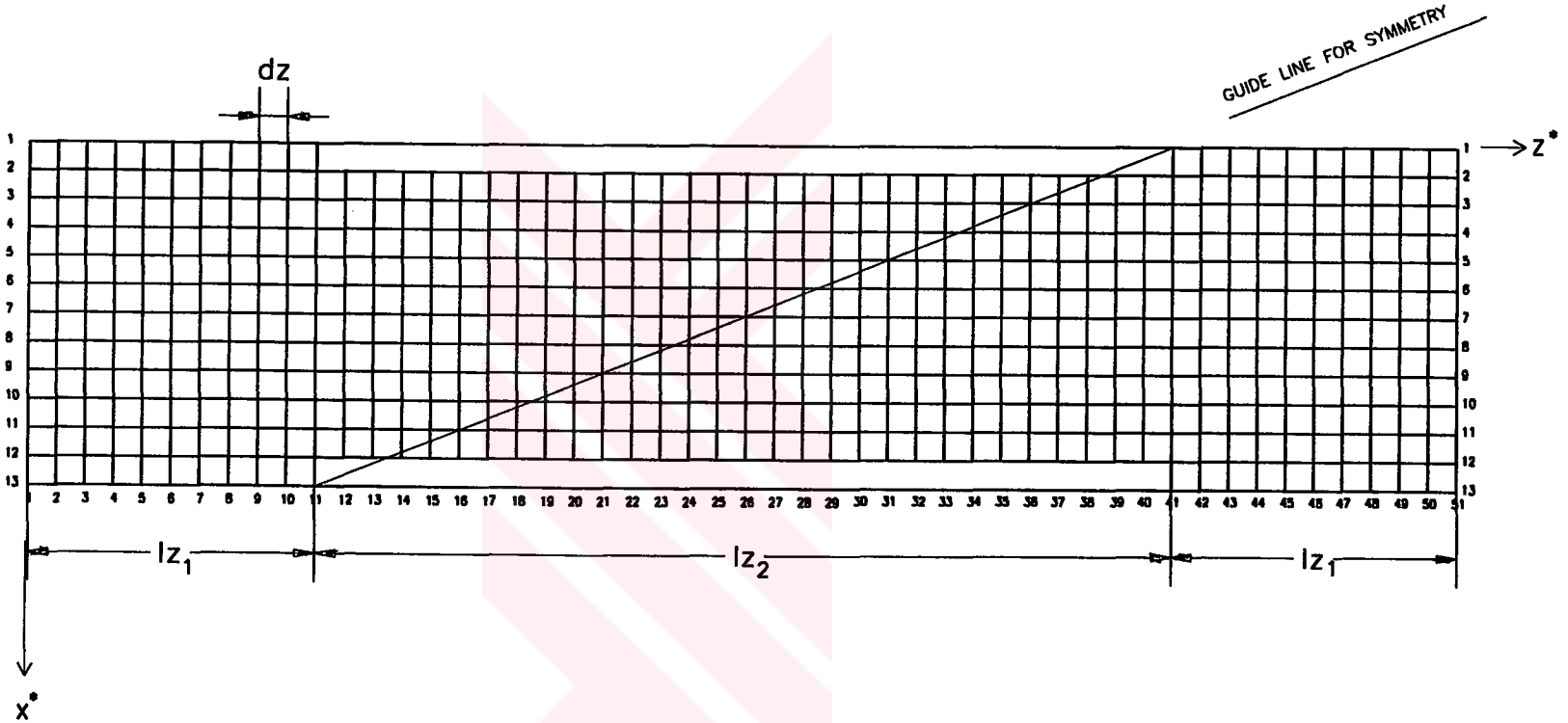

Fig.3.4b. Gridding for finite difference for l = 12, h = 5, c = 13 on x^*z^* plane. ($lz_1 = 10$, $lz_2 = 30$)

3.4.1 SAMPLE DERIVATION OF BASIC FINITE DIFFERENCE EQUATIONS

Sample derivation of finite difference equations for the nodes shown in the Fig. 3.4 will be demonstrated in the followings. Two sample nodes are selected. One of them is on the outer surface and the other is in the pipe (fluid side).

General definitions for temperature elements are as follows:

$T_{x,y,z}^{P}$ is the temperature for the pointer node (or center node) of any rectangular prismatic nodal element at certain Z plane at any time t. The x,y represents the node number on x-y plane, z represents the plane number on z direction. $T_{x,y,z}^{P+1}$ is the temperature for the pointer node (or center node) of any rectangular prismatic nodal element at any time $t + \Delta t$. The temperature values of the neighboring nodes at the south, east, north and west are called $T_{x,Y-1,z}^{P+1}$, $T_{X+1,y,z}^{P+1}$, $T_{x,Y+1,z}^{P+1}$, $T_{X-1,y,z}^{P+1}$ respectively at any time $t + \Delta t$. $T_{x,y,Z+1}^{P+1}$ and $T_{x,y,Z-1}^{P+1}$ are also neighboring nodes located at +Z and -Z direction relative to $T_{x,y,z}^{P+1}$ respectively.

Similarly values $T_{x,y,z}^{P}$, $T_{x,y,z}^{P+1}$, $T_{x,Y-1,z}^{P+1}$, $T_{X+1,y,z}^{P+1}$, $T_{x,Y+1,z}^{P+1}$, $T_{X-1,y,z}^{P+1}$, $T_{x,y,Z+1}^{P+1}$ and $T_{x,y,Z-1}^{P+1}$ can be expressed in terms of their corresponding non-dimensional temperature values $\theta_{x,y,z}^{P}$, $\theta_{x,y,z}^{P+1}$, $\theta_{x,Y-1,z}^{P+1}$, $\theta_{X+1,y,z}^{P+1}$, $\theta_{x,Y+1,z}^{P+1}$, $\theta_{X-1,y,z}^{P+1}$, $\theta_{x,y,Z+1}^{P+1}$ and $\theta_{x,y,Z-1}^{P+1}$.

3.4.1.1 SAMPLE NODE ON THE OUTER SURFACE

Fig. 3.5 shows the sample node on the outer surface. With dimensional temperature, following energy balance equation can be written:

$$k\,S_{ym1}\,(T_{x,Y-1,z}^{P+1} - T_{x,y,z}^{P+1}) + k\,S_{xp1}\,(T_{X+1,y,z}^{P+1} - T_{x,y,z}^{P+1}) + k\,S_{yp1}\,(T_{\infty} - T_{x,y,z}^{P+1})$$
$$+ k\,S_{xm1}\,(T_{X-1,y,z}^{P+1} - T_{x,y,z}^{P+1}) + k\,S_{zp1}\,(T_{x,y,Z+1}^{P+1} - T_{x,y,z}^{P+1}) + k\,S_{zm1}\,(T_{x,y,Z-1}^{P+1} - T_{x,y,z}^{P+1})$$

$$= \rho V c_p \frac{T_{x,y,z}^{P+1} - T_{x,y,z}^{P}}{\Delta t} \qquad (3.6)$$

where S_{yml}, S_{xpl}, S_{ypl}, S_{xml}, S_{zpl}, S_{zml} are shape factors. For conduction heat transfer, shape factor is the ratio of heat transfer area to the distance between related nodes. On the other hand for convection heat transfer, shape factor is the heat transfer area. V is the nodal volume.

Applying the non-dimensional parameters,

$$S^*_{yml}(\theta_{x,Y-1,z}^{P+1} - \theta_{x,y,z}^{P+1}) + S^*_{xpl}(\theta_{X+1,y,z}^{P+1} - \theta_{x,y,z}^{P+1}) - Bi_\infty S^*_{ypl}\theta_{x,y,z}^{P+1}$$
$$+ S^*_{xml}(\theta_{X-1,y,z}^{P+1} - \theta_{x,y,z}^{P+1}) + S^*_{zpl}(\theta_{x,y,Z+1}^{P+1} - \theta_{x,y,z}^{P+1}) + S^*_{zml}(\theta_{x,y,Z-1}^{P+1} - \theta_{x,y,z}^{P+1})$$

$$= \frac{V^*}{Fo}(\theta_{x,y,z}^{P+1} - \theta_{x,y,z}^{P}) \qquad (3.7)$$

where Fo is incremental Fourier Number that is defined as follows:

$$Fo = \frac{\alpha \Delta t}{R^2} \qquad (3.8)$$

According to Fig. 3.5, the shape factors are:

$$S^*_{yml} = \frac{dx\,dz}{dy} \qquad S^*_{xpl} = \frac{dy\,dz}{2\,dx} \qquad S^*_{ypl} = dx\,dz \qquad S^*_{xpl} = \frac{dy\,dz}{2\,dx}$$

$$S^*_{zpl} = \frac{dx\,dy}{2\,dz} \qquad S^*_{zml} = \frac{dx\,dy}{2\,dz} \qquad (3.9)$$

Nodal area on x^*y^* plane, $A_0 = 0.5\,dx\,dy$ (3.10)

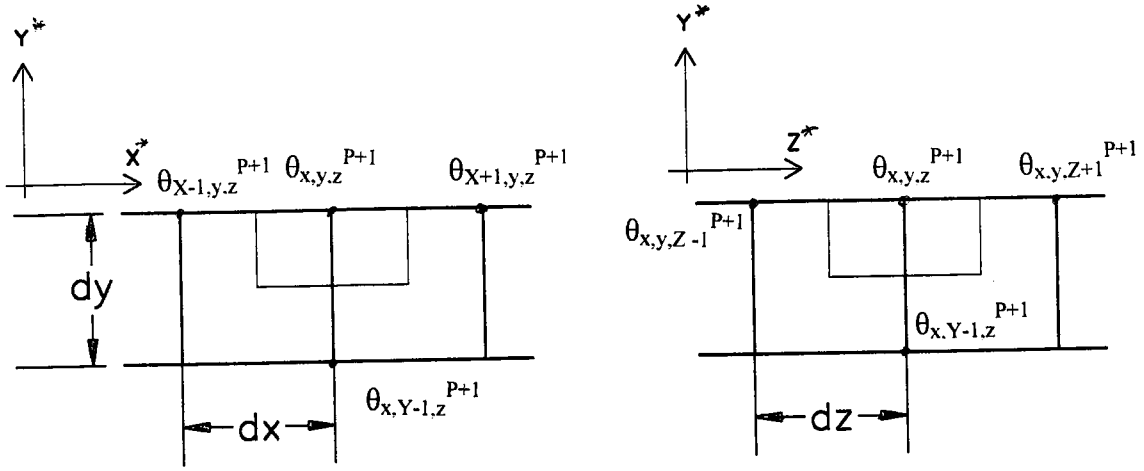

Figure 3.5. Sample node at outer surface at x^*y^* & y^*z^* planes.

Nodal Volume, $V^* = A_0\, dz = 0.5\, dx\, dy\, dz$ (3.11)

For simplification of Eqn. (3.7) following coefficients can be defined:

$$K_{ym1} = \frac{S^*_{ym1}}{V^*} Fo \qquad K_{xp1} = \frac{S^*_{xp1}}{V^*} Fo \qquad K_{yp1} = \frac{S^*_{yp1}}{V^*} Bi_\infty Fo$$

$$K_{xm1} = \frac{S^*_{xm1}}{V^*} Fo \qquad K_{zp1} = \frac{S^*_{zp1}}{V^*} Fo \qquad K_{zm1} = \frac{S^*_{zm1}}{V^*} Fo \qquad (3.12)$$

Using Eqn. 3.12, Eqn. 3.7 can be written as:

$$K_{ym1}(\theta_{x,Y-1,z}^{P+1} - \theta_{x,y,z}^{P+1}) + K_{xp1}(\theta_{X+1,y,z}^{P+1} - \theta_{x,y,z}^{P+1}) - K_{yp1}\,\theta_{x,y,z}^{P+1}$$
$$+ K_{xm1}(\theta_{X-1,y,z}^{P+1} - \theta_{x,y,z}^{P+1}) + K_{zp1}(\theta_{x,y,Z+1}^{P+1} - \theta_{x,y,z}^{P+1}) + K_{zm1}(\theta_{x,y,Z-1}^{P+1} - \theta_{x,y,z}^{P+1})$$

$$= \theta_{x,y,z}^{P+1} - \theta_{x,y,z}^{P} \qquad (3.13)$$

Sum of the coefficients, S_m, can be defined as:

$$S_m = K_{ym1} + K_{xp1} + K_{yp1} + K_{xm1} + K_{zp1} + K_{zm1} \qquad (3.14)$$

So, Eqn. (3.13) can be simplified as:

$$K_{yml}\,\theta_{x,Y-1,z}^{P+1} + K_{xpl}\,\theta_{X+1,y,z}^{P+1} + K_{xml}\,\theta_{X-1,y,z}^{P+1} + K_{zpl}\,\theta_{x,y,Z+1}^{P+1} + K_{zml}\theta_{x,y,Z-1}^{P+1}$$
$$- S_m\,\theta_{x,y,z}^{P+1} = \theta_{x,y,z}^{P+1} - \theta_{x,y,z}^{P} \qquad (3.15)$$

The coefficients in the Eqn. 3.12 are called as nodal coefficients and will be used for generalization of finite difference equations. $\theta_{x,y,z}^{P}$ is known from the initial condition and the other non-dimensional temperature values are the unknowns to be determined.

3.4.1.2 SAMPLE NODE IN THE PIPE

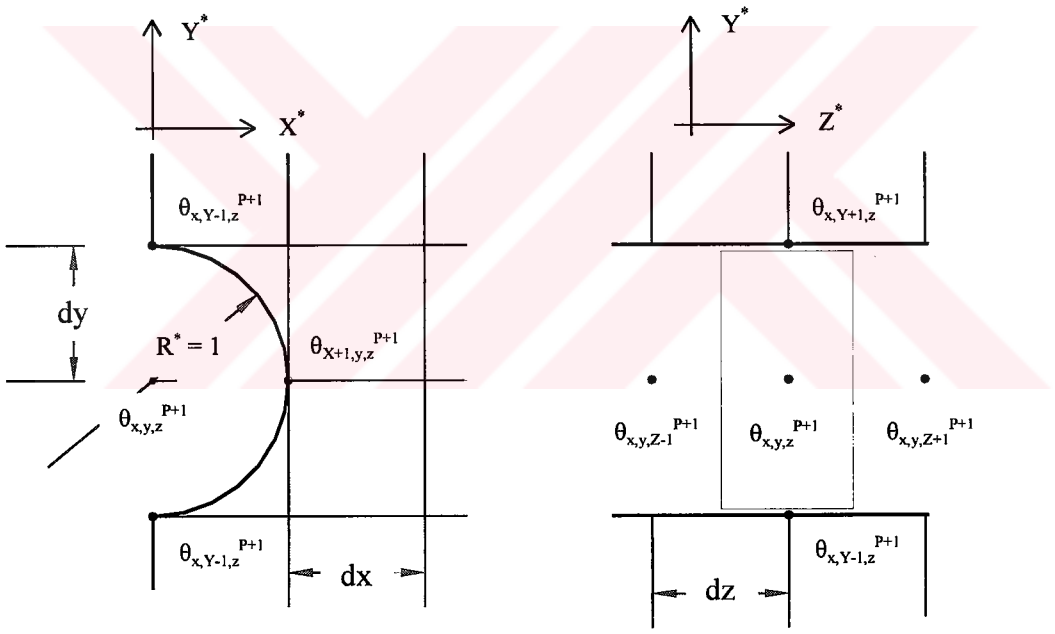

Figure 3.6. Sample node in the pipe at x^*y^* and y^*z^* planes

Unlike the previous node, there is a mass flow in and mass flow out to the control volume shown in Fig. 3.6. The energy balance equation can be written as:

$$m\, i_{x,y,Z-1} + Q = \frac{dE}{dt} + m\, i_{x,y,z} \qquad (3.16)$$

where

m: Mass flow rate in the pipe

$i_{x,y,Z-1}$: Enthalpy inflow to the control volume

Q: Heat transfer to the control volume

dE/dt: Rate of change of internal energy within the control volume

$m\, i_{x,y,z}$: Enthalpy outflow from the control volume

When the terms are rearranged:

$$m\, c_{pw} (T_{x,y,Z-1}^{P+1} - T_{x,y,z}^{P+1}) + Q = \frac{dE}{dt} \qquad (3.17)$$

also

$$Q = 2\, [\, h_m S_{ym1} (T_{x,Y-1,z}^{P+1} - T_{x,y,z}^{P+1}) + h_m S_{xp1} (T_{X+1,y,z}^{P+1} - T_{x,y,z}^{P+1}) + h_m S_{ym1} (T_{x,Y+1,z}^{P+1} - T_{x,y,z}^{P+1})] \qquad (3.18)$$

Since total mass flow in the pipe is considered, heat transfer of the half circle is multiplied by 2. The shape factors are the heat transfer areas in dimensional form. Therefore, they are multiplied by R^2.

$$S_{ym1} = 0.25\, \pi\, dz\, R^2$$

$$S_{xp1} = 0.50\, \pi\, dz\, R^2$$

$$S_{yp1} = 0.25\, \pi\, dz\, R^2 \qquad (3.19)$$

Using Eqn. (3.4), in terms of non-dimensional temperature values,

$$Q = 2\ h_m\ R^2\ (T_b - T_\infty)\ dz\ [0.25\ \pi\ (\theta_{x,Y-1,z}^{P+1} - \theta_{x,y,z}^{P+1}) + 0.50\ \pi\ (\theta_{X+1,y,z}^{P+1} - \theta_{x,y,z}^{P+1}) + 0.25\ \pi\ (\theta_{x,Y+1,z}^{P+1} - \theta_{x,y,z}^{P+1})] \quad (3.20)$$

The rate of change of internal energy can be detailed as:

$$\frac{dE}{dt} = 2\ \rho_w\ 0.5\ \pi\ dz\ c_{pw}\ R^3 \frac{T_{x,y,z}^{P+1} - T_{x,y,z}^{P}}{\Delta t} \quad (3.21)$$

$$\frac{dE}{dt} = \rho_w\ R^3\ c_{pw}\ (T_b - T_\infty)\ \pi\ dz\ \frac{\theta_{x,y,z}^{P+1} - \theta_{x,y,z}^{P}}{\Delta t} \quad (3.22)$$

Equations (3.22) and (3.20) are substituted into Eqn. (3.17) and $(T_b - T_\infty)$ from both sides is eliminated. So, the energy balance equation becomes:

$$m\ c_{pw}\ (\theta_{x,y,Z-1}^{P+1} - \theta_{x,y,z}^{P+1}) + h_m\ R^2\ dz\ \pi\ [0.5\ (\theta_{x,Y-1,z}^{P+1} - \theta_{x,y,z}^{P+1}) + (\theta_{X+1,y,z}^{P+1} - \theta_{x,y,z}^{P+1}) + 0.5\ (\theta_{x,Y+1,z}^{P+1} - \theta_{x,y,z}^{P+1})] = \rho_w\ R^3\ c_{pw}\ \pi\ dz\ \frac{\theta_{x,y,z}^{P+1} - \theta_{x,y,z}^{P}}{\Delta t} \quad (3.23)$$

Dividing both sides of the Eqn. (3.23) by $\frac{\Delta t}{\rho_w\ R^3\ c_{pw}\ \pi\ dz}$ gives two important non-dimensional coefficients on the left side of the equation.

$$A^* = \frac{m\ \Delta t}{\rho_w\ R^3\ \pi\ dz} \qquad B^* = \frac{h_m\ R\ \Delta t}{\rho_w\ c_{pw}\ R^2} \quad (3.24)$$

So, the Eqn. 3.23 is simplified as:

$$A^*(\theta_{x,y,Z-1}^{P+1} - \theta_{x,y,z}^{P+1}) + 0.5\,B^*(\theta_{x,Y-1,z}^{P+1} - \theta_{x,y,z}^{P+1}) + B^*(\theta_{X+1,y,z}^{P+1} - \theta_{x,y,z}^{P+1})$$

$$+ 0.5\,B^*(\theta_{x,Y+1,z}^{P+1} - \theta_{x,y,z}^{P+1}) = \theta_{x,y,z}^{P+1} - \theta_{x,y,z}^{P} \qquad (3.25)$$

To apply general form as in Eqn. (3.15) nodal coefficients are defined as:

$$K_{zm1} = A^* \qquad K_{ym1} = 0.5\,B^* \qquad K_{xp1} = B^* \qquad K_{yp1} = 0.5\,B^* \qquad (3.26)$$

Since S_m is the sum of nodal coefficients as defined in Eqn. (3.14), the Eqn. (3.25) is simplified as:

$$K_{zm1}\,\theta_{x,y,Z-1}^{P+1} + K_{ym1}\theta_{x,Y-1,z}^{P+1} + K_{xp1}\,\theta_{X+1,y,z}^{P+1} + K_{yp1}\,\theta_{x,Y+1,z}^{P+1} - S_m\,\theta_{x,y,z}^{P+1}$$

$$= \theta_{x,y,z}^{P+1} - \theta_{x,y,z}^{P} \qquad (3.27)$$

It is necessary to consider in detail the non-dimensional coefficients A^* and B^*.

$$A^* = \frac{m\,\Delta t}{\rho_w R^3 \pi\, dz} = \frac{4\,m}{\pi D \mu} \frac{\mu}{\rho_w} \frac{1}{\alpha_w} \frac{\alpha_w \Delta t}{R^2} \frac{1}{2\,dz} \qquad (3.28)$$

It is obvious that Reynolds Number, Prandtl Number and Fourier Number based on fluid parameters are appeared at the right hand side of the Eqn. (3.28). Simply, the coefficient A^* is:

$$A^* = Re_D\,Pr\,Fo_w \frac{1}{2\,dz} \qquad (3.29)$$

Similarly, for coefficient B^*,

$$B^* = \frac{h_m R\,\Delta t}{\rho_w c_{pw} R^2} = \frac{h_m R}{k_w} \frac{k_w}{\rho_w c_{pw}} \frac{\Delta t}{R^2}$$

It is the product of Nusselt Number and Fourier Number based on fluid parameters.

$$B^* = Nu_R \, Fo_w \qquad (3.30)$$

3.4.2 THE GUIDE LINE FOR SYMMETRY

In Figures 3.1 and 3.4b there is a guide line for symmetry. Since the flow pattern is considered as cross flow such a line is defined. This line is actually not a symmetry line for temperature distribution. In other words, the slope of temperature at the cross-section plane defined by this line is not zero. As the name implies it is a guide line for symmetry.

The equation of this line can be written as:

$$z^* = \left(nz_1 + nz_2 - \frac{nz_2 + 1}{2\,l}\, x^*\right) dz$$

where

z^*: Non-dimensional coordinate value (shown in Fig. 3.4b)

nz_1: Number of nodes in z^* direction of Solid-1 (shown in Fig. 3.4b as the region with dimension lz_1)

nz_2: Number of nodes in z^* direction of Solid-2 (shown in Fig. 3.4b as the region with dimension lz_2)

x^*: Non-dimensional coordinate value in x^* direction (shown in Fig. 3.4b)

dz: Grid length in z^* direction (shown in Fig. 3.4b)

Considering three-dimensional structure, there is a relation between the nodes before and beyond the cross-sectional plane defined by this line. Coordinate index of any node and coordinate index of any corresponding symmetrical node is given in Table 3.1.

Table 3.1. General symmetry rule with respect to guide line

Coordinate Index Of Any Node	Coordinate Index Of Corresponding Node
x	nx + 1 – x
y	y
z	nztotal + 1 – z

In this table:

nx: The number of nodes in x direction (In Fig. 3.4b, this value is 13)

nztotal: The total number of nodes in z direction (In Fig. 3.4b, this value is 51)

It is necessary to point out the distinction between coordinate index and coordinate value. For example in Fig. 3.4b, for the non-dimensional temperature $\theta_{3,14,12}$ coordinate index value x is 3, y is 14 and z is 12. The coordinate values for this node in x^*, y^* and z^* directions are,

$x^* = (3-1)\,dx$

$y^* = (14-1)\,dy$

$z^* = (12-1)\,dz$

In Figures 3.4a and 3.4b, dx, dy and dz are taken to be unity.

According to Table 3.1 corresponding symmetrical non-dimensional temperature is $\theta_{11,14,40}$. In other words the coordinate index value x is 11, y is 14 and z is 40. Similar to Table 3.1 for coordinate values, Table 3.2 is given at the end of this section.

As another example, the finite difference equation for the non-dimensional temperature $\theta_{4,14,33}$ (a sample node in outer surface, Eqn.(3.15)) can be given as:

$$K_{ym1}\,\theta_{x,Y-1,z}^{P+1} + K_{xp1}\,\theta_{X+1,y,z}^{P+1} + K_{xm1}\,\theta_{X-1,y,z}^{P+1} + K_{zp1}\,\theta_{x,y,Z+1}^{P+1} + K_{zm1}\theta_{x,y,Z-1}^{P+1}$$
$$- S_m\,\theta_{x,y,z}^{P+1} = \theta_{x,y,z}^{P+1} - \theta_{x,y,z}^{P}$$

Considering Fig. 3.4b, $\theta_{X+1,y,z}^{P+1}$ and $\theta_{x,y,Z+1}^{P+1}$ are beyond the guide line for symmetry. So their corresponding symmetric nodes according to Table-3.1, should be taken into account. Consequently the equation should be:

$$K_{ym1}\,\theta_{x,Y-1,z}^{P+1} + K_{xp1}\,\theta_{nx-x,\,y,\,nztotal+1-z}^{P+1} + K_{xm1}\,\theta_{nx+1-x,y,\,nztotal-z}^{P+1}$$
$$+ K_{zp1}\,\theta_{x,y,Z+1}^{P+1} + K_{zm1}\theta_{x,y,Z-1}^{P+1} - S_m\,\theta_{x,y,z}^{P+1} = \theta_{x,y,z}^{P+1} - \theta_{x,y,z}^{P} \qquad (3.31)$$

Same consideration should be applied to other nodes neighboring to the guide line for symmetry.

Table 3.2. General symmetry rule with respect to guide line for coordinates

Coordinate Of Any Node	Coordinate Of Corresponding Node
x^*	$1 - x^*$
y^*	y^*
z^*	$2\,lz_1 + lz_2 - z^*$

3.4.3 NUMERICAL SOLUTION APPROACH TO THE FINITE DIFFERENCE EQUATIONS

Basically, there are maximum six faces for heat transfer either in the form of conduction or convection modes, for the nodes in –y, +x, +y, -x, +z, -z directions. For the first node in the pipe fluid with non-dimensional temperature θ_i enters to the control volume. It can be shown that using the derivation procedure explained in section 3.4.1.2 another nodal coefficient of K_i is equal to A^* and the finite difference equation takes the following form:

$$K_i(\theta_i - \theta_{x,y,z}^{P+1}) + K_{yml}(\theta_{x,Y-1,z}^{P+1} - \theta_{x,y,z}^{P+1}) + K_{xpl}(\theta_{X+1,y,z}^{P+1} - \theta_{x,y,z}^{P+1}) + K_{ypl}(\theta_{x,Y+1,z}^{P+1} - \theta_{x,y,z}^{P+1}) + K_{xml}(\theta_{X-1,y,z}^{P+1} - \theta_{x,y,z}^{P+1}) + K_{zpl}(\theta_{x,y,Z+1}^{P+1} - \theta_{x,y,z}^{P+1}) + K_{zml}(\theta_{x,y,Z-1}^{P+1} - \theta_{x,y,z}^{P+1}) = \theta_{x,y,z}^{P+1} - \theta_{x,y,z}^{P} \quad (3.32)$$

Sum of the coefficients, S_m, can be defined as:

$$S_m = K_i + K_{yml} + K_{xpl} + K_{ypl} + K_{xml} + K_{zpl} + K_{zml} \quad (3.33)$$

So, Eqn. (3.32) can be simplified as:

$$K_i\theta_i + K_{yml}\theta_{x,Y-1,z}^{P+1} + K_{xpl}\theta_{X+1,y,z}^{P+1} + K_{xml}\theta_{X-1,y,z}^{P+1} + K_{ypl}\theta_{x,Y+1,z}^{P+1} + K_{zpl}\theta_{x,y,Z+1}^{P+1} + K_{zml}\theta_{x,y,Z-1}^{P+1} - S_m\theta_{x,y,z}^{P+1} = \theta_{x,y,z}^{P+1} - \theta_{x,y,z}^{P} \quad (3.34)$$

$\theta_{x,y,z}^{P}$ is known from the initial condition and the other non-dimensional temperature values are unknowns to be determined.

For Eqn. (3.34) implicit solution must be performed. In Figures 3.4a and 3.4b there are 8918 unknown nodes. Approximately, half of this value are before the guideline for symmetry.

For numerical solution technique, Gauss-Seidel Iteration Method [7] is used to determine the unknown nodal values at $t + \Delta t$. For each timestep, iterative procedure is performed according to the following equation

$$\theta_{x,y,z}^{P+1} = \frac{1}{1 + S_m}(K_i\theta_i + K_{yml}\theta_{x,Y-1,z}^{P+1} + K_{xpl}\theta_{X+1,y,z}^{P+1} + K_{xml}\theta_{X-1,y,z}^{P+1} + K_{ypl}\theta_{x,Y+1,z}^{P+1} + K_{zpl}\theta_{x,y,Z+1}^{P+1} + K_{zml}\theta_{x,y,Z-1}^{P+1} + \theta_{x,y,z}^{P}) \quad (3.35)$$

$\theta_{x,y,z}^{P}$ is constant throughout the iteration procedure for each timestep.

In Appendix C the list of computer program in Visual Basic 6.0 for solution of finite difference equations is given. For more simplification of the program, following temperature values are defined:

$$T_{yml} = K_{yml}\,\theta_{x,Y-1,z}^{P+1} \qquad T_{xpl} = K_{xpl}\,\theta_{X+1,y,z}^{P+1} \qquad T_{ypl} = K_{ypl}\,\theta_{x,Y+1,z}^{P+1}$$

$$T_{xml} = K_{xml}\,\theta_{X-1,y,z}^{P+1} \qquad T_{zpl} = K_{zpl}\,\theta_{x,y,Z+1}^{P+1} \qquad T_{zml} = K_{zml}\,\theta_{x,y,Z-1}^{P+1}$$

$$T_n = \theta_{x,y,z}^{P} \qquad T_{ii} = K_i\,\theta_i \qquad (3.36)$$

So, the Eqn. (3.34) is simplified as:

$$\theta_{x,y,z}^{P+1} = \frac{1}{1+S_m}\left(T_{ii} + T_{yml} + T_{xpl} + T_{xml} + T_{ypl} + T_{zpl} + T_{zml} + T_n\right) \qquad (3.37)$$

3.4.4 RESULTS OF THE TEMPERATURE CALCULATIONS

Results of the temperature calculations are plotted in the figures (Fig. 3.7 –3.24). These calculations are performed for both Objective-1 and Objective-2. For the cross-sectional view on x^* - y^* planes, z^* coordinate index values of 12 (first plane of pipe in z^* direction) and of 26 (middle plane of pipe in z^* direction) are selected. For cross-sectional view on x^* - z^* planes, y^* coordinate index are selected as 9 (from pipe centerline) and 14 (from outer surface). The timesteps 5 (t^*=7.5) and 20 (t^*=30) are selected. Steady state value is assumed to be reached at timestep of 81 (t^* = 123.5) for Ojective-1 and 86 (t^* = 129) for Objective-2. All of these temperature distributions are evaluated for non-dimensional supply fluid temperature (θ_i) of 5.41 which corresponds to 80°C according to Eqn. (3.4b), for atmospheric temperature (T_∞) of -12°C and ground temperature (T_b) of +5°C. Reynolds Number for the fluid flowing in the pipe is selected as 10 to observe considerable temperature difference between pipe inlet and exit. Other reference values are given in Appendix-A.

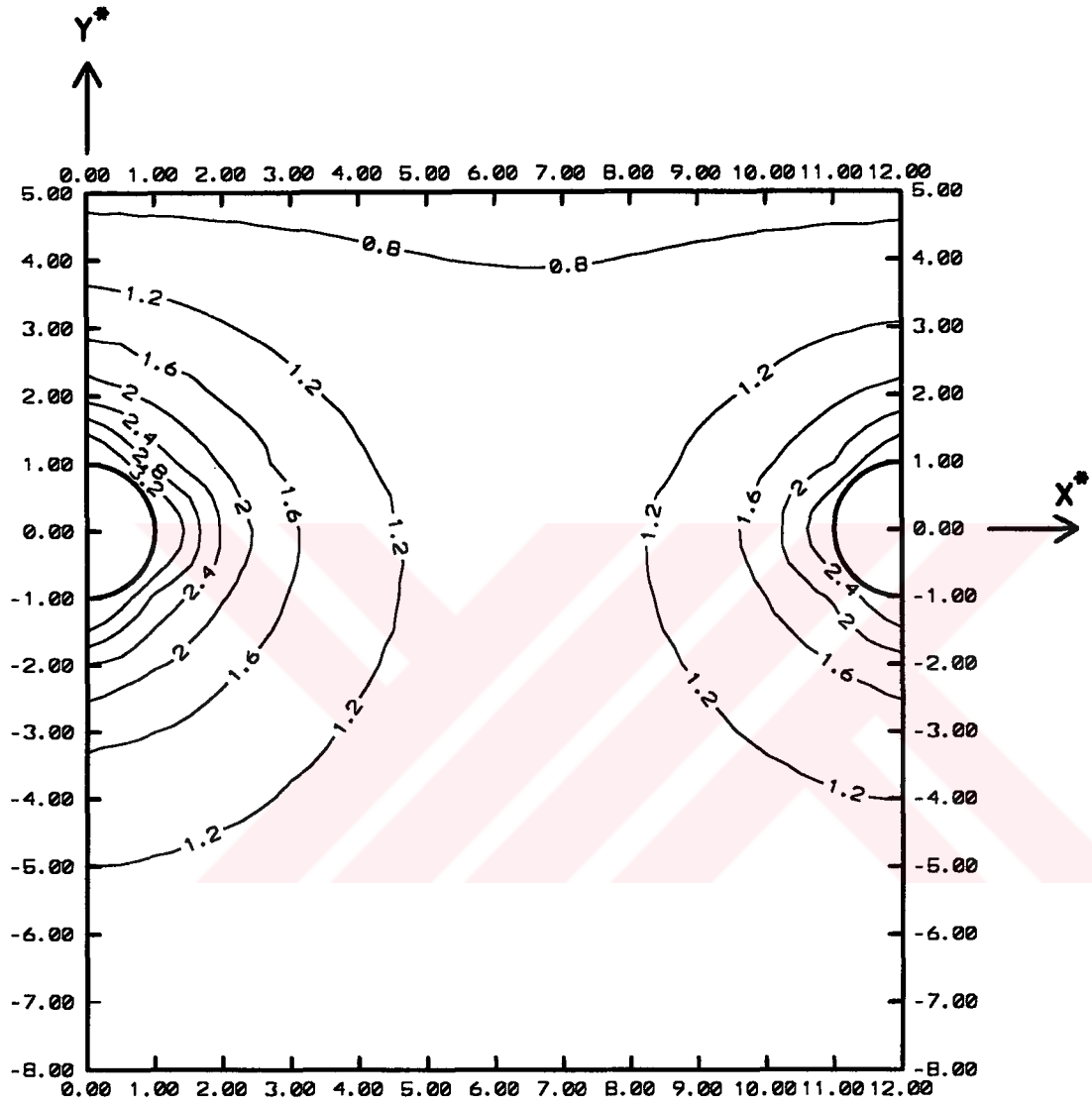

Figure 3.7. Non-dimensional temperature distribution for Objective-1 (Constant Surface Temperature) Timestep = 5, z = 12 ($z^* = 11$), $\theta_i = 5.41$ and $\theta_{mo} = 3.728864$

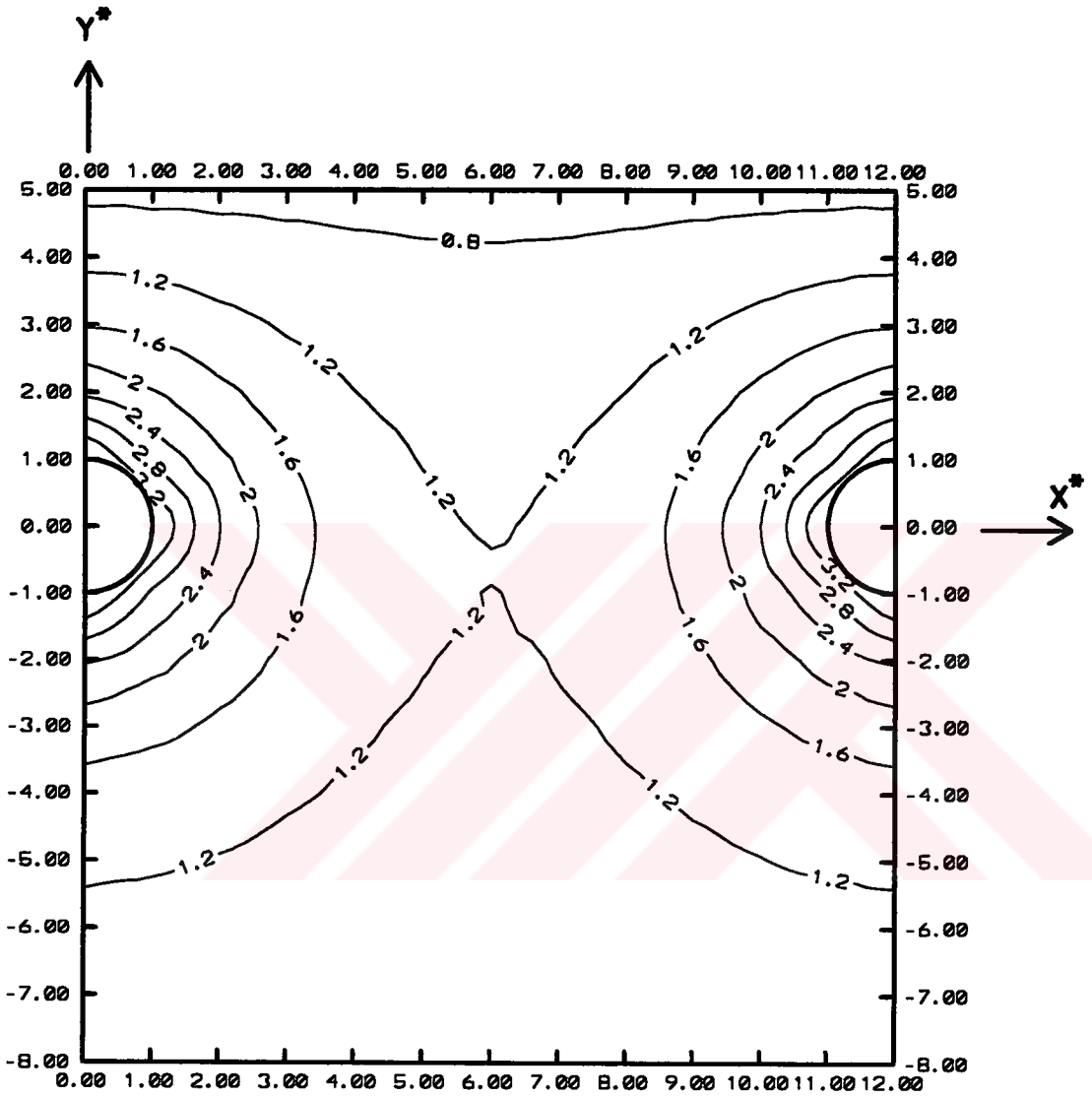

Figure 3.8. Non-dimensional temperature distribution for Objective-1 (Constant Surface Temperature) Timestep = 5, z = 26 ($z^* = 25$), $\theta_i = 5.41$ and $\theta_{mo} = 3.728864$

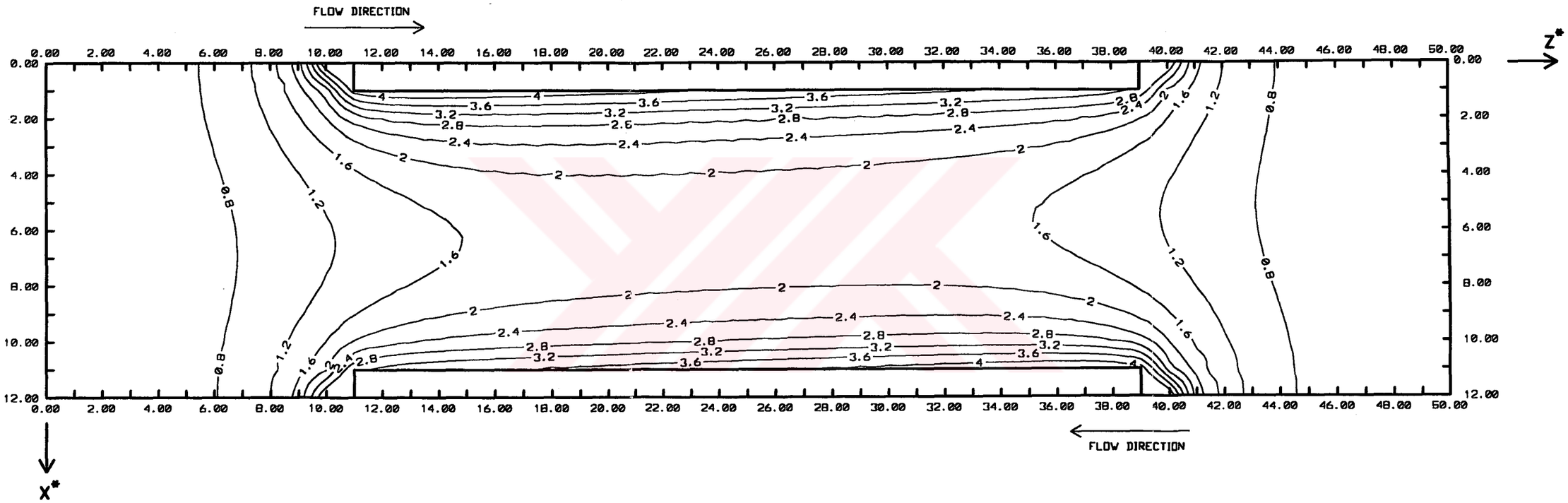

Figure 3.9. Non-dimensional temperature distribution for Objective-1 (Constant Surface Temperature) Timestep = 5, section from pipe center ($y^* = 0$), $\theta_i = 5.41$ and $\theta_{mo} = 3.728864$

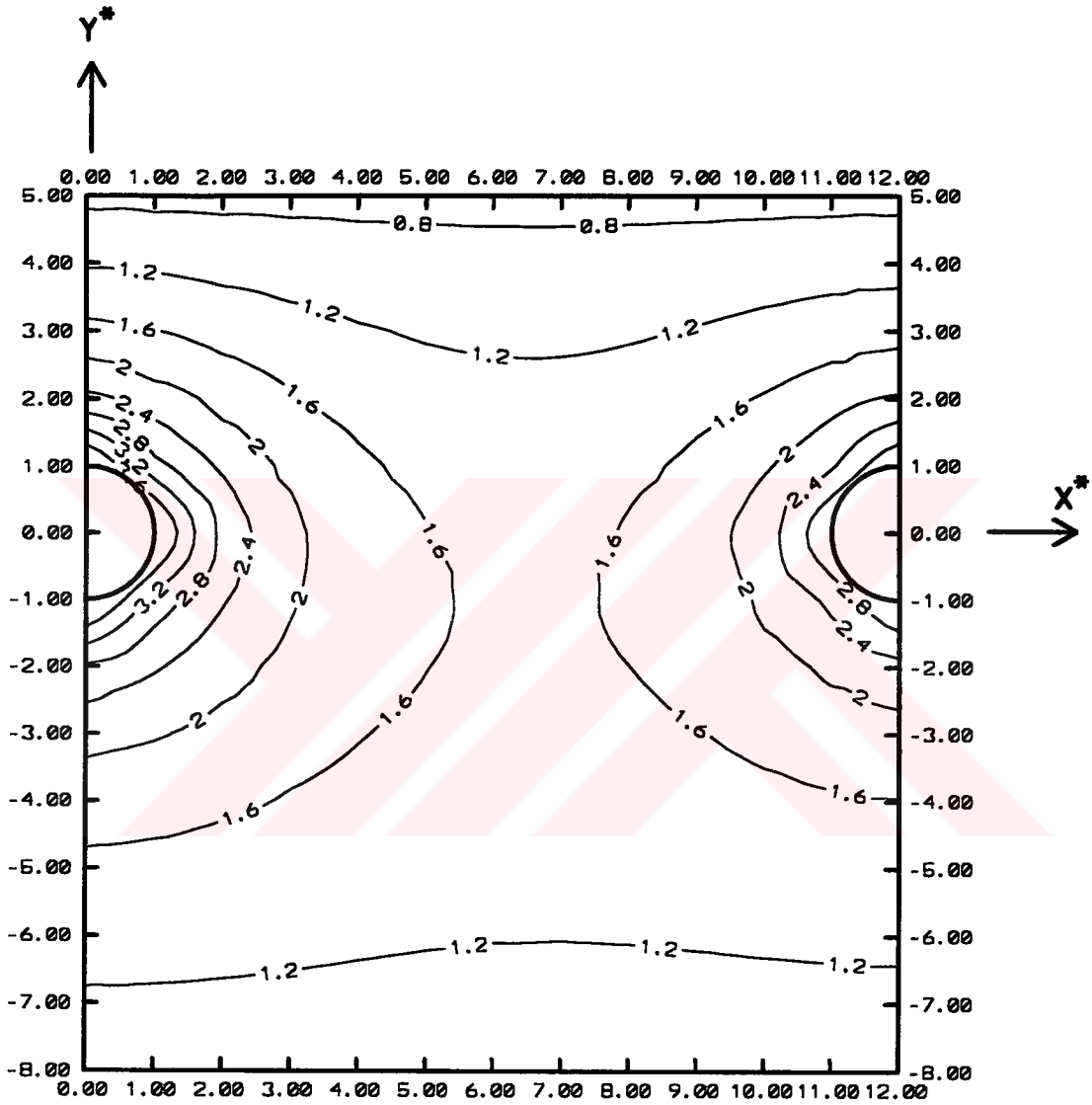

Figure 3.10. Non-dimensional temperature distribution for Objective-1 (Constant Surface Temperature) Timestep = 20, z = 12 ($z^* = 11$), $\theta_i = 5.41$ and $\theta_{mo} = 3.993906$

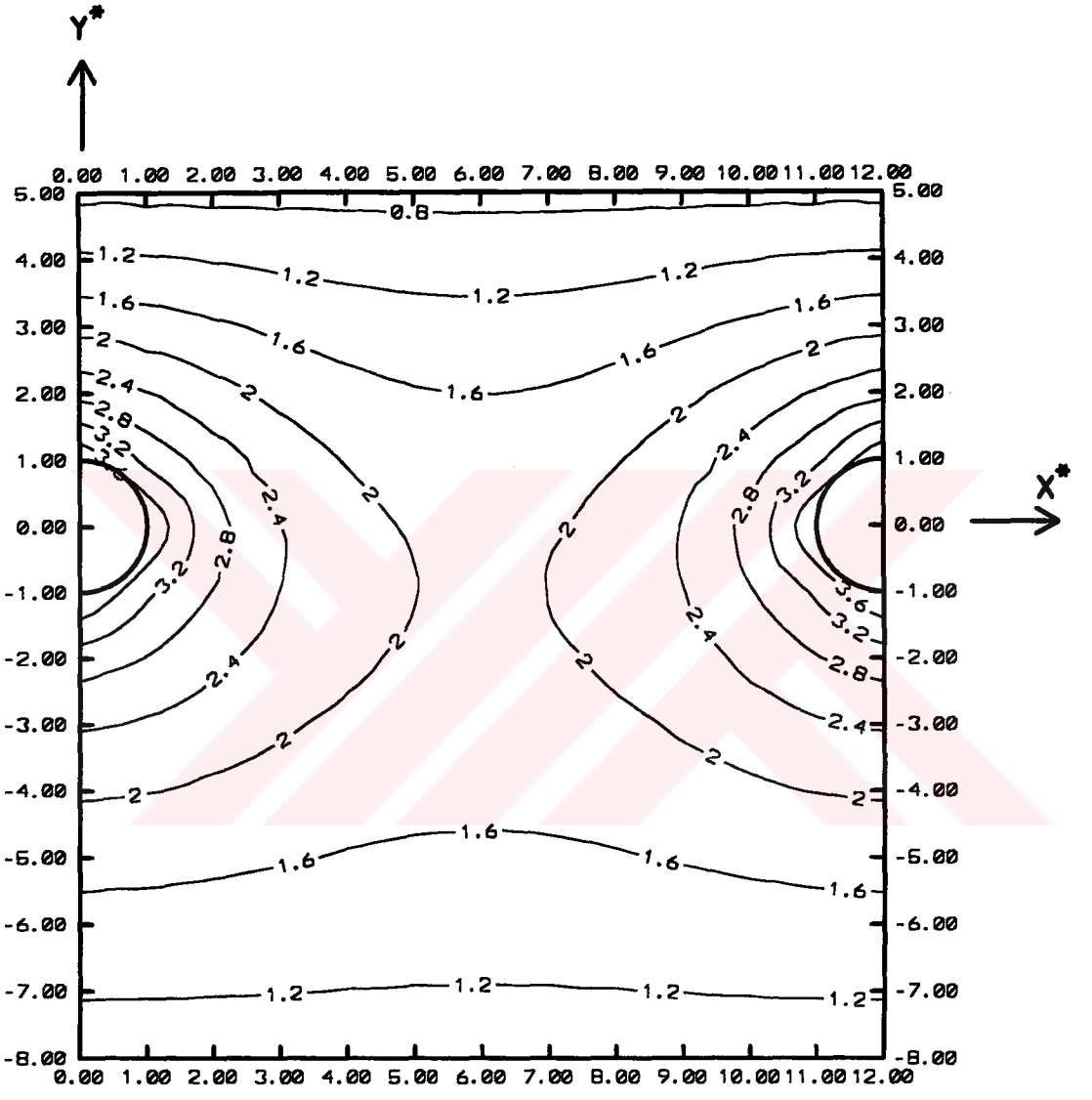

Figure 3.11. Non-dimensional temperature distribution for Objective-1 (Constant Surface Temperature) Timestep = 20, z = 26 (z^* = 25), θ_i = 5.41 and θ_{mo} = 3.993906

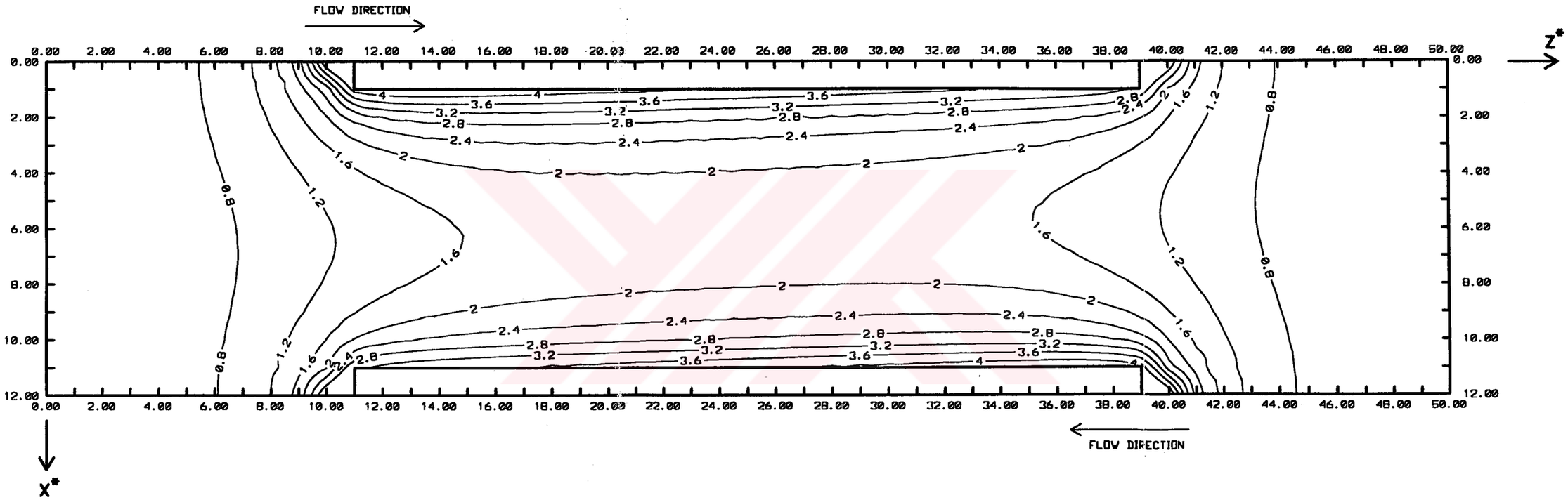

Figure 3.12. Non-dimensional temperature distribution for Objective-1 (Constant Surface Temp.) Timestep = 20, section from pipe center ($y^* = 0$), $\theta_i = 5.41$ and $\theta_{mo} = 3.993906$

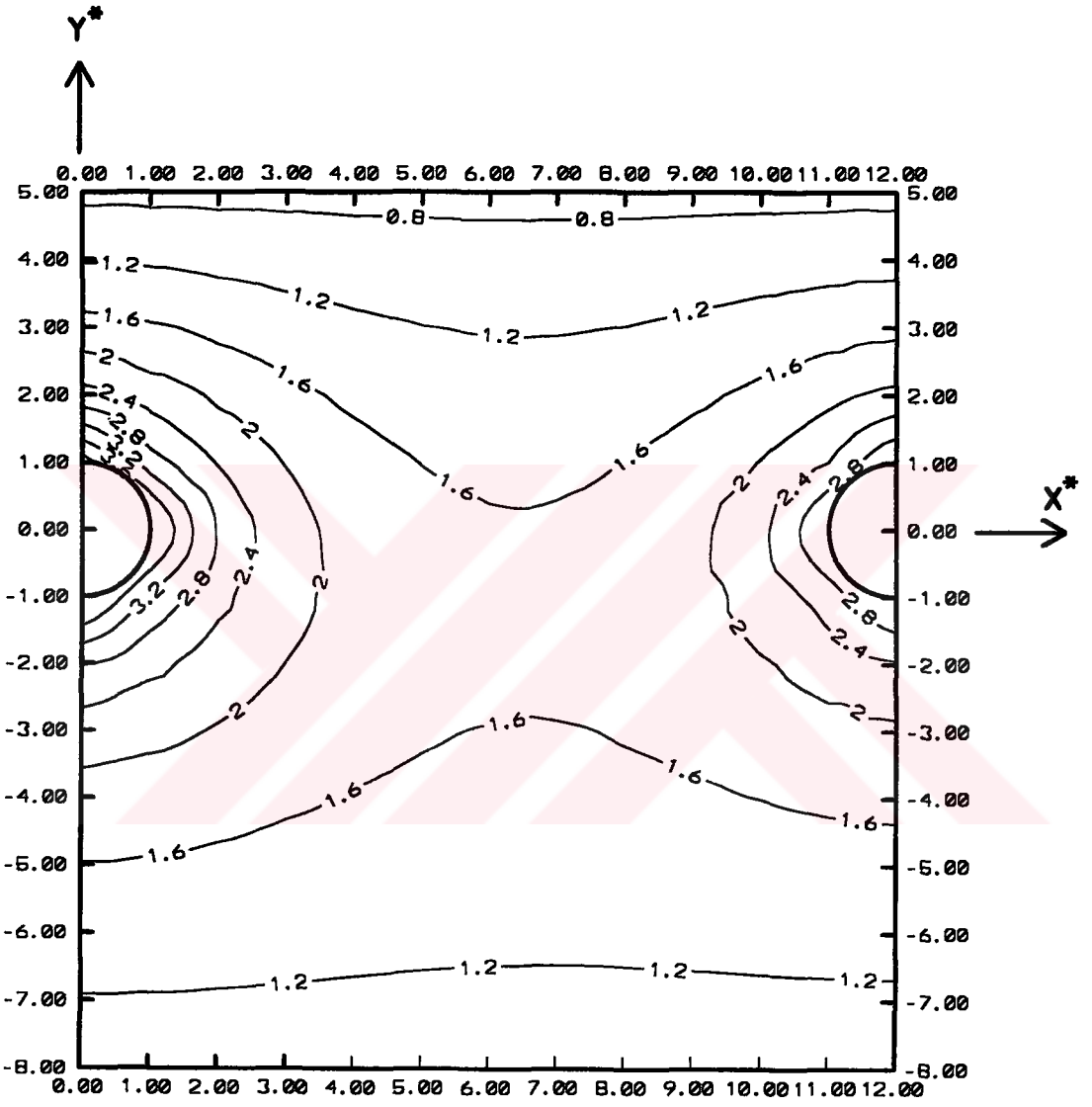

Figure 3.13. Non-dimensional temperature distribution for Objective-1 (Constant Surface Temperature) Timestep = 81 (Steady State), z = 12 (z^* =11), θ_i = 5.41 and θ_{mo} = 4.033008

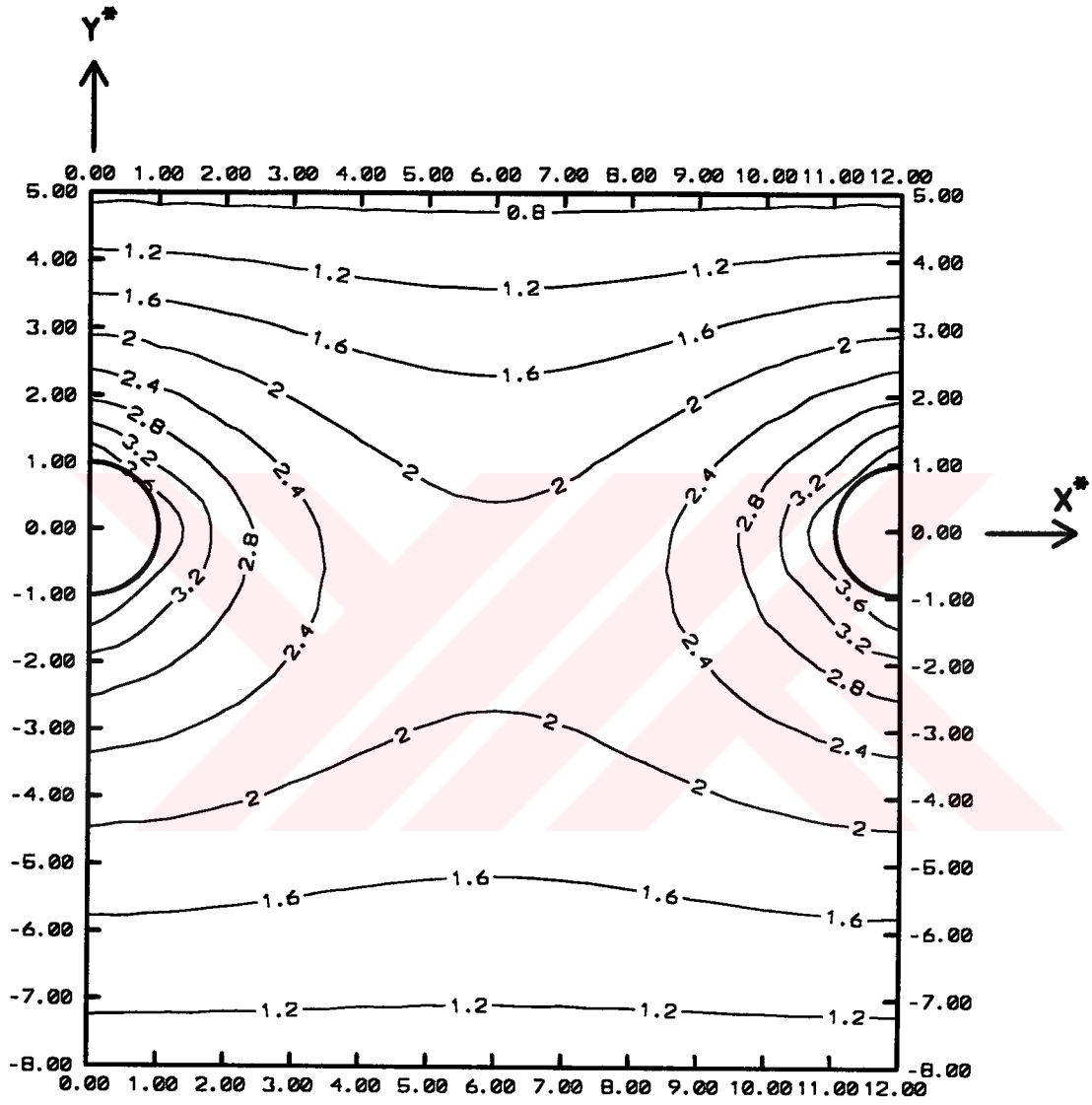

Figure 3.14. Non-dimensional temperature distribution for Objective-1 (Constant Surface Temperature) Timestep = 81 (Steady State), z = 26 ($z^* = 25$), $\theta_i = 5.41$ and $\theta_{mo} = 4.033008$

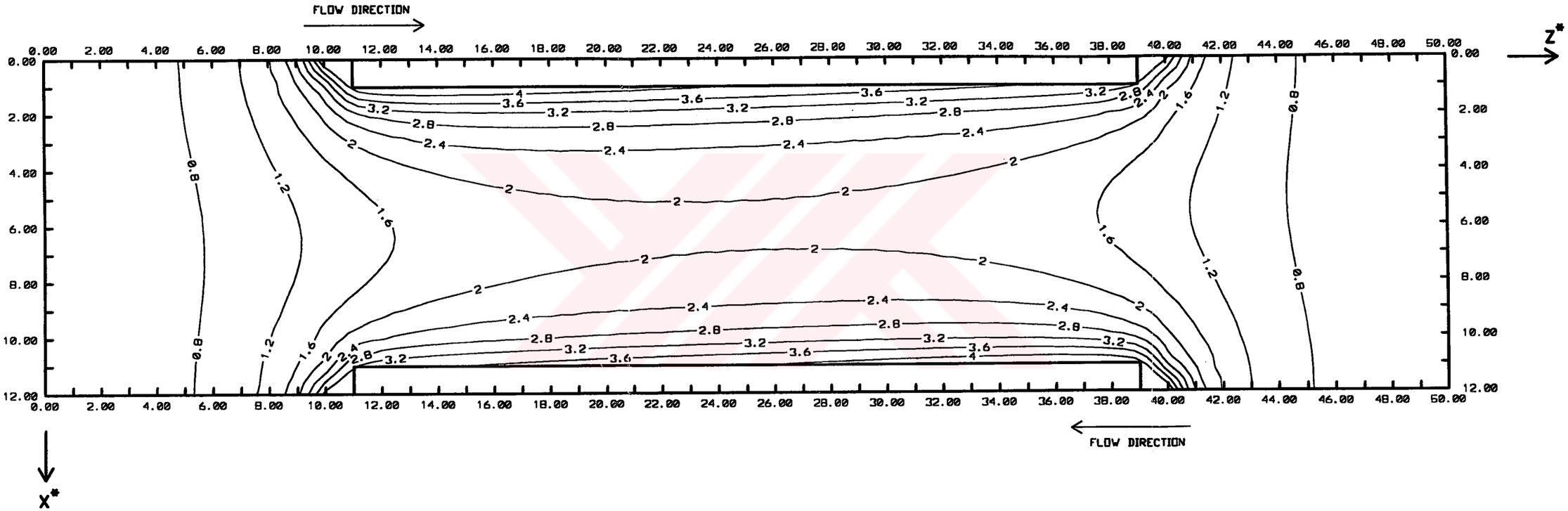

Figure 3.15. Non-dimensional temperature distribution for Objective-1 (Constant Surface Temp.) Timestep = 81 (Steady State), Section from pipe center ($y^* = 0$), $\theta_i = 5.41$ and $\theta_{mo} = 4.033008$

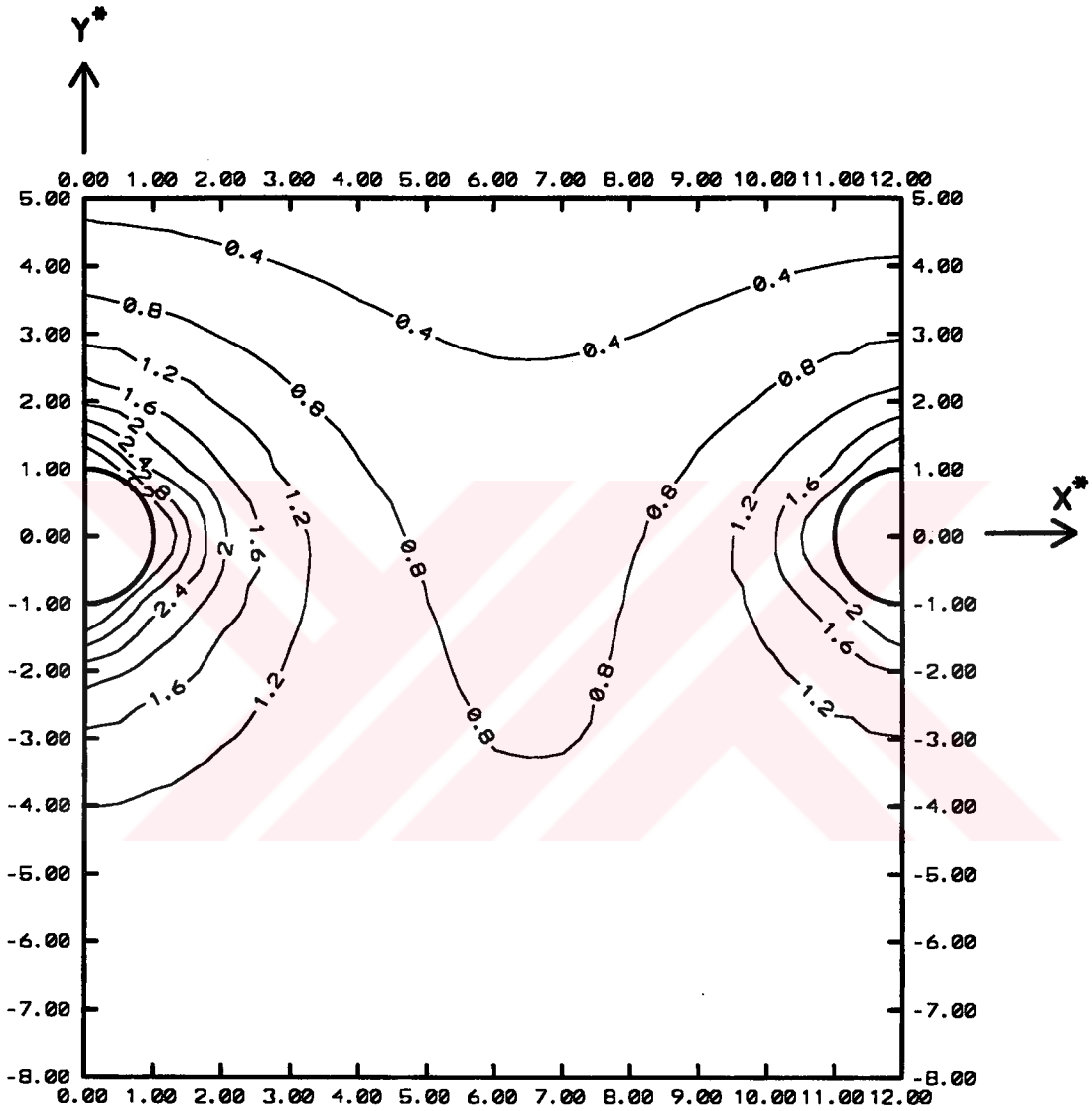

Figure 3.16. Non-dimensional temperature distribution for Objective-2 (Convective Boundary Condition) Timestep = 5, z = 12 ($z^* = 11$), $\theta_i = 5.41$ and $\theta_{mo} = 3.583439$

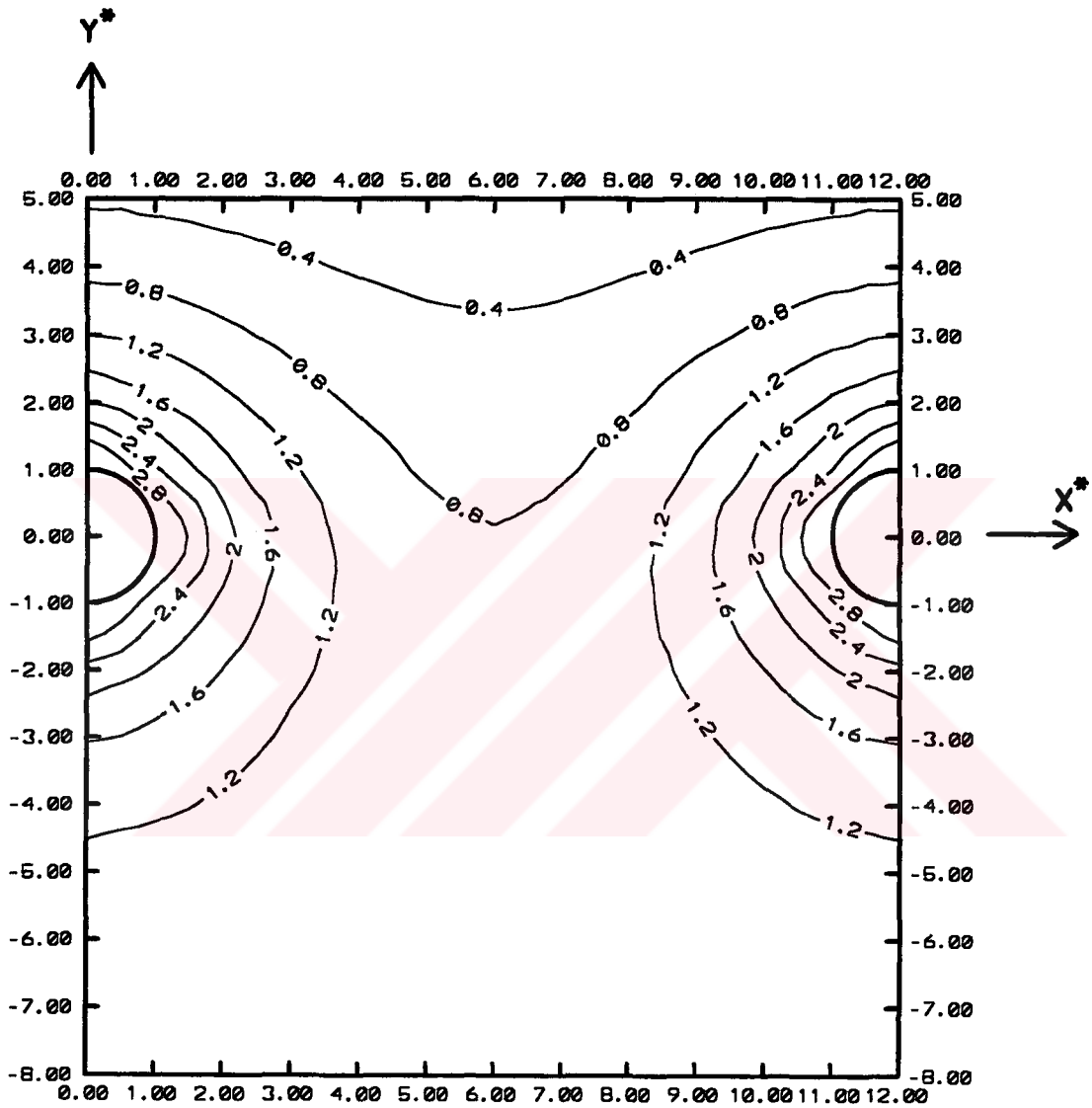

Figure 3.17. Non-dimensional temperature distribution for Objective-2 (Convective Boundary Condition) Timestep = 5, z = 26 (z^* = 25), θ_i = 5.41 and θ_{mo} = 3.583439

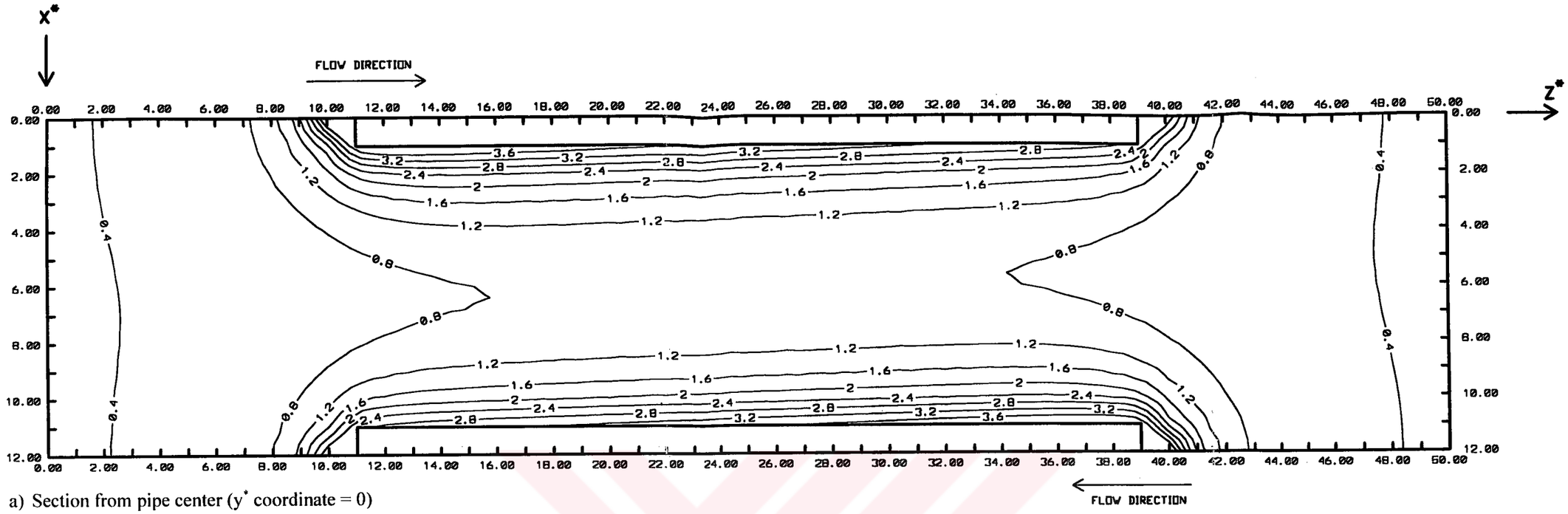

a) Section from pipe center (y^* coordinate = 0)

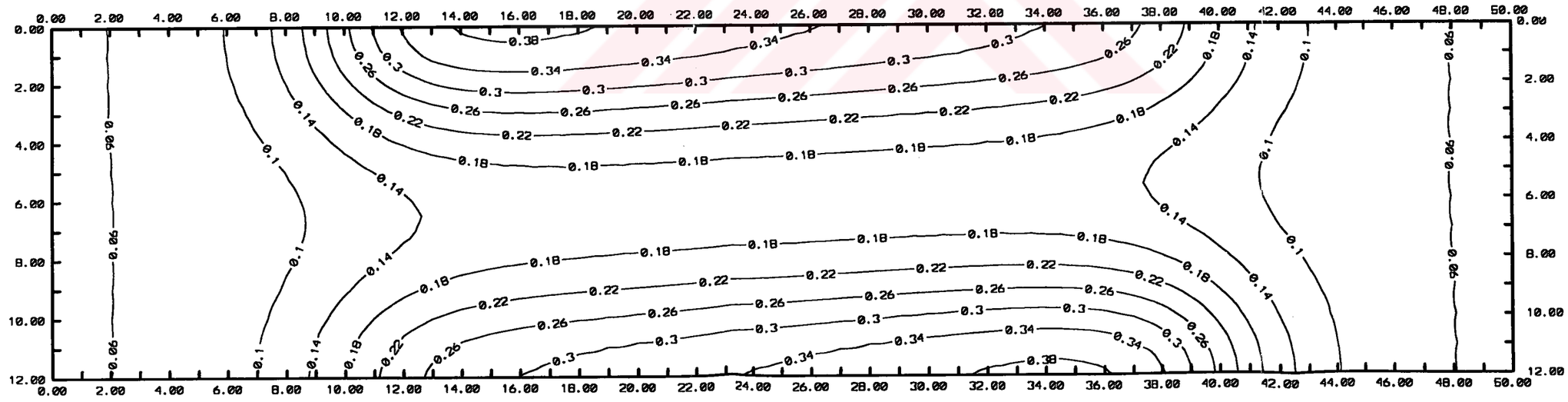

b) Outer Surface

Figure 3.18. Non-dimensional temperature distribution for Objective-2 (Convective Boundary Condition) Timestep = 5, θ_i = 5.41 and θ_{mo} = 3.583439

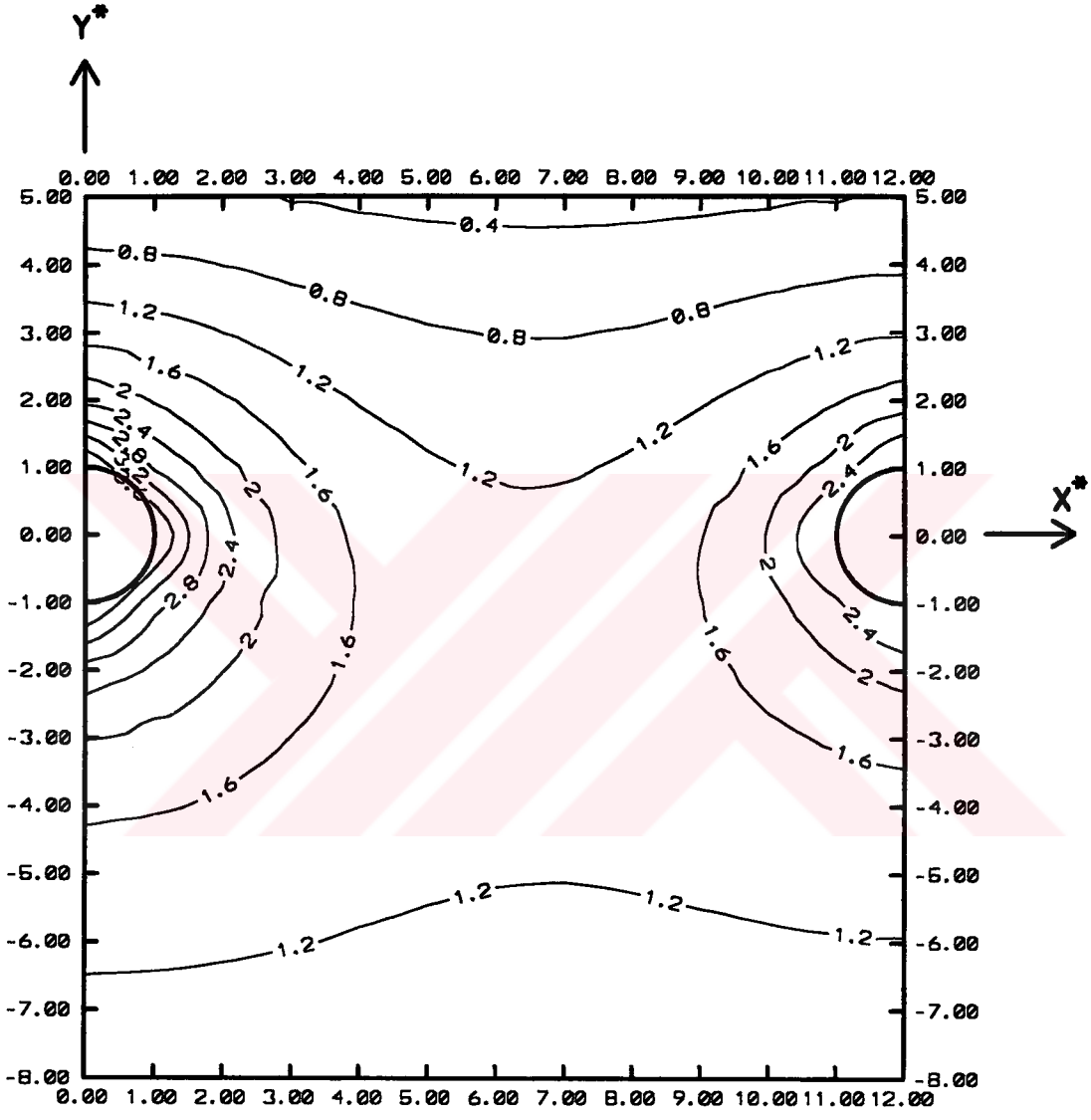

Figure 3.19. Non-dimensional temperature distribution for Objective-2 (Convective Boundary Condition) Timestep = 20, z = 12 (z^* = 11), θ_i = 5.41 and θ_{mo} = 3.924572

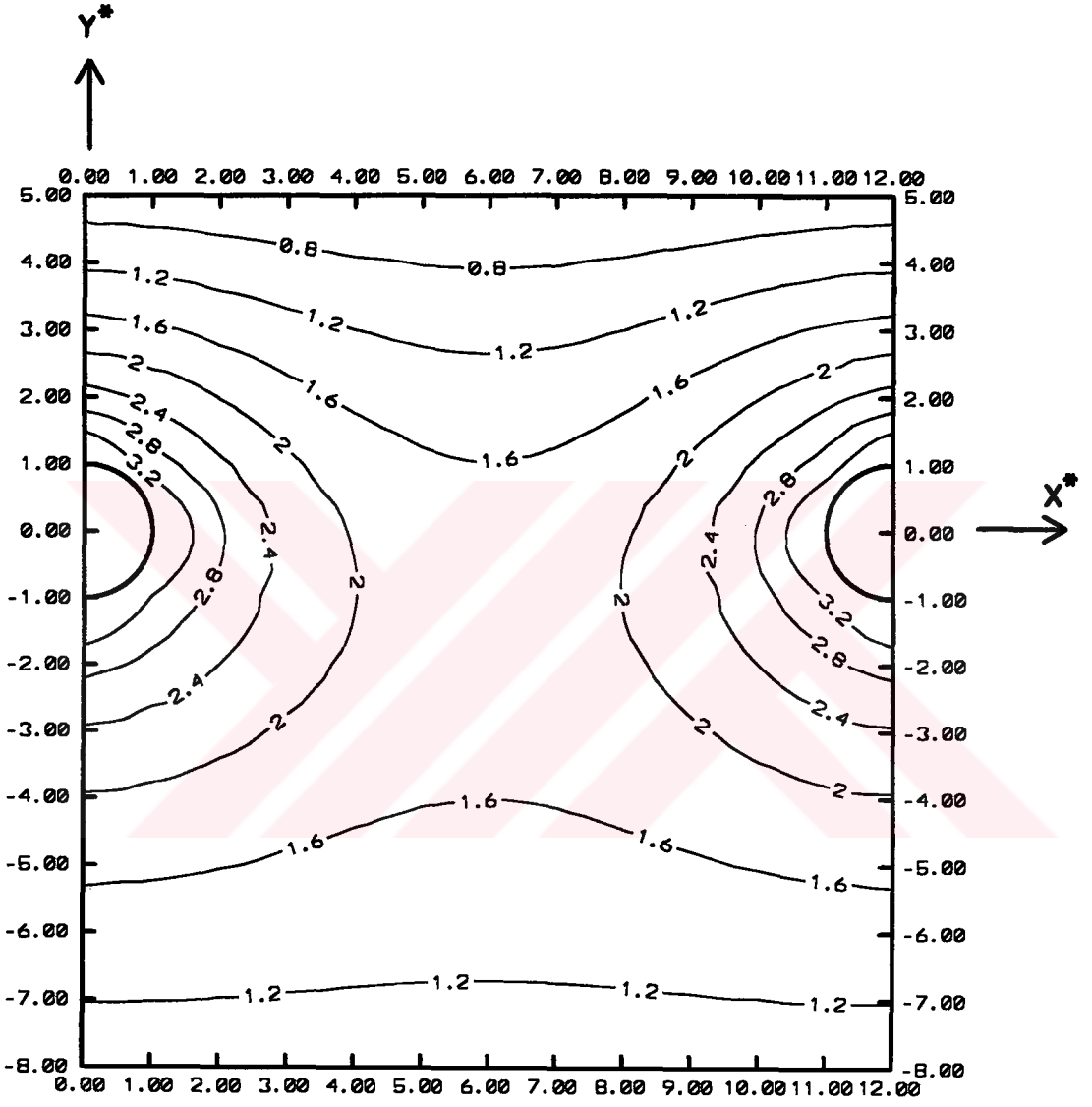

Figure 3.20. Non-dimensional temperature distribution for Objective-2 (Convective Boundary Condition) Timestep = 20, z = 26 ($z^* = 25$), $\theta_i = 5.41$ and $\theta_{mo} = 3.924572$

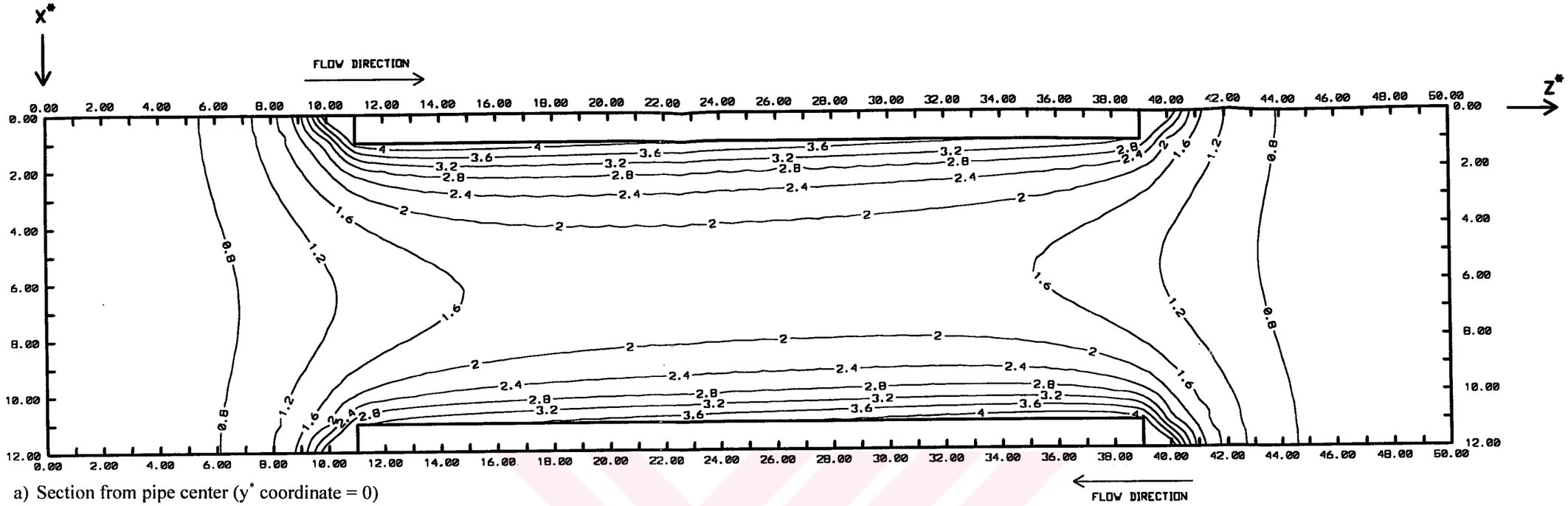

a) Section from pipe center (y^* coordinate = 0)

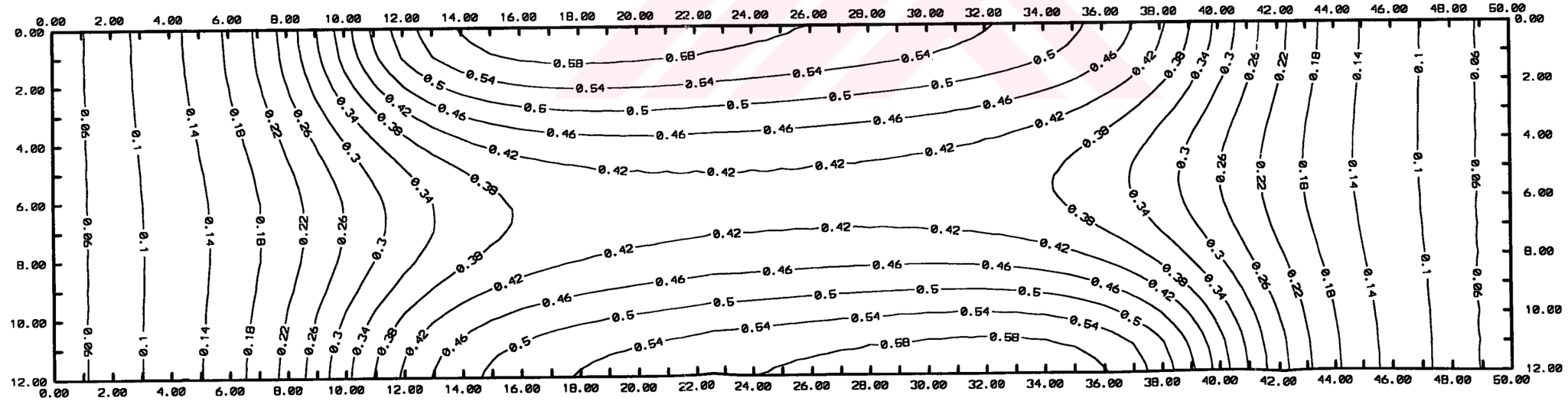

b) Outer Surface

Figure 3.21. Non-dimensional temperature distribution for Objective-2 (Convective Boundary Condition) Timestep = 20, θ_i = 5.41 and θ_{mo} = 3.924572

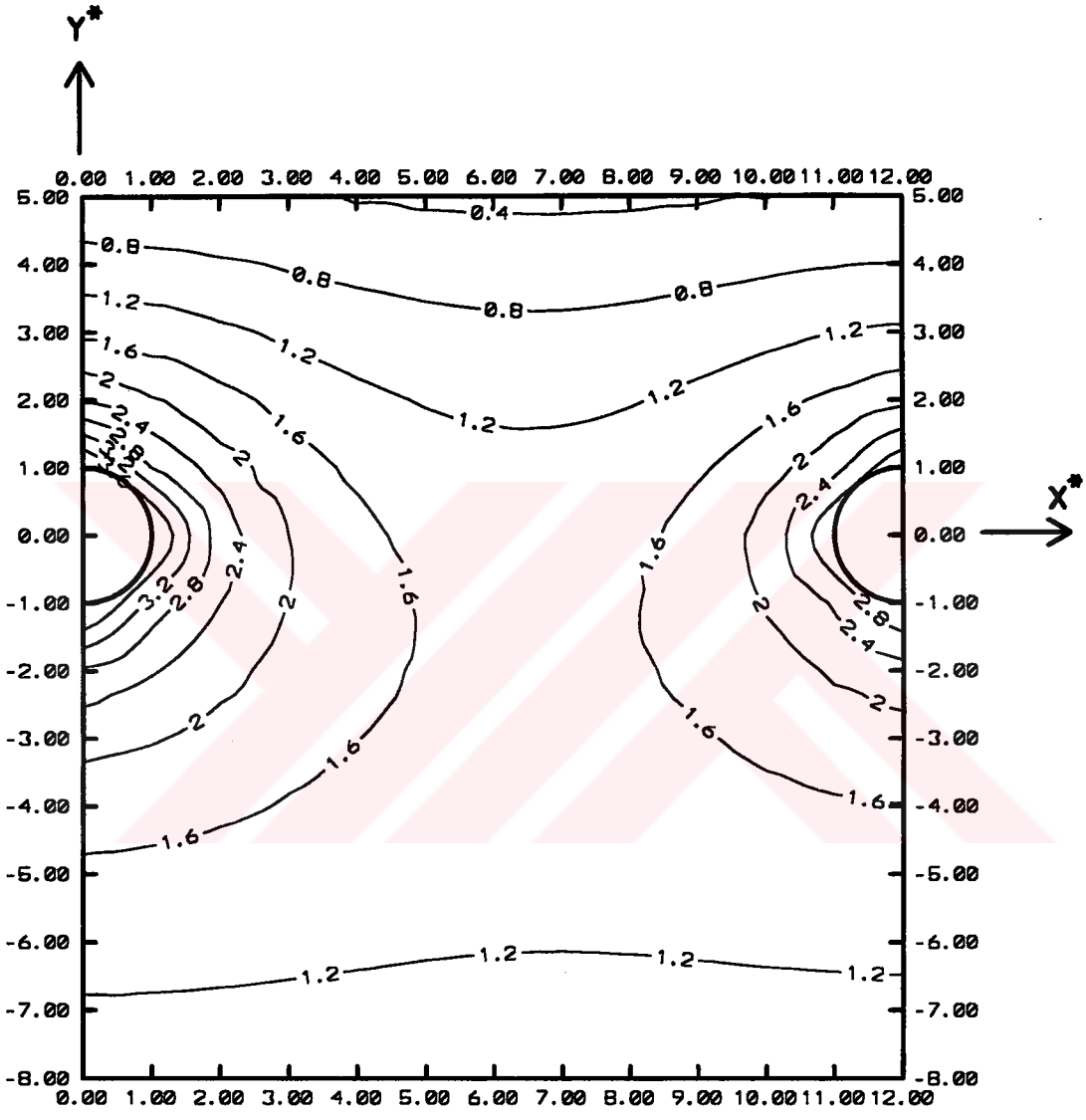

Figure 3.22. Non-dimensional temperature distribution for Objective-2 (Convective Boundary Condition) Timestep = 86 (Steady State), z = 12 ($z^* = 11$), $\theta_i = 5.41$ and $\theta_{mo} = 3.987736$

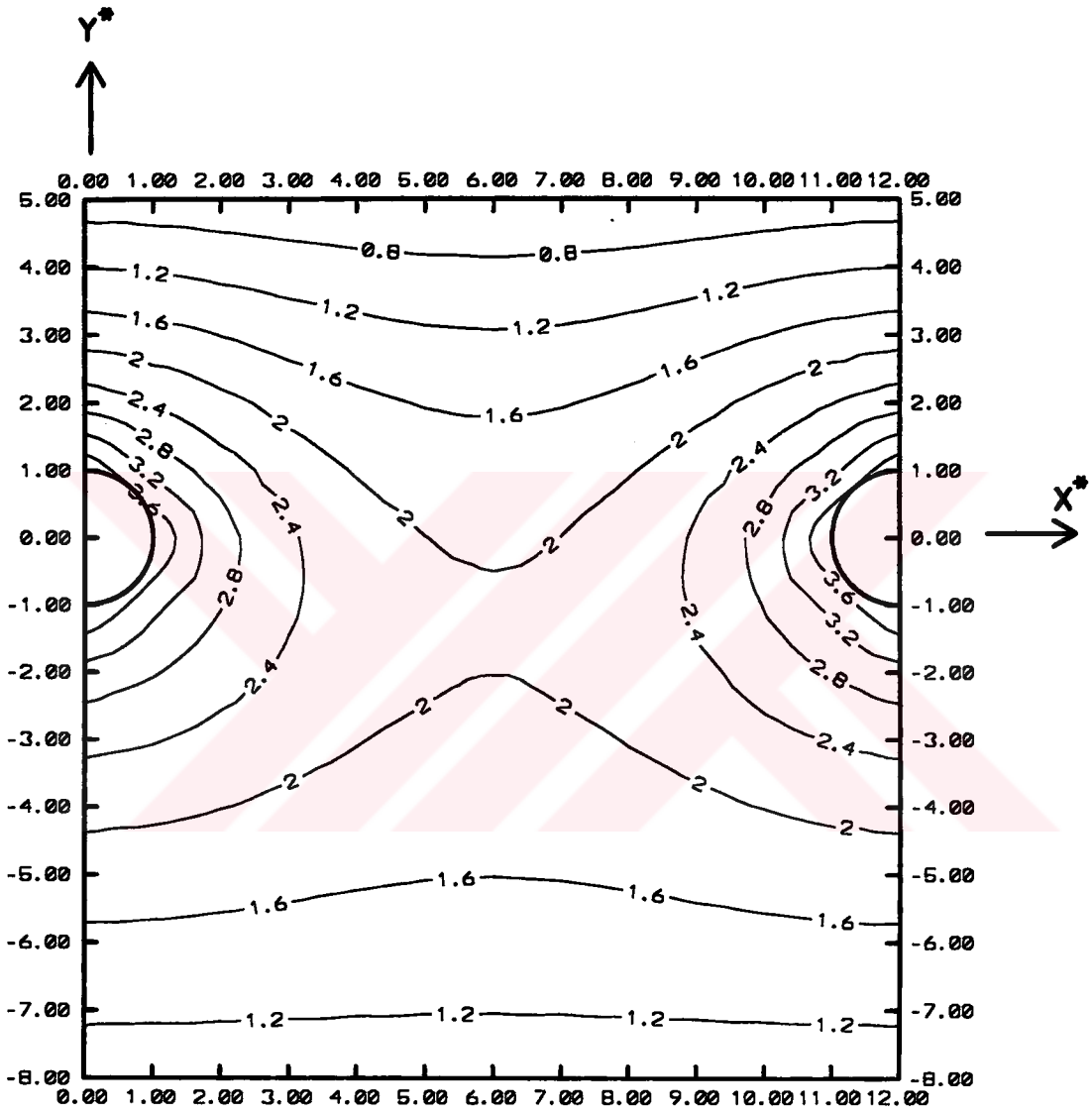

Figure 3.23. Non-dimensional temperature distribution for Objective-2 (Convective Boundary Condition) Timestep = 86 (Steady State), z = 26 ($z^* = 25$), $\theta_i = 5.41$ and $\theta_{mo} = 3.987736$

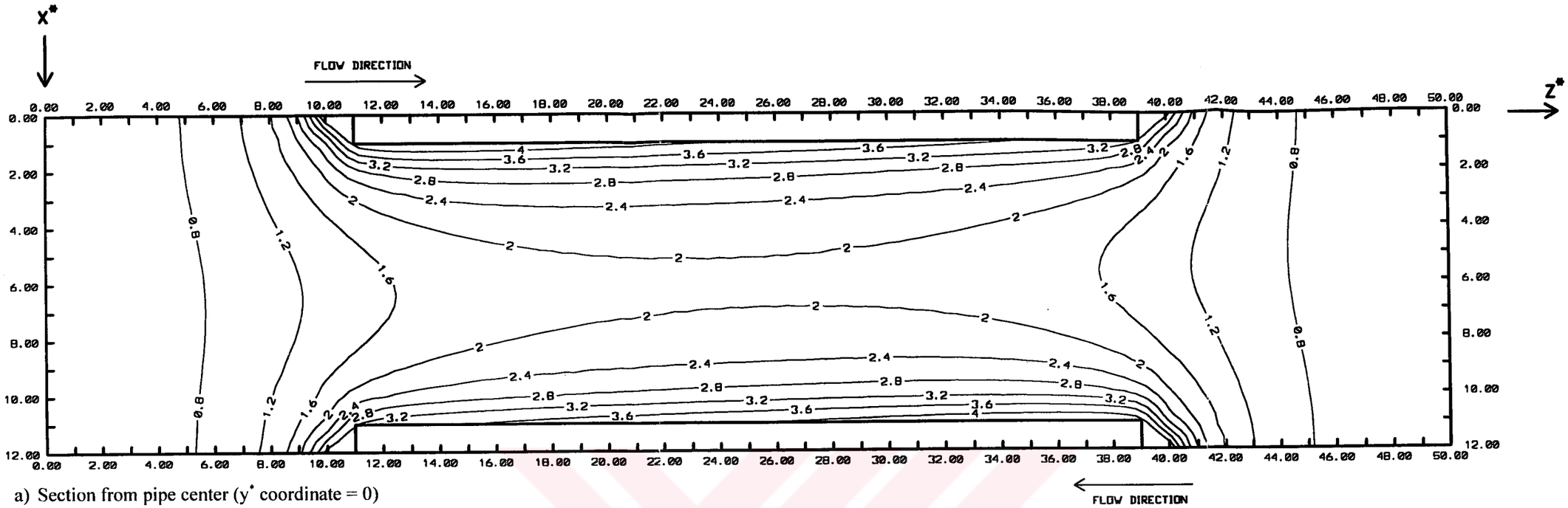

a) Section from pipe center (y^* coordinate = 0)

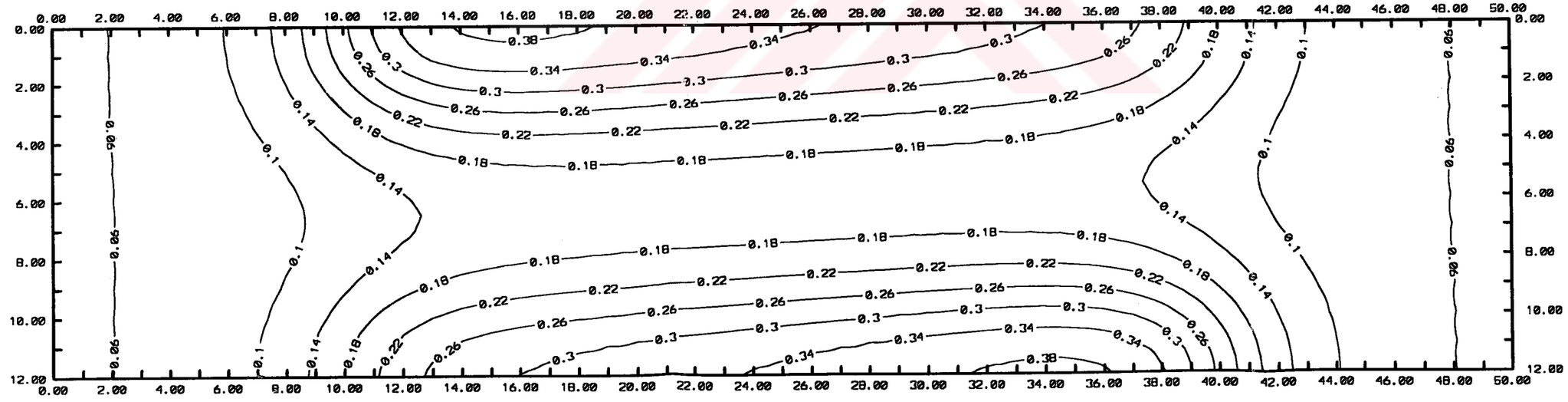

b) Outer Surface

Figure 3.24. Non-dimensional temp. distribution for Objective-2 (Convective B. Condition) Timestep = 86 (Steady State), $\theta_i = 5.41$ and $\theta_{mo} = 3.987736$

CHAPTER 4

HEAT TRANSFER EVALUATION

In the previous chapter, three-dimensional transient temperature distributions were evaluated. These results depends upon many parameters such as supply fluid temperature (θ_i), Biot Number for atmosphere (Bi_∞) and pipe spacing. Before going into details of temperature variations, it is important to calculate heat transfer values through the boundaries and to investigate their variations. Using the temperature distribution, it is possible to obtain heat transfer values for various geometry's similar to Figures 3.4a and 3.4b.

4.1 DETERMINATION OF HEAT TRANSFER COMPONENTS

As it is stated before, the source of heat transfer is the fluid supplied to the pipe at a certain non-dimensional temperature θ_i. Fluid leaves the pipe at θ_{mo} that is less than θ_i. Obviously, this difference is a result of heat transfer from the pipe to the surrounding solid. Some portion of this heat is transferred to the atmosphere through the outer surface or y = ny. Important portion of heat is transferred through the base plane or y =1 to the ground which has non-dimensional temperature θ_b. From Eqn. 3.4b, θ_b is equal to 1. Some heat is transferred to the ground through the side planes at z = 1 and z = nztotal (nztotal is 51 according to Fig. 3.4b).

4.1.1 HEAT TRANSFER TO ATMOSPHERE

For an arbitrary node on the outer surface the rate of heat transfer, Q_{UP}, can be written as:

$$Q_{UP} = - k F \frac{\partial T}{\partial y} \qquad (4.1)$$

where

F: Area of heat transfer between the node and the atmosphere.

From Equation 3.4b, dimensional temperature can be written as:

$$T = T_\infty + (T_b - T_\infty)\,\theta \qquad (4.2)$$

Partial differentiation of both sides of Eqn. (4.2) with respect to y, yields:

$$\frac{\partial T}{\partial y} = \frac{(T_b - T_\infty)}{R} \frac{\partial \theta}{\partial y^*} \qquad (4.3)$$

At this point, heat transfer area, F, can be written in terms of its non-dimensional value, F^*. So,

$$F = F^* R^2 \qquad (4.4)$$

Substitution of Equations (4.4) and (4.3) into Eqn. (4.1) results in the following equation:

$$.Q_{UP} = - k R (T_b - T_\infty) F^* \frac{\partial \theta}{\partial y^*} \qquad (4.5)$$

Division of both sides by "k R (T_b - T_∞)" results in following non-dimensional equation:

$$\frac{Q_{UP}}{k\,R\,(T_b - T_\infty)} = -F^* \frac{\partial\theta}{\partial y^*} \qquad (4.6)$$

The value of F^* is "dx dz" for any interior node at the outer surface. For the nodes at the edges except corners this value is "0.5 dx dz" and for corner nodes this is "0.25 dx dz". In addition to Equations (3.4a) and (3.4b), from the left side of Eqn. (4.6) a new non-dimensionalization equation is obtained.

$$Q_{UP}^* = \frac{Q_{UP}}{k\,R\,(T_b - T_\infty)} = -F^* \frac{\partial\theta}{\partial y^*} \qquad (4.7)$$

In Eqn. (4.7), Q_{UP}^* is non-dimensional heat transfer rate for any node at upper surface (y = 14, according to Fig. 3.4). At the right side of Eqn. (4.6) the term $\partial\theta/\partial y^*$ is actually time dependent. So, Q_{UP}^* is also time-dependent. Total non-dimensional heat transfer rate, Q_{UPSUM}^*, is the sum of all Q_{UP}^* values at the upper surface.

$$Q_{UPSUM}^* = \sum_{z=1}^{nztotal} \sum_{x=1}^{nx} -F^* \frac{\partial\theta}{\partial y^*} \qquad (4.8)$$

The term $\partial\theta/\partial y^*$ should be evaluated numerically for each node at the surface at any timestep. Since it is desired to evaluate numerical derivative at the top node of y^* direction, backward difference approximation has to be used. Determination of best method for numerical differentiation is examined in Appendix-B. As a result of this analysis in Appendix-B, differentiation of Third Order Lagrange Interpolating Polynomial gave the best result. Therefore, for a node at upper surface numerical differentiation can be written as:

$$\frac{\partial\theta}{\partial y^*} = \frac{1}{3\,dy}(5.5\,\theta_{x,y,z}^{P+1} - 9\,\theta_{x,Y-1,z}^{P+1} + 4.5\,\theta_{x,Y-2,z}^{P+1} - \theta_{x,Y-3,z}^{P+1}) \qquad (4.9)$$

where,

$\theta_{x,y,z}^{P+1}$: Non-dimensional temperature value at the surface.

As it is shown in Figure 4.1, $\theta_{x,Y-1,z}^{P+1}$, $\theta_{x,Y-2,z}^{P+1}$ and $\theta_{x,Y-3,z}^{P+1}$ are subsequent neighboring nodes.

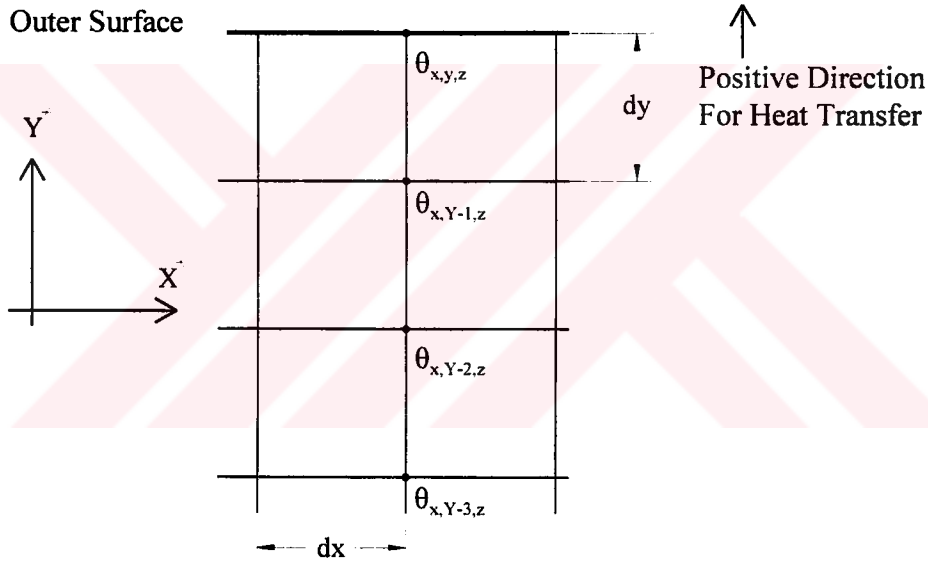

Figure 4.1. Illustration of heat transfer to the atmosphere

After performing the summation shown in Eqn. 4.8, instantaneous heat transfer rate to atmosphere is evaluated in non-dimensional form.

4.1.2 HEAT TRANSFER TO GROUND

Similar to previous section for an arbitrary node on the base plane, the rate of heat transfer, Q_{DOWN} , can be written as:

$$Q_{DOWN} = k\,F\,\frac{\partial T}{\partial y} \qquad (4.10)$$

This equation is quite different from Eqn. (4.1). Minus sign is not appeared since the positive direction of heat flux is considered in -y direction. Due to the initial conditions, initially heat is transferred from ground to the control volume. Therefore, initially the heat transfer to the ground has a negative value.

Similar derivation procedure is followed as in previous section and following non-dimensional equation is obtained:

$$Q_{DOWN}^{*} = \frac{Q_{DOWN}}{k\,R\,(T_b - T_\infty)} = F^{*}\,\frac{\partial \theta}{\partial y^{*}} \qquad (4.11)$$

The value of F^{*} is exactly same as in previous section. Total non-dimensional heat transfer rate, $Q_{DOWNSUM}^{*}$, is the sum of all Q_{DOWN}^{*} values at the base plane.

$$Q_{DOWNSUM}^{*} = \sum_{z=1}^{nztotal} \sum_{x=1}^{nx} F^{*}\,\frac{\partial \theta}{\partial y^{*}} \qquad (4.12)$$

The term $\partial\theta/\partial y^{*}$ should be evaluated numerically for each node at the base plane at any timestep. Since it is desired to evaluate numerical derivative at the bottom node in y^{*} direction, forward difference approximation has to be used. Therefore, for a node at base plane numerical differentiation can be written as:

$$\frac{\partial\theta}{\partial y^*} = \frac{1}{3\,dy}\left(-5.5\,\theta_{x,y,z}^{P+1} + 9\,\theta_{x,Y+1,z}^{P+1} - 4.5\,\theta_{x,Y+2,z}^{P+1} + \theta_{x,Y+3,z}^{P+1}\right) \qquad (4.13)$$

where,

$\theta_{x,y,z}^{P+1}$: Non-dimensional temperature value at the base plane

As it is shown in Figure 4.2, $\theta_{x,Y+1,z}^{P+1}$, $\theta_{x,Y+2,z}^{P+1}$ and $\theta_{x,Y+3,z}^{P+1}$ are subsequent neighboring nodes.

After performing the summation shown in Eqn. 4.12, instantaneous heat transfer rate to ground is evaluated in non-dimensional form.

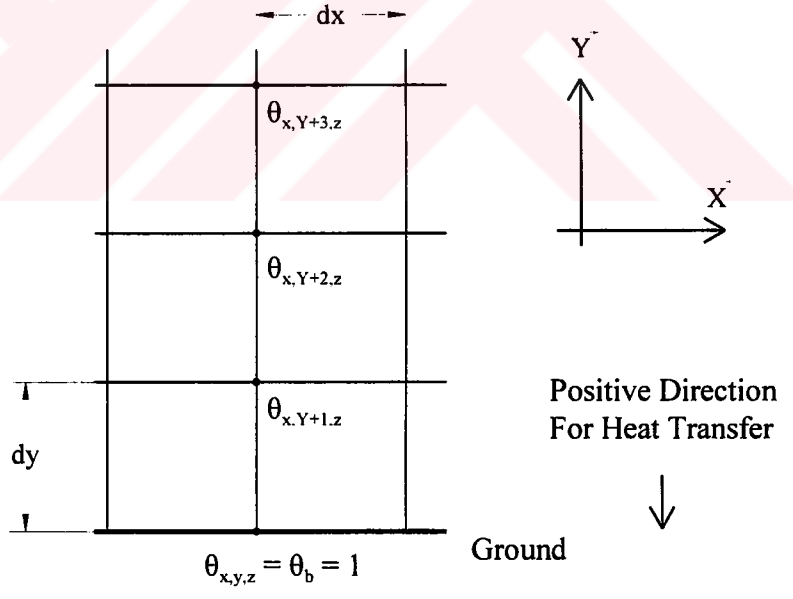

Figure 4.2. Illustration of heat transfer to ground

4.1.3 HEAT TRANSFER TO THE SIDES

Heat transfer also occurs through the side planes (z = 1 and z = nztotal planes according to Figure 3.4). Due to the guide line for symmetry, heat transfer through the first side plane (z = 1) is equal to the one through the last side plane (z = nztotal according to Figure 3.4). Therefore, total heat transfer through the sides is twice of the heat transfer through first side plane (z = 1).

For an arbitrary node on the first side plane, the rate of heat transfer, Q_{SIDES} , can be written as:

$$Q_{SIDES} = 2\,k\,F\,\frac{\partial T}{\partial z} \qquad (4.14)$$

Initially temperature varies along only in y direction. In other words $\partial T/\partial z$ term is zero. Therefore, initially heat transferred through the sides is zero. Similar derivation procedure followed as in previous section, following non-dimensional equation is obtained:

$$Q_{SIDES}^{*} = \frac{Q_{SIDES}}{k\,R\,(T_b - T_\infty)} = 2\,F^{*}\,\frac{\partial \theta}{\partial z^{*}} \qquad (4.15)$$

The value of F^{*} is equal to the product "dx dy" for any interior node at the first side plane. For the nodes at the edges except corners this value is "0.5 dx dy" and for corner nodes this is "0.25 dx dy". Total non-dimensional heat transfer rate, $Q_{SIDESSUM}^{*}$, is the sum of all Q_{SIDES}^{*} values at the first side plane.

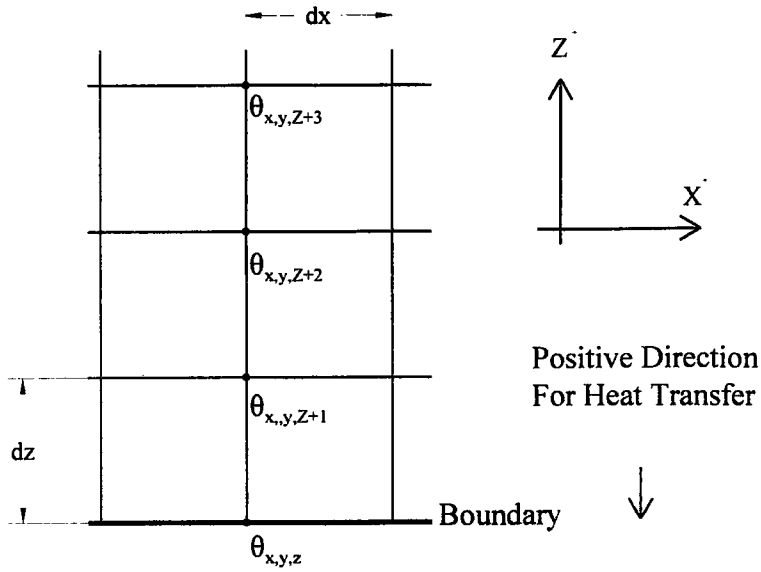

Figure 4.3. Illustration of heat transfer to first side plane

$$Q_{SIDESSUM}^{*} = 2 \sum_{x=1}^{nx} \sum_{y=1}^{ny} F^{*} \frac{\partial \theta}{\partial z^{*}} \qquad (4.16)$$

The term $\partial\theta/\partial z^{*}$ should be evaluated numerically for each node at the first side plane at any timestep. Since it is desired to evaluate numerical derivative at the first node of z^{*} direction, forward difference approximation has to be used. Therefore, for a node at first side plane numerical differentiation can be written as:

$$\frac{\partial \theta}{\partial z^{*}} = \frac{1}{3\,dz}(-5.5\,\theta_{x,y,z}^{P+1} + 9\,\theta_{x,y,Z+1}^{P+1} - 4.5\,\theta_{x,y,Z+2}^{P+1} + \theta_{x,y,Z+3}^{P+1}) \qquad (4.17)$$

where,

$\theta_{x,y,z}^{P+1}$: Non-dimensional temperature value at the first side plane

After performing the summation shown in Eqn. 4.16, instantaneous heat transfer rate to the side planes is evaluated in non-dimensional form.

4.2 STEADY STATE ENERGY BALANCE EQUATION

As it is stated at the beginning of this chapter, temperature difference between the pipe inlet and exit is a result of heat transfer components described in the previous section. At steady state, temperature distribution in the solid and in the pipe does not change with time any longer. Therefore, heat transfer components also does not change with time. Hence, the following energy balance equation can be written at steady state:

$$m\, c_{pw}\, (T_i - T_{mo}) = Q_{UPSUM} + Q_{DOWNSUM} + Q_{SIDESSUM} \qquad (4.18)$$

This equation can be non-dimensionalized by using the same principal for Eqn. (4.6). Division of both sides by "k R ($T_b - T_\infty$)" gives the following result:

$$\frac{m\, c_{pw}}{k\, R}(\theta_i - \theta_{mo}) = Q_{UPSUM}^{*} + Q_{DOWNSUM}^{*} + Q_{SIDESSUM}^{*} \qquad (4.19)$$

At the left side of Eqn. (4.19), another important non-dimensional parameter appears.

$$C^{*} = \frac{m\, c_{pw}}{k\, R} \qquad (4.20)$$

Consequently, Eqn. (4.19) can be simplified as:

$$C^{*}\, (\theta_i - \theta_{mo}) = Q_{UPSUM}^{*} + Q_{DOWNSUM}^{*} + Q_{SIDESSUM}^{*} \qquad (4.21)$$

At this point it is necessary to consider C^{*} in detail.

$$C^* = \frac{m\, c_{pw}}{k\, R} = \frac{4\, m}{\pi\, D\, \mu} \frac{\mu\, c_{pw}}{k_w} \frac{k_w}{k} \frac{\pi}{2} \qquad (4.22)$$

It is quite obvious that Reynolds Number and Prandtl Number appear at right hand side of Eqn. (4.22).

$$C^* = Re_D\, Pr \frac{k_w}{k} \frac{\pi}{2} \qquad (4.23)$$

Total heat transfer rate, Q_{TOTAL}^*, can be defined as:

$$Q_{TOTAL}^* = Q_{UPSUM}^* + Q_{DOWNSUM}^* + Q_{SIDESSUM}^* \qquad (4.24)$$

Combining Equations (4.21), (4.23) and (4.24) gives the following result:

$$Re_D\, Pr \frac{k_w}{k} \frac{\pi}{2} (\theta_i - \theta_{mo}) = Q_{TOTAL}^* \qquad (4.25)$$

Once the steady state non-dimensional temperature distribution is determined, both side of Eqn. (4.25) can be evaluated. Therefore, Eqn. (4.25) can be used to verify temperature distribution and heat transfer values.

4.3 CONCEPT OF USEFUL HEAT, HEAT LOSS AND EFFICIENCY

In Section 4.1 determination of the heat transfer components were described. But the portion of heat to melt snow (useful heat) and heat loss are not clarified. At any timestep useful heat, Q_{USE}^*, is the heat transfer to the atmosphere through the outer surface of Solid-2. In other words heat transfer through the outer surface above the

pipe is called as used heat. At any timestep, heat transfer to the atmosphere through the outer surface of Solid-1, heat transfer to the ground and heat transfer to the sides are called as heat loss, Q_{LOSS}^*. Sum of used heat and heat loss is actually total heat transfer rate, Q_{TOTAL}^*, defined in Eqn. (4.24).

At this point thermal efficiency, η, can be defined as the ratio of used heat to the total heat. Therefore,

$$\eta = \frac{Q_{USED}^*}{Q_{TOTAL}^*} \qquad (4.26)$$

4.4 CUMULATIVE HEAT TRANSFER

In preceding sections of this chapter the considered heat transfer values are in rate (power) form. But to melt existing snow or ice certain amount of energy has to be given per unit mass. Therefore, time integration of used heat transfer rate (Q_{USED}) is necessary to find the energy given to the snow or ice at the outer surface. So, cumulative used heat transfer, $Q_{USEDCUM}$, can be written as:

$$Q_{USEDCUM} = \int_0^t Q_{USED} \; dt \qquad (4.27)$$

Similar to Eqn. (4.7), Q_{USED} can be written in terms of its non-dimensional value Q_{USED}^*.

$$Q_{USED} = k\, R\, (T_b - T_\infty)\, Q_{USED}^* \qquad (4.28)$$

Using Eqn. (3.4a) dt can also be written in terms of non-dimensional value dt^*

$$dt = \frac{R^2}{\alpha} dt^* \qquad (4.29)$$

Substitution of Equations (4.29) and (4.28) into Eqn (4.27) gives the following:

$$Q_{USECUM} = \int_0^t k R (T_b - T_\infty) Q_{USE}^* (R^2/\alpha) dt^* \qquad (4.30)$$

Thermal diffusivity of solid (α) is given as

$$\alpha = \frac{k}{\rho c_p} \qquad (4.31)$$

Substituting Eqn. (4.31) into Eqn. (4.30) and rearranging the terms results in

$$Q_{USECUM} = \rho c_p R^3 (T_b - T_\infty) \int_0^t Q_{USE}^* dt^* \qquad (4.32)$$

Division of both sides by "$\rho c_p R^3 (T_b - T_\infty)$" results in the following non-dimensional equation:

$$\frac{Q_{USECUM}}{\rho c_p R^3 (T_b - T_\infty)} = \int_0^t Q_{USE}^* dt^* \qquad (4.33)$$

In addition to Equations (3.4a), (3.4b) and (4.7), from the left side of Eqn. (4.33) a new non-dimensionalization equation is obtained.

$$Q_{USECUM}^* = \frac{Q_{USECUM}}{\rho c_p R^3 (T_b - T_\infty)} = \int_0^t Q_{USE}^* dt^* \qquad (4.34)$$

The integral at the right side of Eqn. 4.34 should be evaluated numerically. In this study Trapezoidal Rule [7] is used for this purpose.

4.5 CALCULATION OF HEATING LOAD

According to Objective-1 it is necessary to melt the snow or ice (if exists). Therefore according to the amount of snow, the system should supply necessary heat in cumulative form as described in Section 4.4, to the surface. Heating load (Q_{LOAD}) is equal to the mass of snow multiplied by the latent heat for melting per unit mass (I_L).

$$Q_{LOAD} = m_S I_L \qquad (4.35)$$

Mass of snow (m_S) can be expressed as:

$$m_S = \rho_S A_{SOLID\text{-}2} t_S \qquad (4.36)$$

where

ρ_S : Density of snow (kg /m^3)

$A_{SOLID\text{-}2}$: Outer surface area of solid above the pipe (= lz_2 l, m^2)

t_S: Thickness of snow or ice on $A_{SOLID\text{-}2}$ (m)

Substituting Eqn. (4.36) into Eqn. (4.35) and dividing of both sides of the equation by the term "$\rho\, c_p\, R^3\, (T_b - T_\infty)$" makes the heat load non-dimensional.

$$Q_{LOAD}^{*} = \frac{\rho_S}{\rho} \frac{A_{SOLID\text{-}2}}{R^2} \frac{t_S}{R} \frac{I_L}{c_P (T_b - T_\infty)} \qquad (4.37)$$

Consequently,

$$Q_{LOAD}^{*} = \frac{\rho_S}{\rho} A_{SOLID\text{-}2}^{*} \; t_S^{*} \; I_L^{*} \qquad (4.38)$$

where I_L^{*} is non-dimensional form of latent heat of melting per unit mass.

When cumulative non-dimensional heat transfer (Q_{USECUM}^{*}) stated in Eqn. (4.34) exceeds the heat load Q_{LOAD}^{*}, the system completely melts the snow or ice.

Non-dimensional melted snow thickness (t_{SM}^{*}) can be written as

$$t_{SM}^{*} = \frac{Q_{USECUM}^{*}}{(\rho_S / \rho) \, A_{SOLID\text{-}2}^{*} \, I_L^{*}} \qquad (4.39)$$

CHAPTER 5

RESULTS AND DISCUSSIONS

Up to this point, three-dimensional transient temperature distribution was obtained and plotted for a sample geometry shown in Figures 3.4a and 3.4b. In the previous chapter, evaluation of heat transfer values and efficiency were described. In this chapter, results obtained up to this point will be discussed and the effect of some important parameters will be studied.

5.1 DISCUSSIONS ON TEMPERATURE DISTRIBUTIONS

In Fig. 3.7 non-dimensional temperature distribution of Objective-1 for timestep = 5, z = 12 and $\theta_i = 5.41$ (corresponding to 80°C for T_∞ = -12°C and T_b = 5°C according to Eqn. (3.4b)) is showns. As it is described in Chapter 3, finite difference gridding is performed in Cartesian coordinates. Therefore, contours near the pipe (circular boundary) are not as regular as the contours far from the circular boundary. Even though the sample geometry shown in Figure 3.4b are not long enough in z^* direction, because of reference value of Reynolds number is low, the supply fluid temperature (θ_i) and exit fluid temperature(θ_{mo}) differ considerably. For this reason lower non-dimensional temperature contours at right side and higer non-dimensional temperature values at left side are observed.

When the Fig. 3.7 and Fig. 3.8 is compared the gap between contours near the pipe is higher in Fig. 3.8. Non-dimensional temperature in the middle of the solid is also higher in Fig. 3.8 showing the middle plane (z = 26) of the pipe in z^* direction.

As it is expected, as the timestep increases, non-dimensional temperature between the pipes becomes larger. For timestep of 81 (steady state), non-dimensional temperature distribution reaches the highest value for supply fluid temperature value of 5.41. The other important parameters are Biot Number ($Bi_\infty = 0.88$ as reference) and Reynolds Number ($Re_D = 10$ as reference).

For Objetive-2 (Figures 3.16 – 3.24) similar behavior of contours is observed. However, near the outer surface, very low non-dimensional temperature values are observed. Even at steady state the surface temperature can never be reached to the constant surface temperature (θ_S) defined for Objective-1. Therefore, higher supply fluid temperature and lower Biot number must be considered.

5.2 PARAMETRIC ANALYSIS FOR OBJECTIVE-1

As it is described in Chapter 3, the first objective of this system is to melt the snow or ice on the surface. Therefore it is necessary to supply enough heat to melt snow or ice within a certain time limit. For this reason useful heat transfer rate should be kept as high as possible.

Useful heat rate, heat loss rate and total heat transfer rate are plotted in Fig. 5.1. As it is stated in Section 4.2, initially heat loss rate has a negative value. As the time goes by, heat is transferred from the pipe to the surrounding solid. Consequently temperature in the solid is increased and becomes grater than the base temperature θ_b. As a result of this increase, total heat loss (Q_{LOSS}^*) becomes positive as the time passes. Within this period, total heat transfer (Q_{TOTAL}^*) is less than the useful heat transfer (Q_{USE}^*).

For this chapter reference value of Reynolds number (Re_D) is selected as 100.

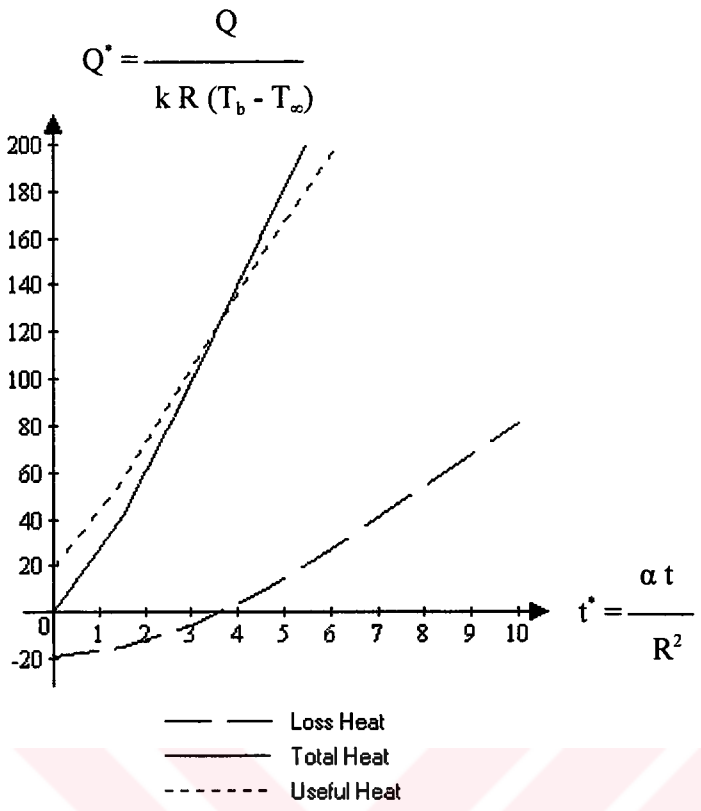

(a) Heat transfer for short time periods

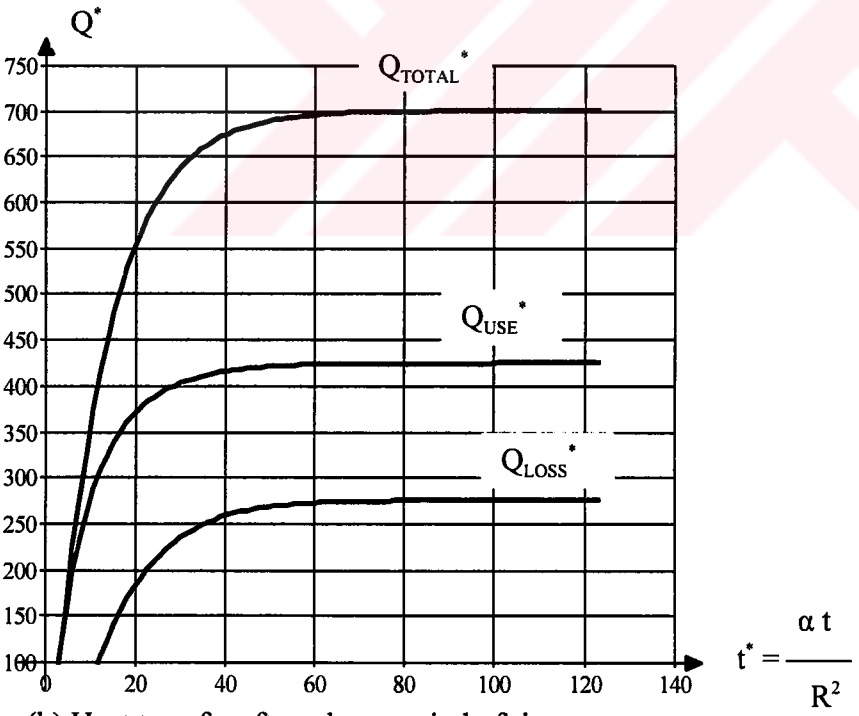

(b) Heat transfer after a long period of time

Figure 5.1 Variation of total, useful and lost heat transfer as a function of time (Objective-1)

As it is seen in Fig. 5.1b, heat transfer values increases with time and reaches its steady value. Steady state is reached at timestep of 81. Since value of non-dimensional time increment (Incremental Fourier Number, Fo) is taken as 1.5 for each timestep, non-dimensional time (t^*) of steady state corresponds to 121.5. At this value, total heat loss (Q_{LOSS}^*) is 275.94, useful heat (Q_{USE}^*) is 425.08 and total heat (Q_{TOTAL}^*) is 701.02. From the non-dimensional temperature distribution in steady state non-dimensional temperature at he exit of the pipe (θ_{mo}) is determined as 5.0555. From steady state energy balance equation, following relation should hold according to Eqn. (4.25)

$$Re_D \, Pr \, \frac{k_w}{k} \, \frac{\pi}{2} (\theta_i - \theta_{mo}) = Q_{TOTAL}^*$$

when the reference values are inserted,

$$100 \times 12 \, \frac{0.546}{0.52} \, \frac{\pi}{2} (5.41 - 5.0555) = 701.63$$ is obtained.

If this value is compared with Q_{TOTAL}^* in Fig. 5.1. the difference is very small and percent relative error is 0.09.

5.2.1 PARAMETRIC ANALYSIS WITH DIFFERENT PIPE SPACINGS

Pipe spacing (l) one of the important parameters for this system. The value range is selected from 4 to 16 . The first parameter is useful heat transfer rate (Q_{USE}^*) that is described in Fig. 5.2. For low non-dimensional time values, useful heat transfer does not show considerable variation with respect to pipe spacing. But, after the non-dimensional time value of 8, useful heat starts to change drastically. For small pipe

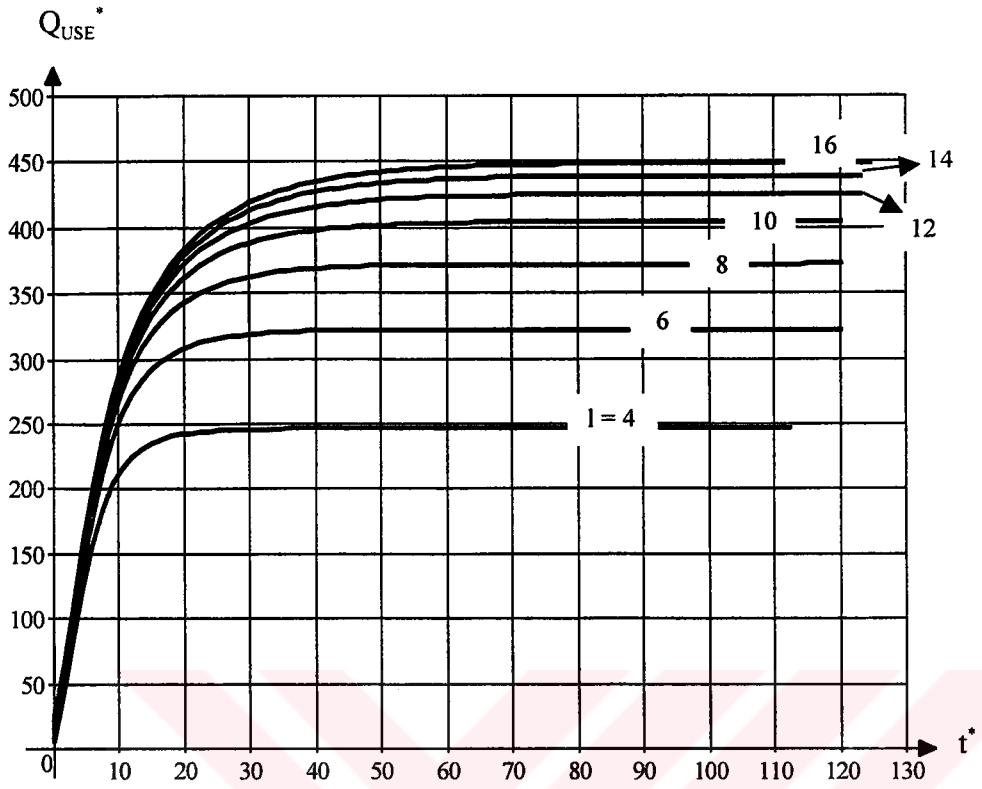

Figure 5.2 Time variation of useful heat transfer for different pipe spacing (l) values (Objective-1).

spacing, useful heat rate (Q_{USE}^*) is also small. When the pipe spacing is increased from 4 to 6, a considerable increase of useful heat rate is observed. Similar behavior is observed up to the pipe spacing value of 10. After this value, change in useful heat transfer rate is not so significant. As the pipe spacing increases system reaches the steady state at a longer time period.

Second parameter is efficiency (η) which is shown in Fig. 5.3. Initially, total heat transfer rate (Q_{TOTAL}^*) is zero, consequently, efficiency can not be defined there. As it is explained in Fig. 5.1a for early values of non-dimensional time , total heat loss rate (Q_{LOSS}^*) is negative. This means that total heat transfer rate (Q_{TOTAL}^*) is less than

useful heat transfer rate (Q_{USE}^*). Therefore, the efficiency is grater than unity for this period.

$$\eta = \frac{Q_{USE}^*}{Q_{TOTAL}^*}$$

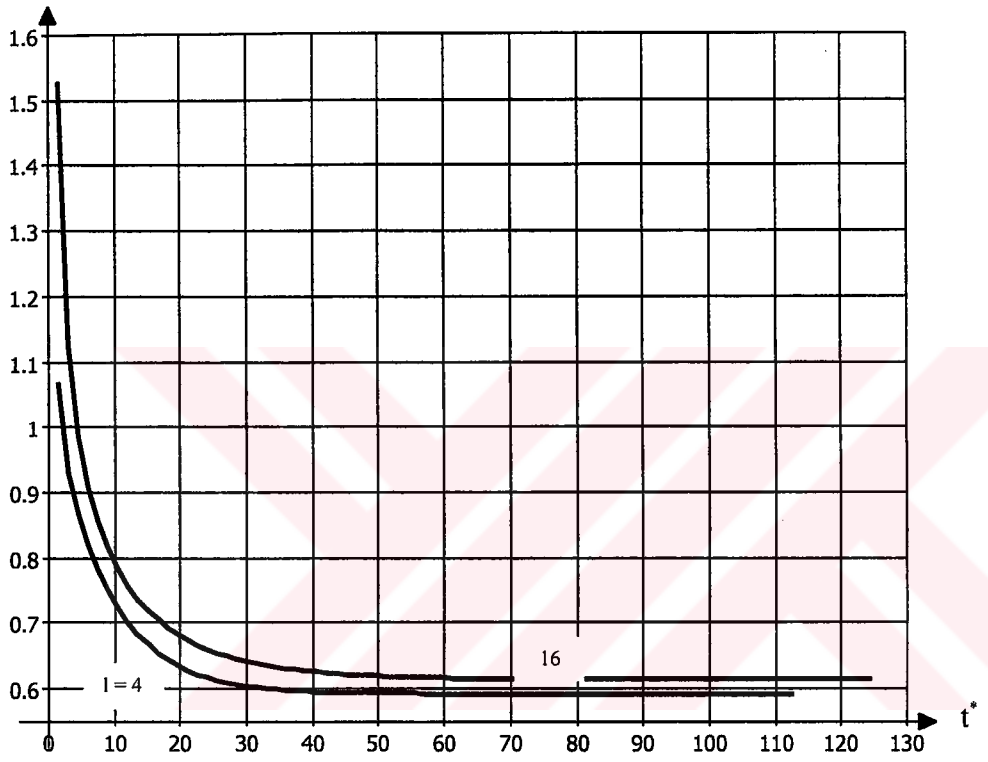

Figure 5.3 Time variation of efficiency for different pipe spacing (l) values (Objective-1).

Initial efficiency exhibit a big difference between pipe spacing of 4 and 16. However, as the non-dimensional time increases, efficiency at different pipe spacing approaches to each other. Near steady state, efficiency gets values close to 0.6.

Third parameter is cumulative heat transfer (Q_{USECUM}^*) defined in Eqn. (4.34). It is actually the integration of Q_{USE}^* shown in Fig. 5.2.with respect to non-dimensional time. The time variation of cumulative heat transfer is shown in Fig. 5.4.

$$Q_{USECUM}^* = \frac{Q_{USECUM}}{\rho\, c_p\, R^3\, (T_b - T_\infty)}$$

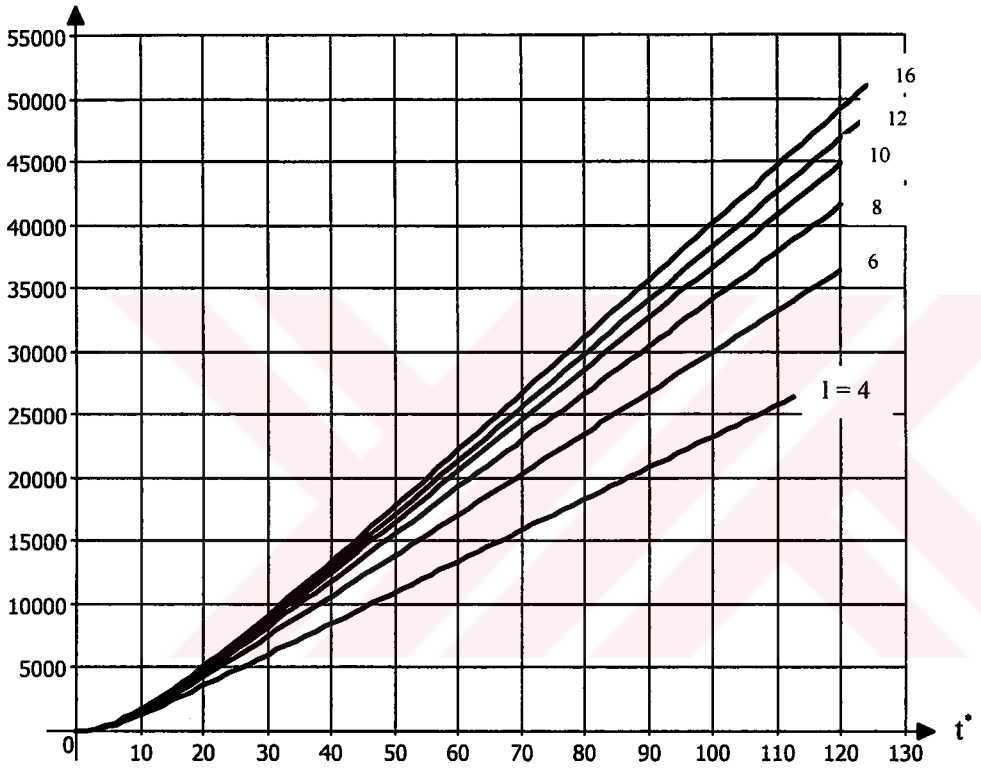

Figure 5.4 Time variation of cumulative heat transfer for different pipe spacing (l) values (Objective-1).

For the non-dimensional time larger than 20, the behavior of curves is almost linear. For shorter times, curves are very close to each other. As it is expected for smaller pipe spacing, cumulative heat transfer (Q_{USECUM}^*) is smaller. For higher pipe spacing, cumulative heat transfer (Q_{USECUM}^*) is larger.

$$t_{SM}^{*} = \frac{Q_{USECUM}^{*}}{(\rho_S / \rho)\, A_{SOLID\text{-}2}^{*}\, I_L^{*}}$$

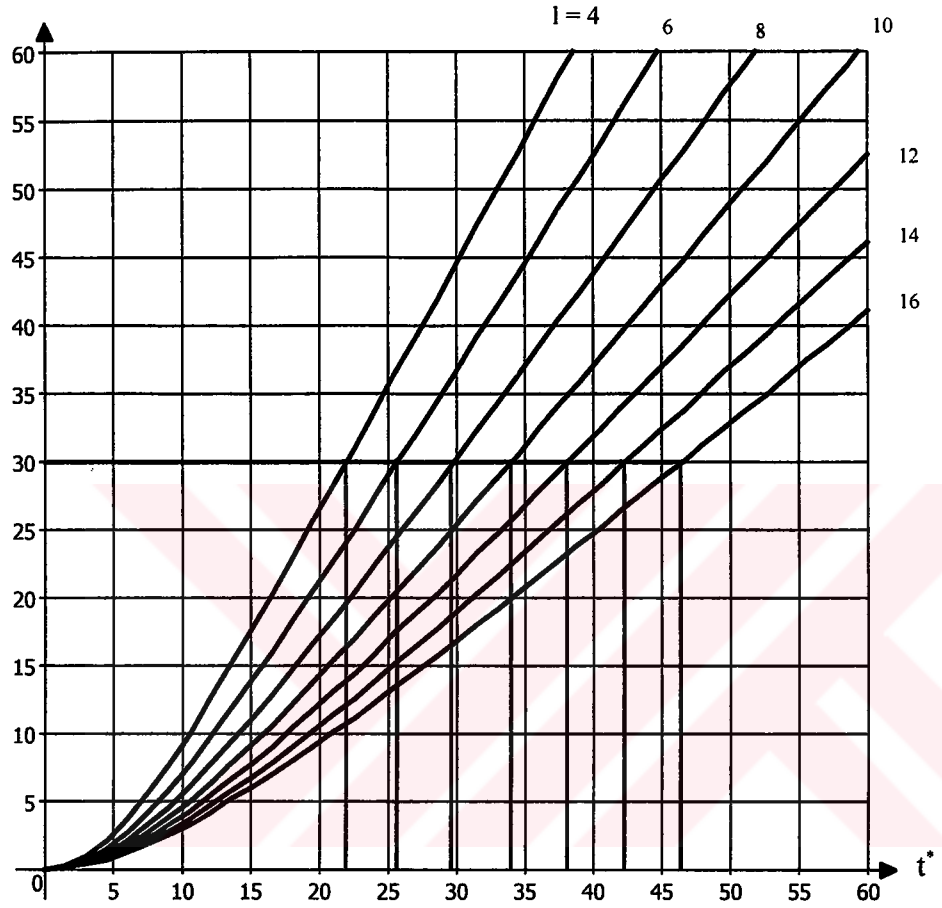

Figure 5.5 Time variation of melted snow thickness for different pipe spacing (l) values (Objective-1).

Time variation of melted snow thickness (t_{SM}^{*}) given by Eqn. (4.39) for different pipe spacing (l) values, is shown in Fig. 5.5. This parameter displays the performance of system as the efficiency. Similar to Fig. 5.4 for non-dimensional time larger than 20, the behavior of curves is almost linear. For shorter time, the curves are very close to each other. As the pipe spacing is increased, the melted snow thickness is decreased.

Area of solid-2 ($A_{SOLID-2}^*$) depends upon pipe spacing (l). As l increases, heating load increases. Even though the system emits higher heat in cumulative form, due to the increase in load, thickness of melted snow is low for large pipe spacings.

As a reference value of snow thickness (t_{SR}^*) 30 is selected. For reference value of pipe radius reference snow thickness corresponds to approximately 50 cm. In Table 5.1, required time values for melting 50 cm snow are shown for different pipe spacings are given.

Table 5.1 Required time values for melting 50 cm snow with following important reference values:
Supply fluid temperature, $\theta_i = 5.41$ (Corresponds to 80°C)
Pipe burial depth, h = 5
Reynolds number, $Re_D = 100$
Thermal conductivity of solid, k = 0.52 W/mK
*All reference values are listed in APPENDIX-A

Pipe Spacing (l)	4	6	8	10	12	14	16
Non-dim. time (t^*)	21.8	25.6	29.5	34.0	38.3	41.7	46.5
Time in hours	12.7	14.9	17.2	19.8	22.3	24.3	27.1

For Table 5.1 thermal conductivity is taken as 0.52 W/mK. When it is increased to 1.5 W/mK, the values are listed in Table 5.2. In this case thermal diffusivity of solid (α) becomes 3.977 10^{-7} m^2/s. Even though the non-dimensional time values in Table 5.2 are higher relative to the values in Table-5.1, time values are considerably smaller.

Table 5.2 Required time values for melting 50 cm snow with following important reference values:
Supply fluid temperature, $\theta_i = 5.41$ (Corresponds to 80°C)
Pipe burial depth, h = 5
Reynolds number, $Re_D = 100$
Thermal conductivity of solid, k = 1.5 W/mK
*All reference values are listed in APPENDIX-A

Pipe Spacing (l)	4	6	8	10	12	14	16
Non-dim. time (t^*)	27	32.5	38.3	43.6	48.5	55.0	60.8
Time in hours	5.4	6.6	7.7	8.8	9.8	11.1	12.3

5.2.2 TIME VARIATION OF SOME IMPORTANT PARAMETERS WITH DIFFERENT SUPPLY FLUID TEMPERATURE VALUES

Supply fluid temperature (θ_i) has also important effects on system performance. It is observed that for Objective-1, efficiency (η) and melted snow thickness (t_{SM}^*) are major indicators of system performance.

As it is considered in previous section, first parameter is useful heat transfer rate (Q_{USE}^*) that is shown in Fig. 5.6. Supply fluid temperature are selected as 4.23, 4.82, 5.41, 6.00, 6.59, 7.18, 7.64, 8.35, 8.94, 9.53 which corresponds to 60, 70, 80, 90, 100, 110, 120, 130, 140 and 150°C respectively according to Eqn. (3.4b) for base temperature (T_b) of 5°C and atmospheric temperature (T_∞) of −12°C.

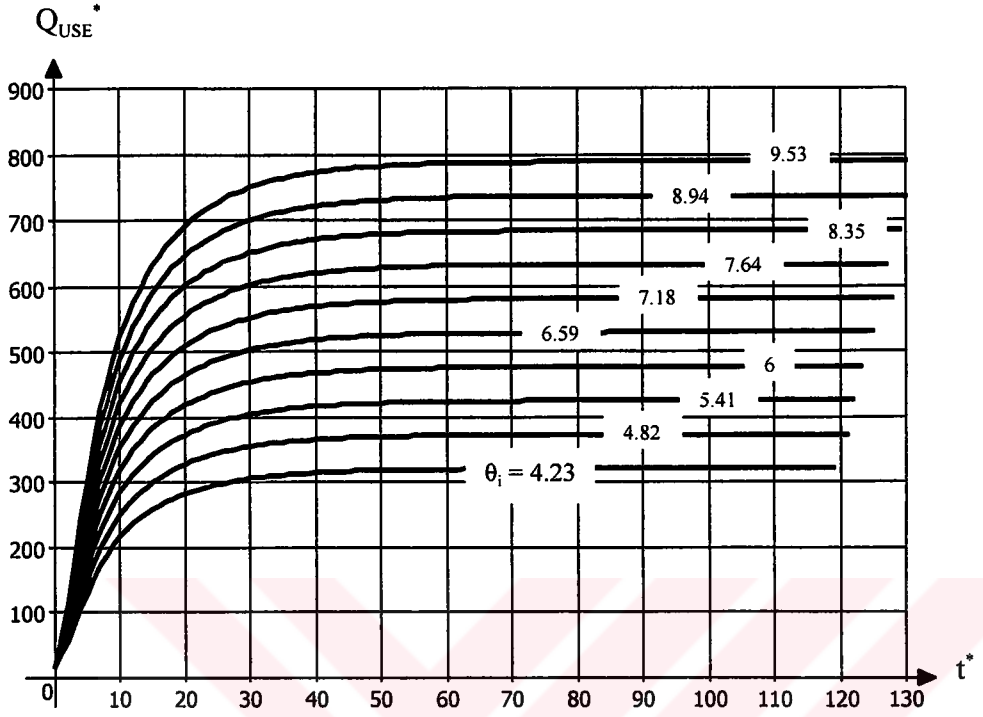

Figure 5.6 Time variation of useful heat transfer for different supply fluid temperature (θ_i) values (Objective-1).

Similar to Fig. 5.2 for low non-dimensional time values, useful heat transfer does not show considerable variation with respect to supply fluid temperature and after the non-dimensional time value of 8, curves begin to separate. When the non-dimensional temperature values increase from 4.23 to 4.82, useful heat transfer rate is also increased. In contrast to Fig. 5.2 the increase of steady state values of useful heat transfer rate (Q_{USE}^*) is almost constant.

Second parameter is efficiency (η) that is shown in Fig. 5.7. Similar behavior is valid as Fig. 5.3. But the curves are closer to each other.

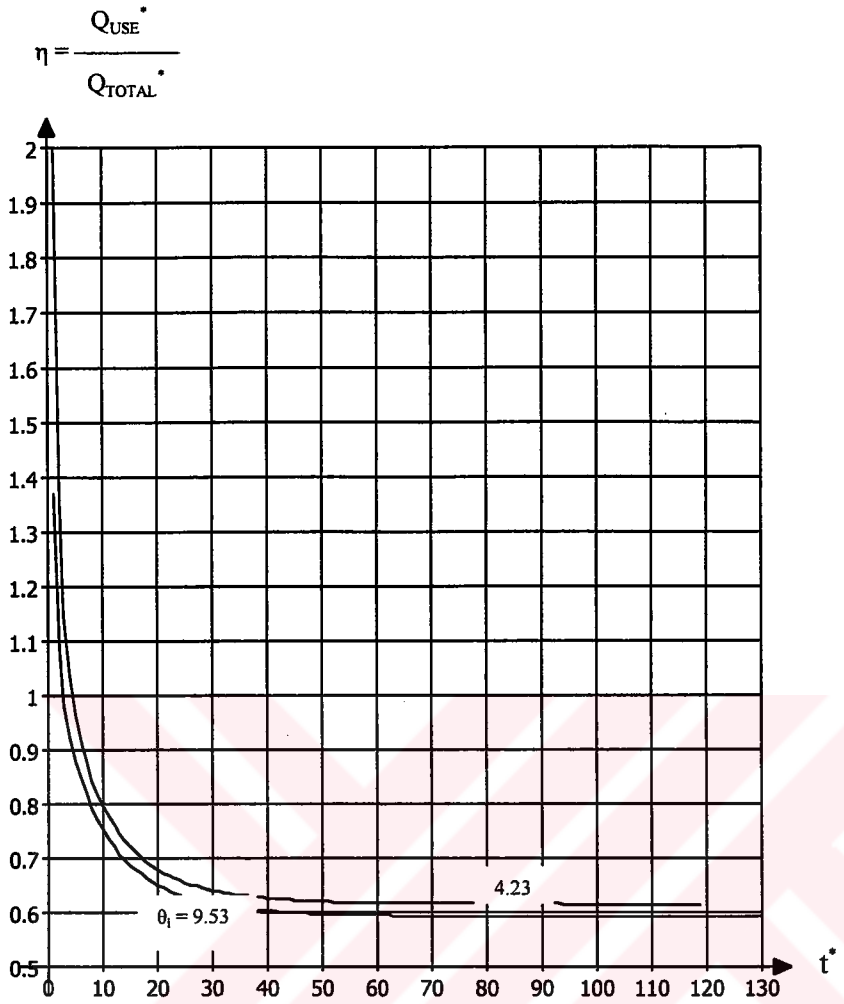

Figure 5.7 Time variation of efficiency for different supply fluid temperature (θ_i) values (Objective-1).

Third parameter is cumulative heat transfer (Q_{USECUM}^*) defined in Eqn. (4.34). This is actually the integration of Q_{USE}^* shown in Fig. 5.6.with respect to non-dimensional time. Similar behavior is observed as in the Fig. 5.4. As it is expected, for larger values of supply fluid temperature (θ_i), cumulative heat transfer is larger

$$Q_{USECUM}^{*} = \frac{Q_{USECUM}}{\rho\, c_p\, R^3\, (T_b - T_\infty)}$$

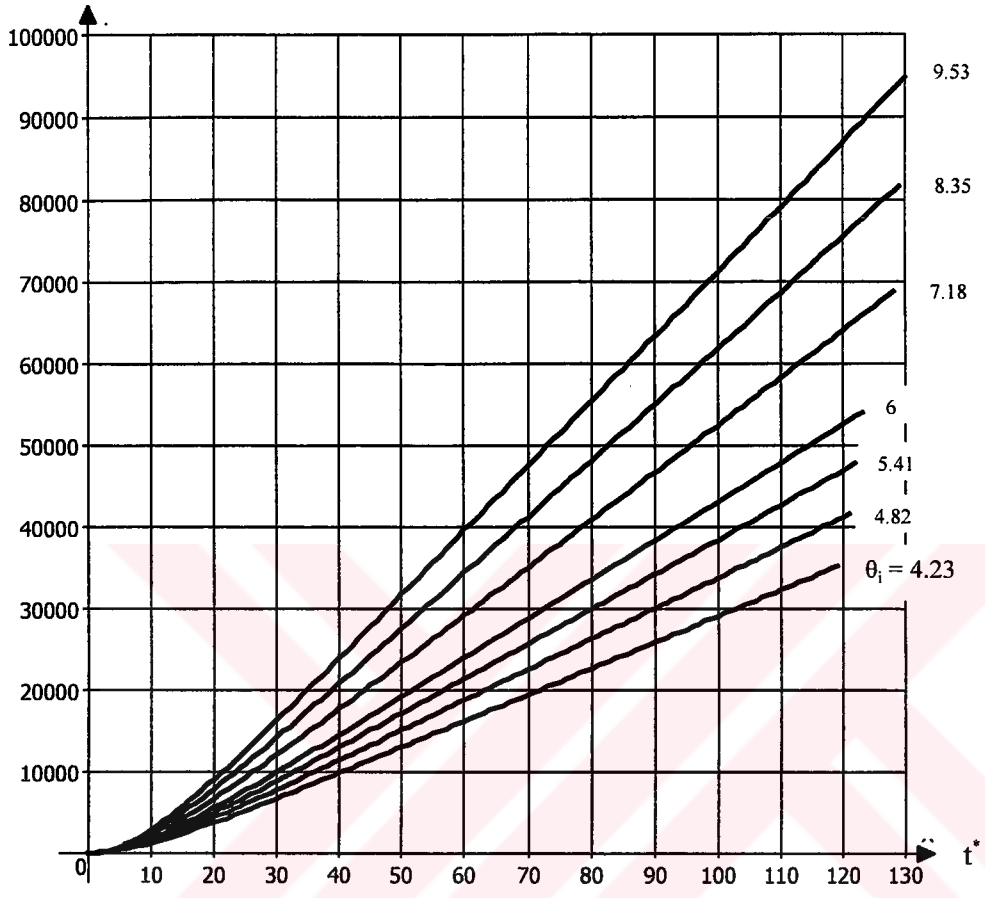

Figure 5.8 Time variation of cumulative heat transfer for different supply fluid temperature (θ_i) values (Objective-1).

Forth parameter is melted snow thickness (t_{SM}^{*}) as described in Eqn. (4.39). Time variation of melted snow thickness for different supply fluid temperature (θ_i) values, is shown in Fig. 5.9. For larger values of supply fluid temperatures, melted snow thickness values are also larger.

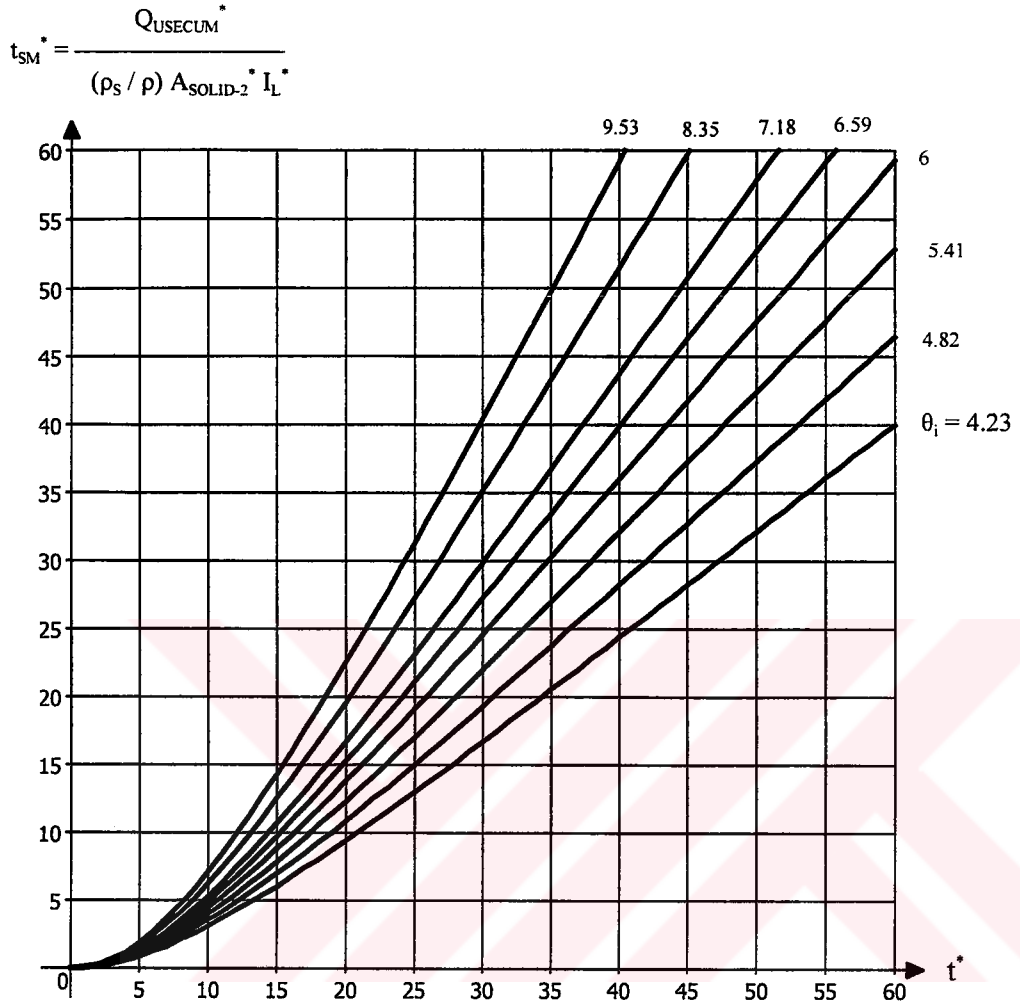

Figure 5.9 Time variation of melted snow thickness for different supply fluid temperature (θ_i) values (Objective-1).

5.2.3 PARAMETRIC ANALYSIS FOR DIFFERENT REYNOLDS NUMBERS

Reynolds Number is very famous parameter in Fluid Mechanics and Heat Transfer. In Section 3.4.1.2, Eqn. (3.28), Reynolds Number is appeared. Therefore it is effective on temperature distribution and heat transfer values. For turbulent flow (Re_D>2300), Reynolds Number affects the Nusselt Number (Nu_R). As a result, it affects the

convective heat transfer coefficient within the pipe (h_m) and Biot Number for pipe (Bi_m). In this section Reynolds Number values are selected as 100, 500, 1000, 10000 and 20000. As in previous sections, first parameter is useful heat transfer (Q_{USE}^*) that

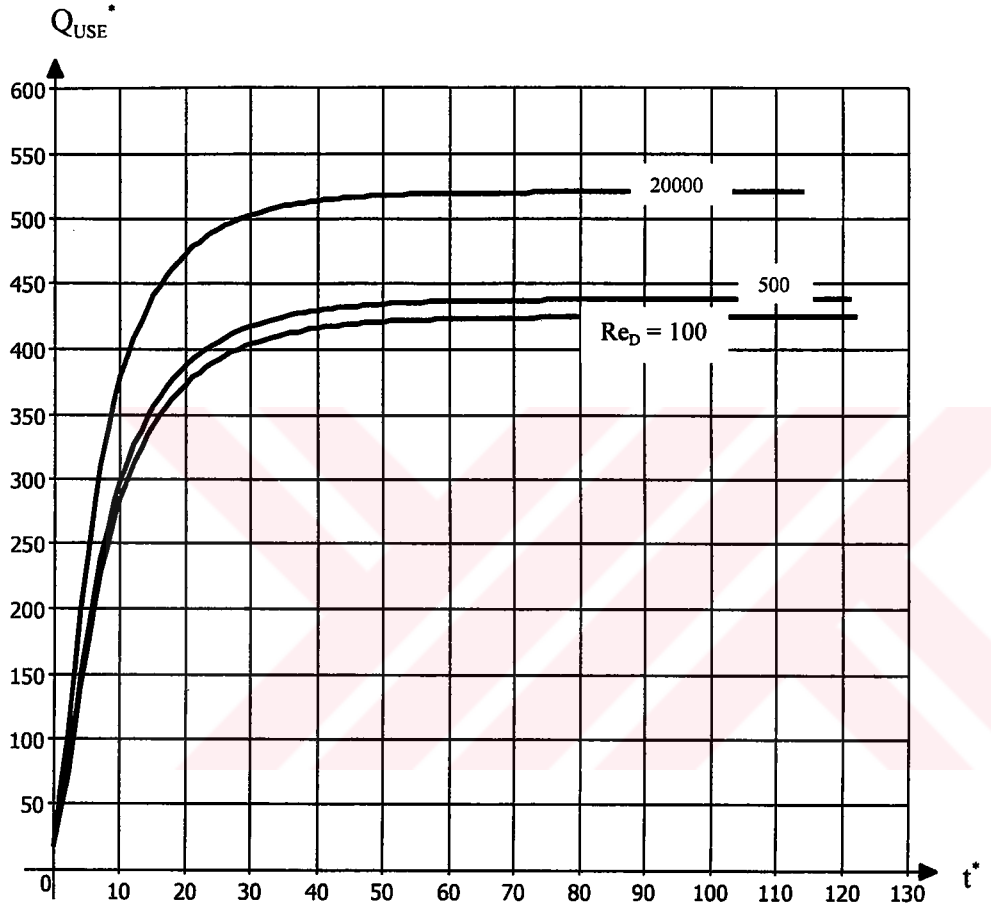

Figure 5.10 Time variation of useful heat transfer for different Reynolds Number(Re_D) values (Objective-1).

is shown in Fig. 5.10. Three Reynolds Numbers are plotted instead of five. Because, curves with Reynolds number values of 10000, 20000 and 500, 1000 are almost

coincident. A considerable difference in useful heat transfer values is observed between laminar and turbulent flow regimes.

Second parameter is efficiency (η) that is shown in Fig. 5.11.

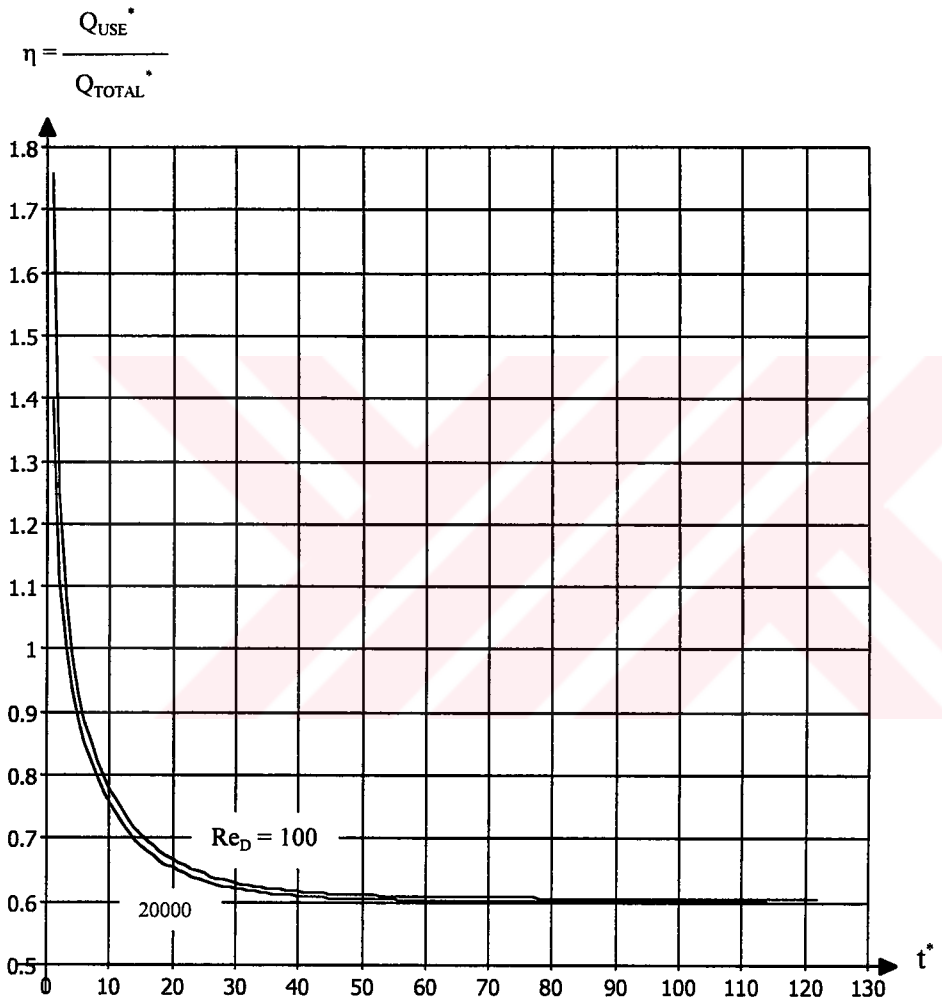

Figure 5.11 Time variation of efficiency for different Reynolds Number(Re_D) values (Objective-1).

There is almost no difference in efficiency values with respect to Reynolds Number. Third parameter is cumulative heat transfer that is shown in Fig. 5.12. Fourth parameter is melted snow thickness shown in Fig. 5.13.

$$Q_{USECUM}^{*} = \frac{Q_{USECUM}}{\rho\, c_p\, R^3\, (T_b - T_\infty)}$$

Figure 5.12 Time variation of cumulative heat transfer for different Reynolds Number(Re_D) values (Objective-1).

$$t_{SM}^{*} = \frac{Q_{USECUM}^{*}}{(\rho_S / \rho)\, A_{SOLID\text{-}2}^{*}\, I_L^{*}}$$

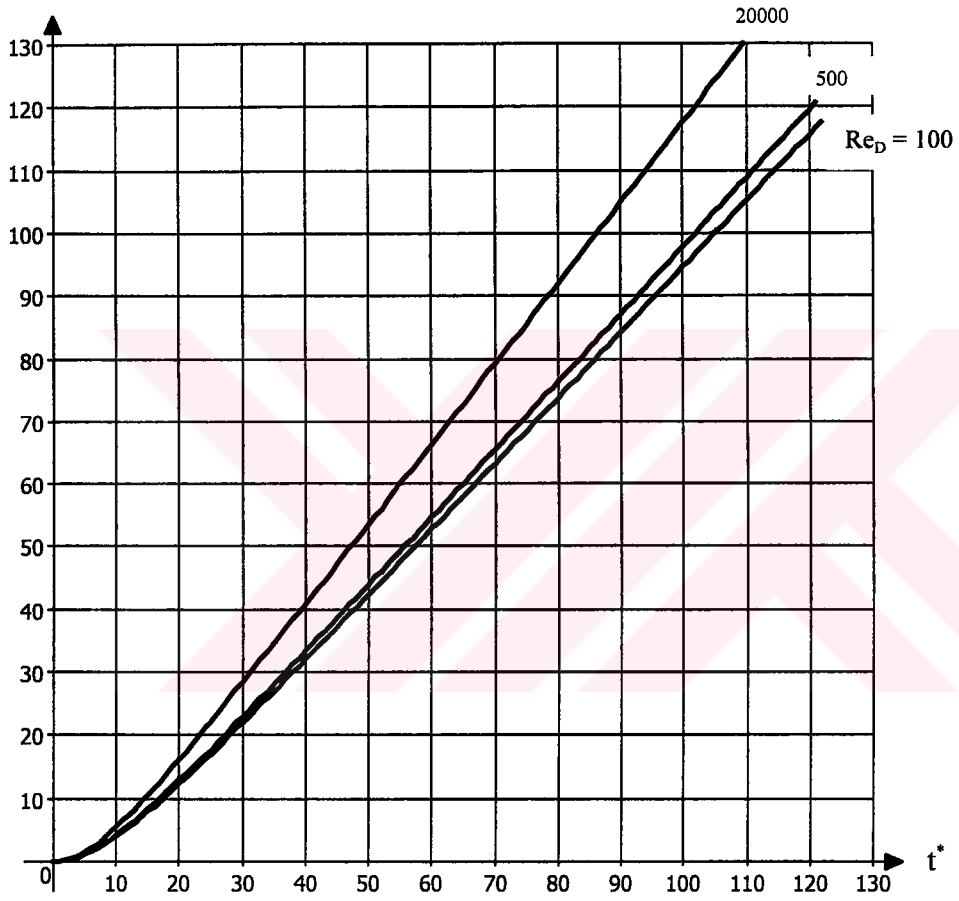

Figure 5.13 Time variation of melted snow thickness for different Reynolds Number(Re_D) values (Objective-1).

5.2.4 PARAMETRIC ANALYSIS FOR DIFFERENT PIPE BURIAL DEPTHS

Pipe burial depth (h) is also effective parameter on system performance. In Figures 5.15 – 5.17, time variation of useful heat transfer, efficiency and melted snow thickness are plotted respectively. For this section reference value of the distance c (Fig. 3.4a) is taken as 30 instead of 13.

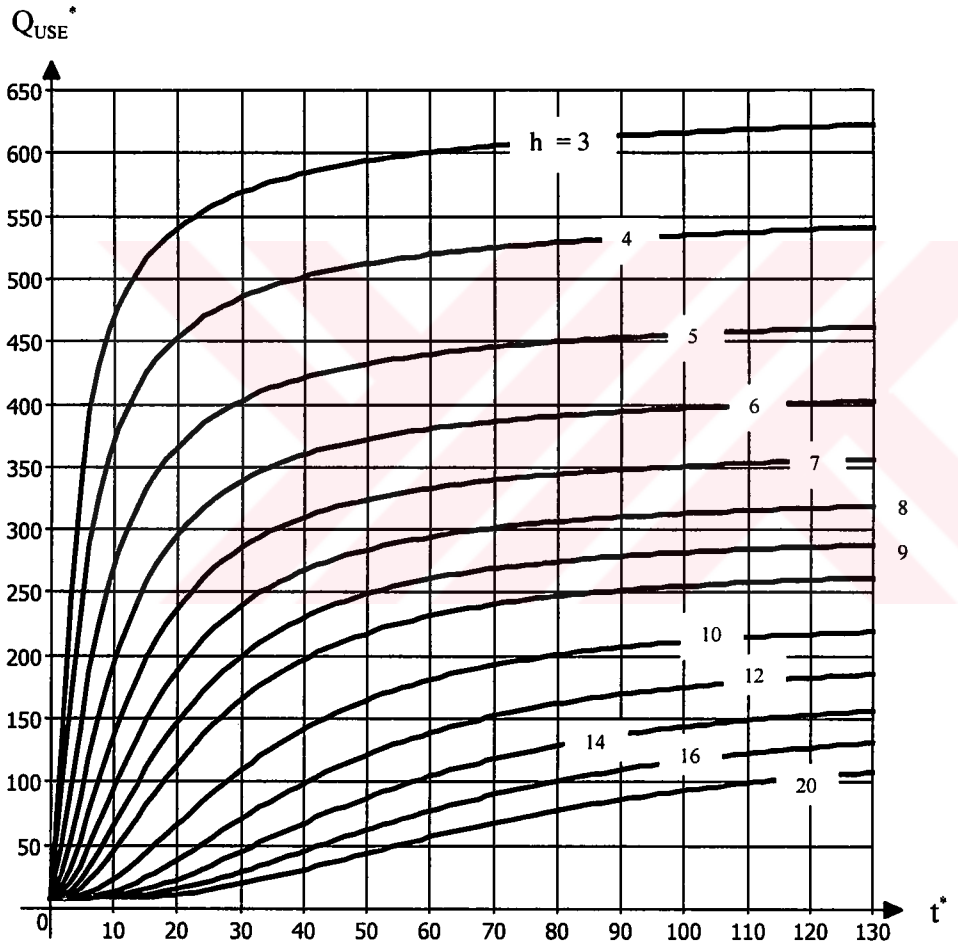

Figure 5.14 Time variation of useful heat transfer for different pipe burial depth (h) values (Objective-1).

In Fig. 5.14, useful heat transfer (Q_{USE}^*) decreases as the pipe burial depth increases. In contrast to preceding sections efficiency (η) is affected by pipe burial depth, as shown in Fig. 5.15

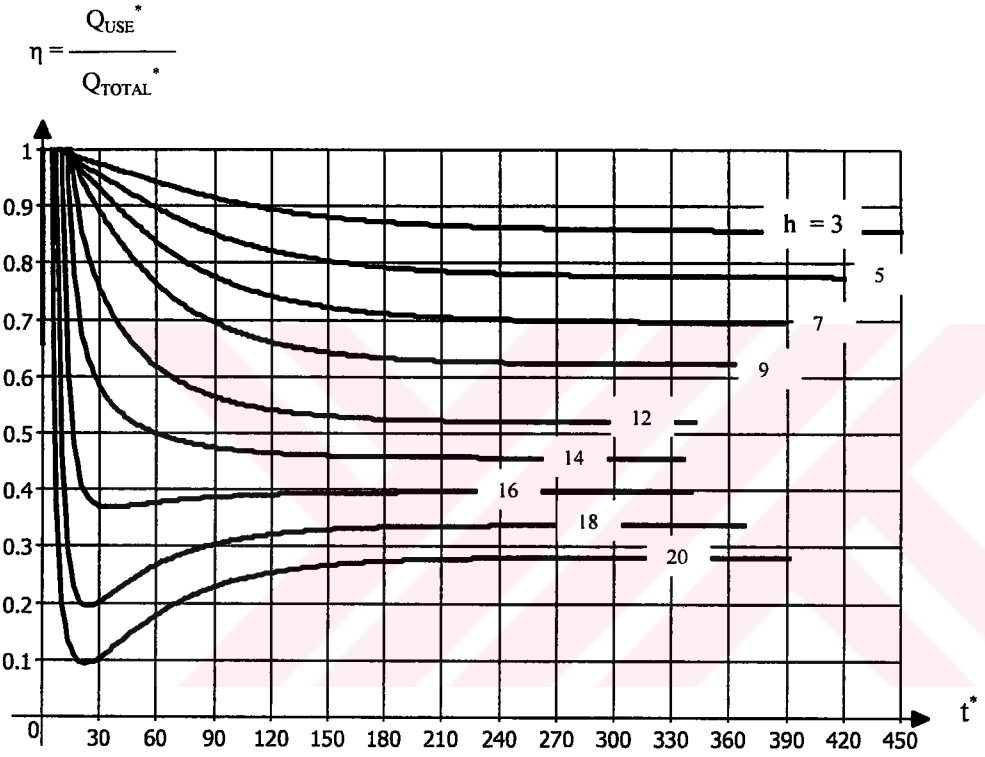

Figure 5.15 Time variation of efficiency for different pipe burial depth (h) values (Objective-1).

In Figure 5.16, melted snow thickness is also strongly affected by pipe burial depth such that melted snow thickness decreases as pipe burial depth increases. For large pipe burial depths, it is necessary to apply higher supply fluid temperatures.

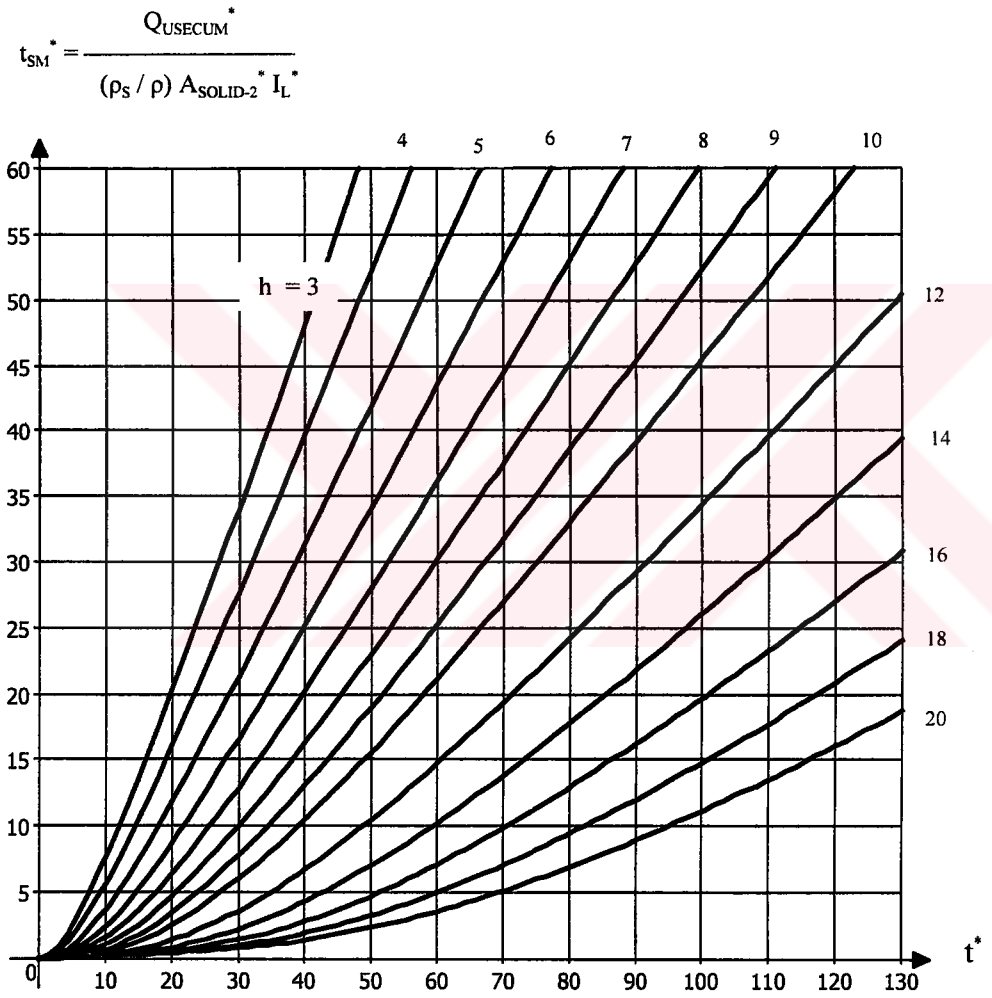

Figure 5.16 Time variation of melted snow thickness for different pipe burial depth (h) values (Objective-1).

5.3 PARAMETRIC ANALYSIS FOR OBJECTIVE-2

As it is shown in Chapter 3, the second objective of this system is to keep the surface temperature above a certain level if there is no snow or ice on the surface. The minimum level of surface temperature is selected as +2°C that corresponds to non-dimensional temperature of 0.823 for ground temperature (T_b) of 5°C and atmospheric temperature of –12°C according to Eqn. (3.4b).

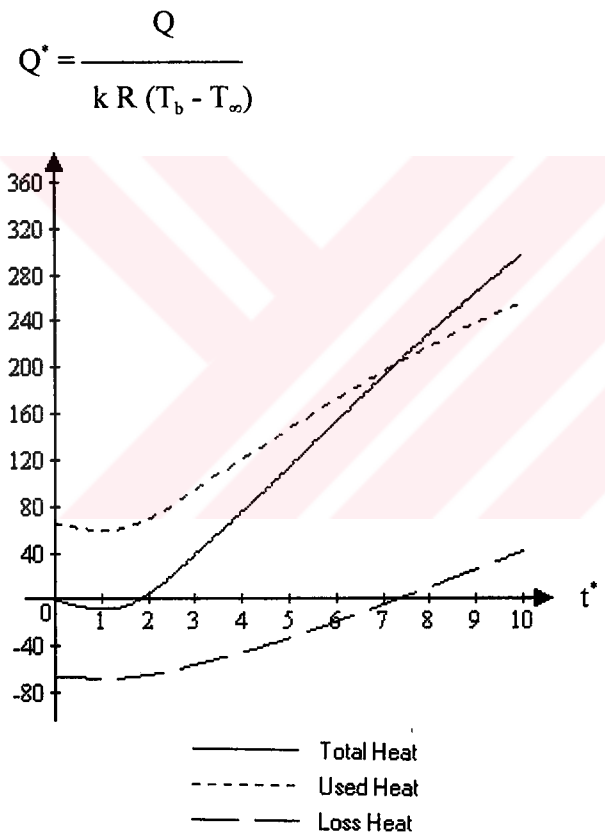

Figure 5.17 Initial behavior of heat transfer values for Objective-2

Before going into details of variations, useful heat rate, heat loss rate and total heat transfer rate are plotted in Fig. 5.17. As it is stated in Section 4.2, initially heat loss rate has a negative value. As the time goes by, heat is transferred from the pipe to the surrounding solid. So temperature in the solid is increased and becomes grater than the base temperature θ_b. As a result of this increase, total heat loss (Q_{LOSS}^*) becomes positive as the time is increased. Within this period, total heat transfer (Q_{TOTAL}^*) is less than the useful heat transfer (Q_{USE}^*). Besides these, up to non-dimensional time value

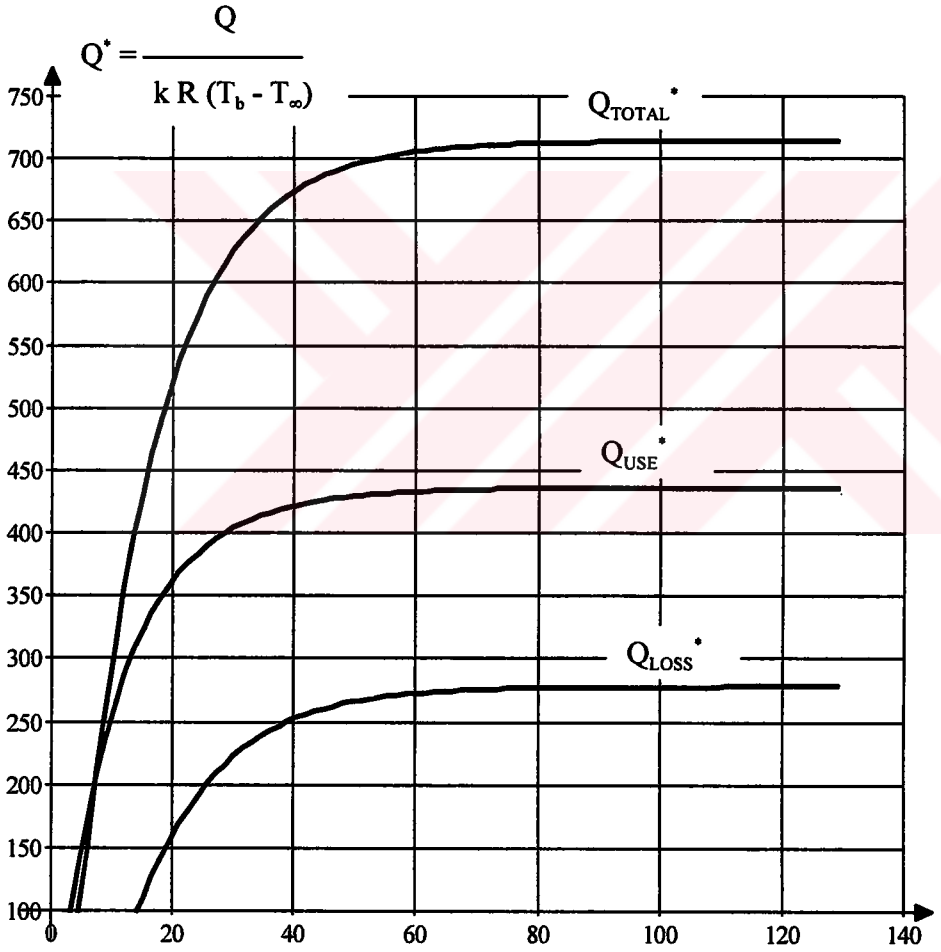

Figure 5.18 Behavior of heat transfer values for large times for Objective-2

of 2, useful heat transfer (Q_{USE}^*) slightly decrease and within this period since total heat loss (Q_{LOSS}^*) is negative so, total heat transfer (Q_{TOTAL}^*) is negative.

As it is seen in Fig. 5.18, heat transfer values increases with time and reaches steady values. As it is stated before steady state is reached at timestep of 86. Since value of non-dimensional time increment (Incremental Fourier Number, Fo) is taken as 1.5 for each timestep. Non-dimensional time (t^*) of steady state corresponds to 129. At this value, total heat loss (Q_{LOSS}^*) becomes 278.15, useful heat (Q_{USE}^*) is 436.07 and total heat (Q_{TOTAL}^*) is 714.22. From the non-dimensional temperature distribution in steady state non-dimensional temperature distribution value at he exit of the pipe (θ_{mo}) is determined as 5.0492. From steady state energy balance equation, following relation should hold according to Eqn. (4.25)

$$Re_D\, Pr \frac{k_w}{k} \frac{\pi}{2} (\theta_i - \theta_{mo}) = Q_{TOTAL}^*$$

when the reference values are inserted,

$$100 \times 12 \frac{0.546}{0.52} \frac{\pi}{2} (5.41 - 5.0492) = 714.08$$ is obtained.

If this value is compared with Q_{TOTAL}^* in Fig. 5.18., the difference is very small and percent relative error is 0.02.

5.3.1 PARAMETRIC ANALYSIS FOR DIFFERENT PIPE SPACINGS

Similar to the section 5.2.1 value range of pipe spacing (l) is selected from 4 to 16 . The first parameter is useful heat transfer rate (Q_{USE}^*) that is shown in Fig. 5.19. For low non-dimensional time values, useful heat transfer does not show considerable variation with respect to pipe spacing. But, after the non-dimensional time value of 8, pipe spacing curves begin to separate. For low pipe spacing, useful heat transfer rate

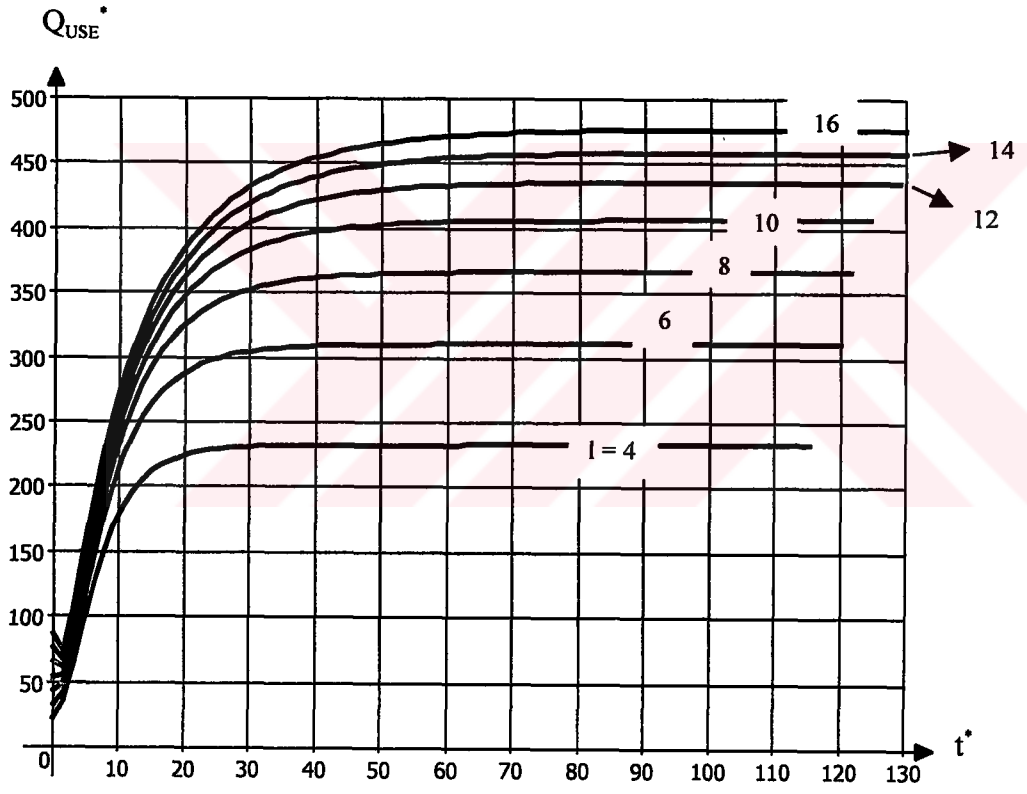

Figure 5.19 Time variation of useful heat transfer for different pipe spacing (l) values (Objective-2).

(Q_{USE}^*) is also low. When the pipe spacing is increased from 4 to 6, a considerable increase of useful heat transfer rate is observed. Similar behavior is observed up to the pipe spacing value of 10. After this value, increase of useful heat transfer rate is not so important. As the pipe spacing increases system reaches the steady state at a later time.

Second parameter is critical surface temperature (θ_C). For Objective-2 since there is convective boundary at the outer surface, temperature is not constant. From the information of temperature distribution surface temperature at the beginning of Solid-2 at the midpoint of x^* direction is critical. In other words once the surface

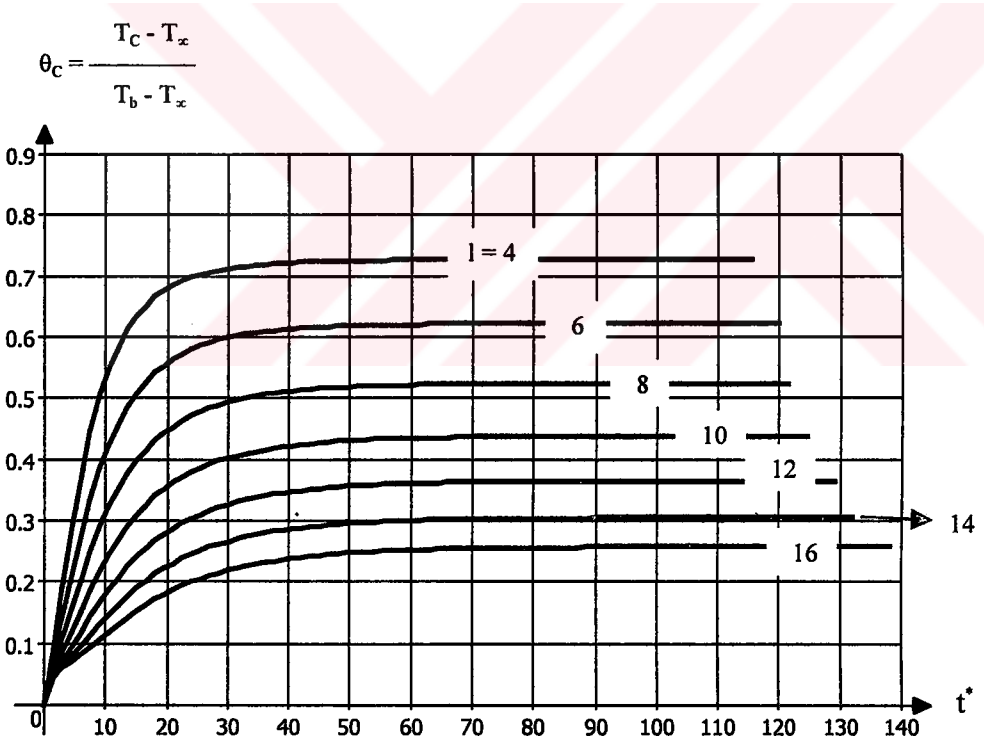

Figure 5.20 Time variation of critical surface temperature for different pipe spacing (l) values (Objective-2).

temperature at that point is satisfied, temperature requirement of all other nodes on the surface is satisfied. According to the Figures 3.4a and 3.4b, critical surface temperature is $\theta_{7,14,12}$. In general it is $\theta_{nxm,ny,nz1+1}$. Here, nxm is integer value of "(nx+1)/2". For various outside temperature values, limit values of critical temperature (θ_{CL}) are given in Table 5.3.

Table 5.3 Critical surface temperature limits (θ_{CL}) with various outside temperatures, for base temperature (T_b) of 5°C and min. surface temperature (T_{CL}) of 2°C, according to Eqn. 3.4b

Atmospheric Temperature (T_∞) °C	-3	-6	-9	-12	-15	-20	-30	-40
Critical surface temperature limits (θ_{CL})	0.625	0.727	0.786	0.823	0.850	0.880	0.914	0.933

From Table 5.3, if the critical surface temperature is kept grater or equal to unity, the system can protect the surface at any outside temperature value.

In Fig. 5.20 critical temperature values are plotted for different pipe spacing values. None of the curves reaches non-dimensional temperature value of 0.823 stated at the beginning of Section 5.3. This means that for outside temperature of –12°C, the system could not be enough to protect the surface with respect to reference values stated in Appendix A. According to maximum values reached in Figure 5.20, in Table 5.4 minimum outside temperatures are given for base temperature (T_b) of 5°C.

Table 5.4 Minimum outside temperatures for system to protect the surface:
Supply fluid temperature, θ_i = 5.41 (Corresponds to 80°C)
Pipe burial depth, h = 5
Reynolds number, Re_D = 100
Biot number for atmosphere, Bi_∞ = 0.88
Thermal conductivity of solid, k = 0.52 W/mK
*All reference values are listed in APPENDIX-A

Pipe Spacing (l)	4	6	8	10	12	14	16
Max. value of critical surface temp. in Fig.5.20	0.7274	0.6221	0.5237	0.4374	0.3647	0.3053	0.2576
Min. outside temperature °C	-6	-2.93	-1.30	-0.33	-	-	-

According to Table 5.4, the system is not effective for pipe spacing (l) values grater than 8. To be more effective, supply fluid temperature (θ_i) should be increased under the reference conditions that will be investigated in Section 5.3.2. One of the important conditions is Biot number for atmosphere ($Bi_\infty = h_\infty R/k$). It is the combination of combined heat transfer coefficient (h_∞) and thermal conductivity of solid. If thermal conductivity of solid is increased from 0.52 to 1.5 that time Biot number for atmosphere is reduced to 0.306. In this case, minimum outside temperatures are reduced as shown in Table 5.5.

Table 5.5 Minimum outside temperatures for system to protect the surface:
Supply fluid temperature, $\theta_i = 5.41$ (Corresponds to 80°C)
Pipe burial depth, $h = 5$
Reynolds number, $Re_D = 100$
Biot number for atmosphere, $Bi_\infty = 0.306$
Thermal conductivity of solid, $k = 1.5$ W/mK
*All reference values are listed in APPENDIX-A

Pipe Spacing (l)	4	6	8	10	12	14	16
Max. value of critical surface temp. in Fig. 5.21	1.3121	1.1107	0.9447	0.8076	0.6942	0.6007	0.5243
Min. outside temperature °C	<-50	<-50	-49.2	-10.6	-3.6	-2.5	-1.3

Third parameter is efficiency that is shown in Figure 5.21. Compared with Fig. 5.3, efficiency values does not also considerably change with respect to pipe spacing (l) for non-dimensional time value grater than 8.

$$\eta = \frac{Q_{USE}^{*}}{Q_{TOTAL}^{*}}$$

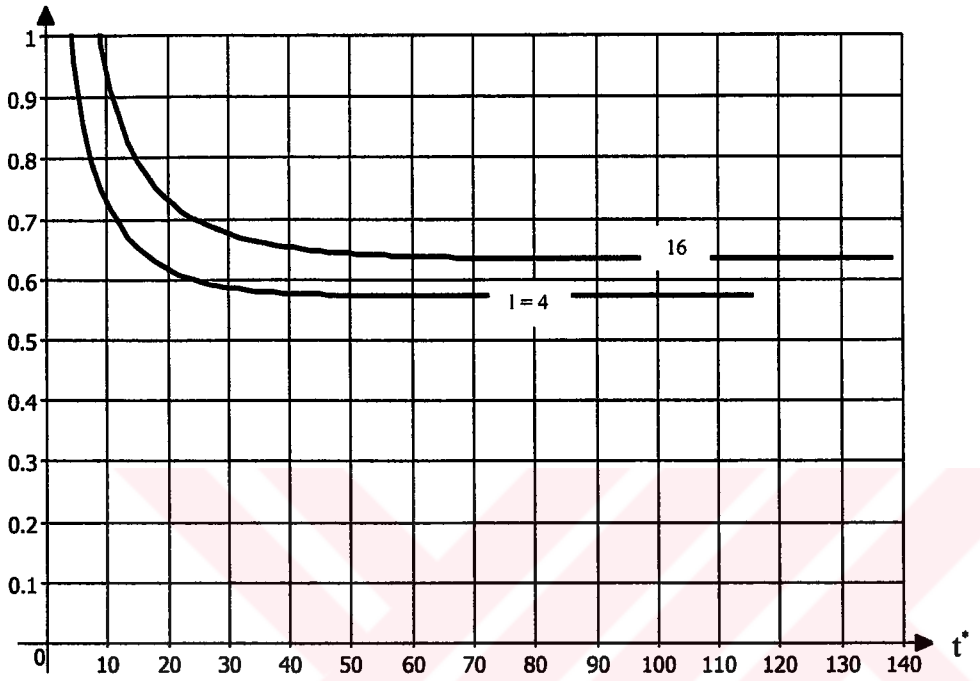

Figure 5.21 Time variation of efficiency for different pipe spacing (l) values (Objective-2).

5.3.2 PARAMETRIC ANALYSIS FOR DIFFERENT SUPPLY FLUID TEMPERATURES

Supply fluid temperature are selected as 4.23, 4.82, 5.41, 6.00, 6.59, 7.18, 7.64, 8.35, 8.94, 9.53 which corresponds to 60, 70, 80, 90, 100, 110, 120, 130, 140 and 150°C respectively according to Eqn. (3.4b) for base temperature (T_b) of 5°C and atmospheric temperature (T_∞) of −12°C.

First parameter is useful heat transfer that is shown in Fig. 5.22.

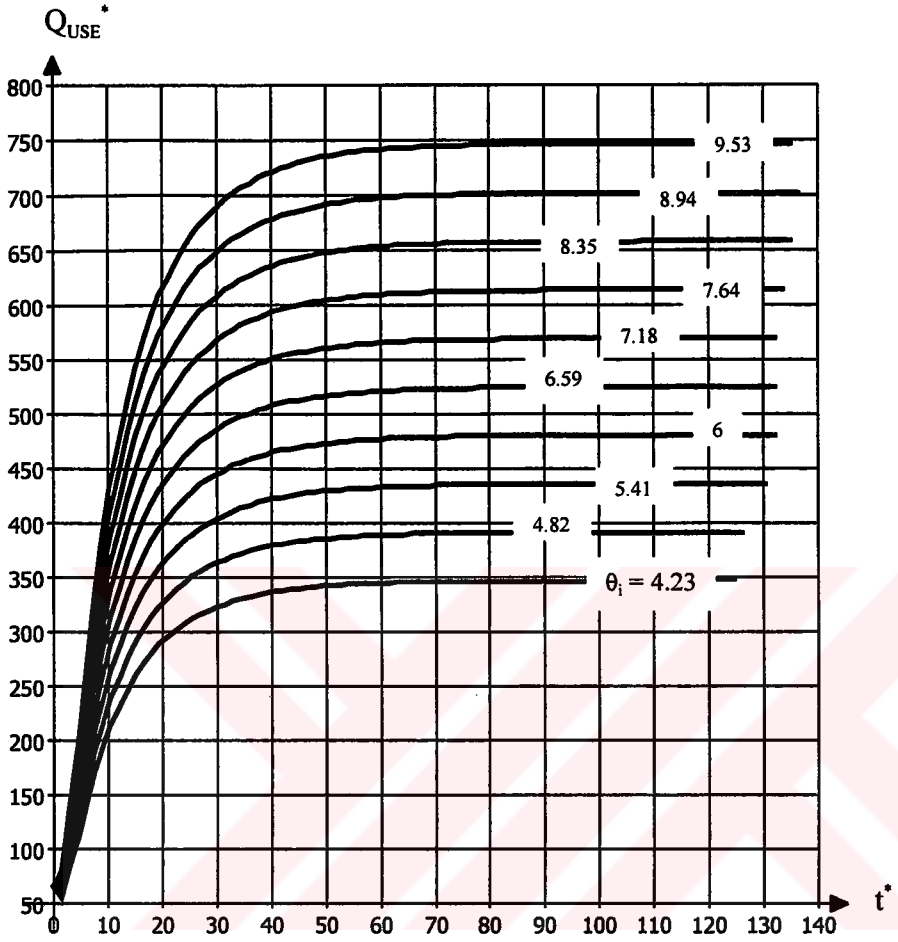

Figure 5.22 Time variation of useful heat transfer for different supply fluid temperature (θ_i) values (Objective-2).

Similar behavior is observed as in Fig. 5.6.

Second parameter is critical surface temperature (θ_C) that is shown in Fig. 5.23. Even though very high supply temperatures are involved, critical surface temperature values are not so high. Of course the reference values of other parameters such that

Biot Number for atmosphere (Bi_∞), pipe spacing (l) pipe burial depth (h) which are very effective on critical surface temperature values.

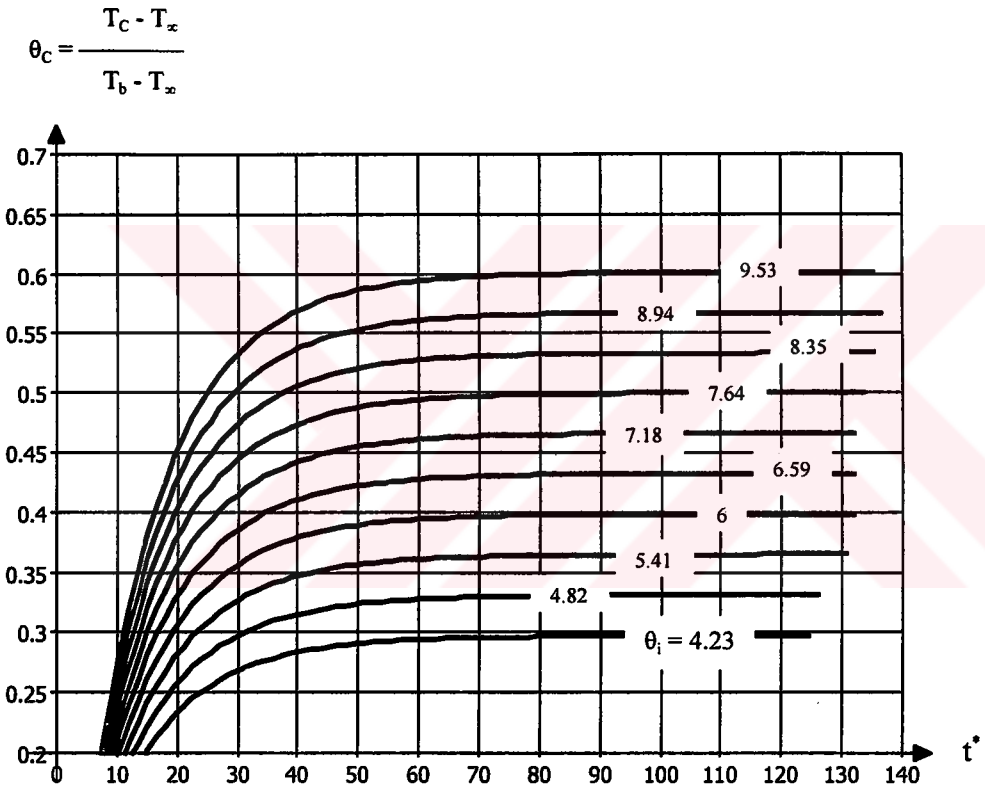

Figure 5.23 Time variation of critical surface temperature for different supply fluid temperature (θ_i) values (Objective-2).

Last parameter for this section is efficiency (η) that is shown in Fig. 5.24

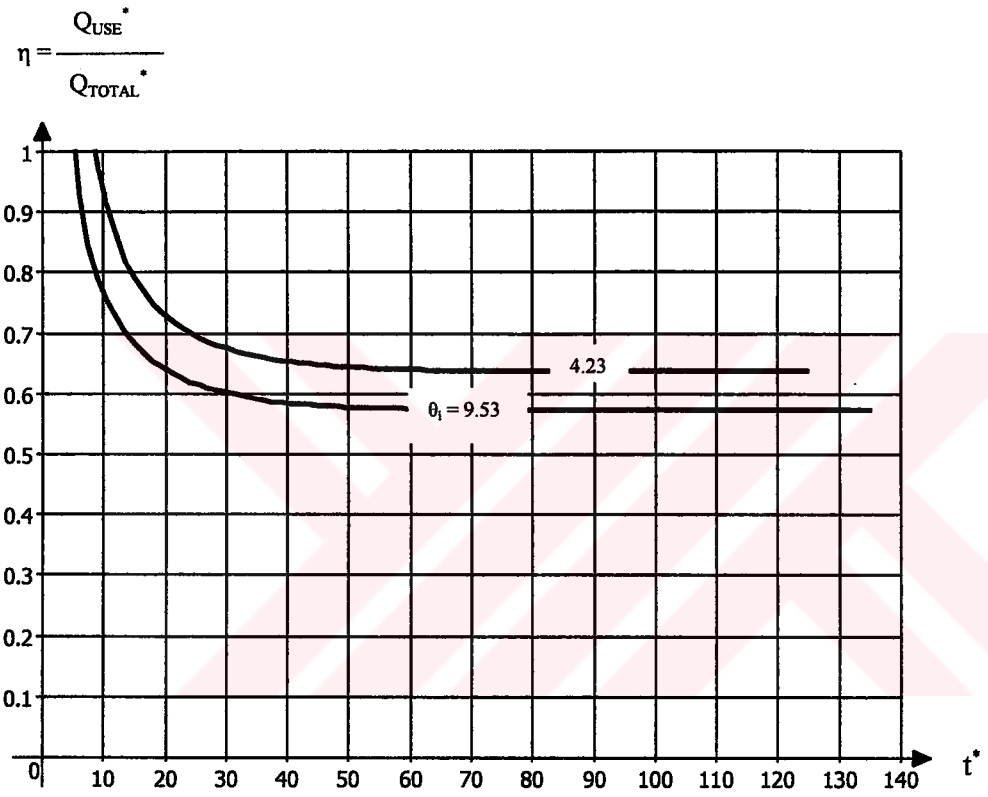

Figure 5.24 Time variation of efficiency for different supply fluid temperature (θ_i) values (Objective-2).

5.3.3 PARAMETRIC ANALYSIS FOR DIFFERENT REYNOLDS NUMBERS

In this section Reynolds Number values are selected as 100, 500, 1000, 2000, 4000, 6000, 8000, 10000 and 20000. As in previous sections, first parameter is useful heat transfer (Q_{USE}^*) that is shown in Fig. 5.25. Even though intermediate values

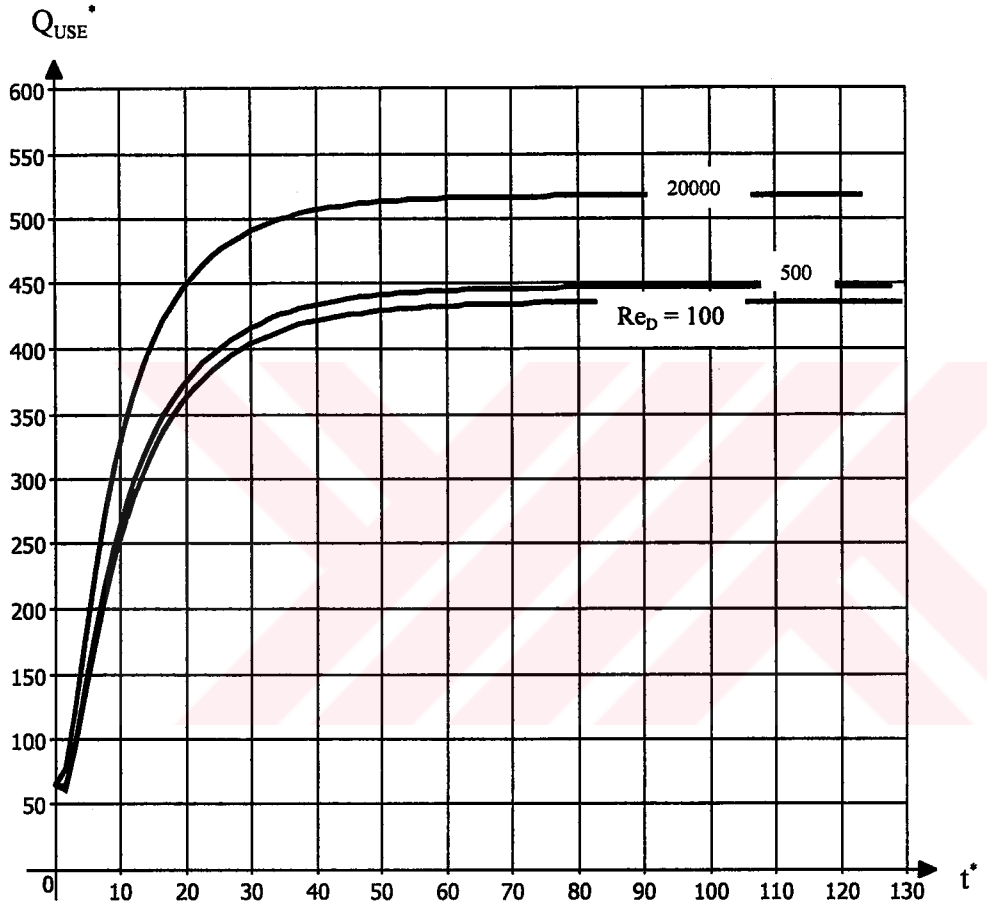

Figure 5.25 Time variation of useful heat transfer for different Reynolds Number(Re_D) values (Objective-2).

between 1000 and 10000 are involved, the result is very similar to Section 5.2.3. Useful heat transfer is slightly higher than the one in Section 5.2.3.

Second parameter is critical surface temperature (θ_C) that is shown in Fig. 5.26. Since the curves with values 2000 – 20000 are very closed to each other only 20000 is shown. Similarly 500 and 1000 are very closed to each other. Only 500 is shown.

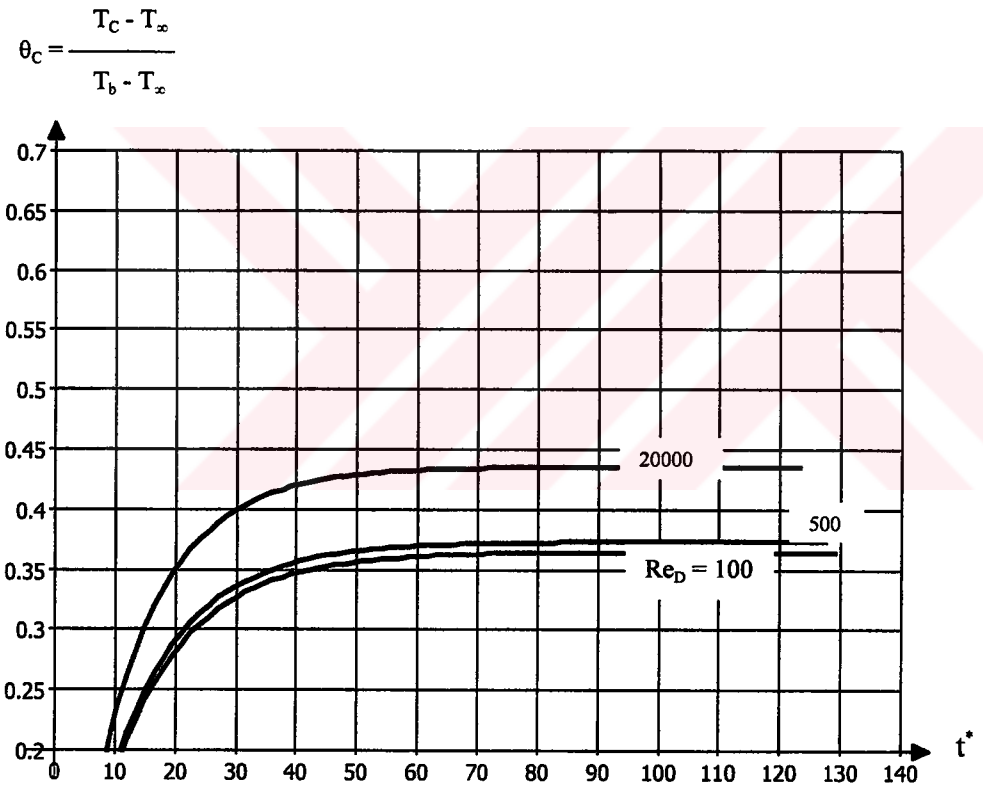

Figure 5.26 Time variation of useful heat transfer for different Reynolds Number(Re_D) values (Objective-2).

Last parameter of this section is efficiency that is shown in Fig.5.27.

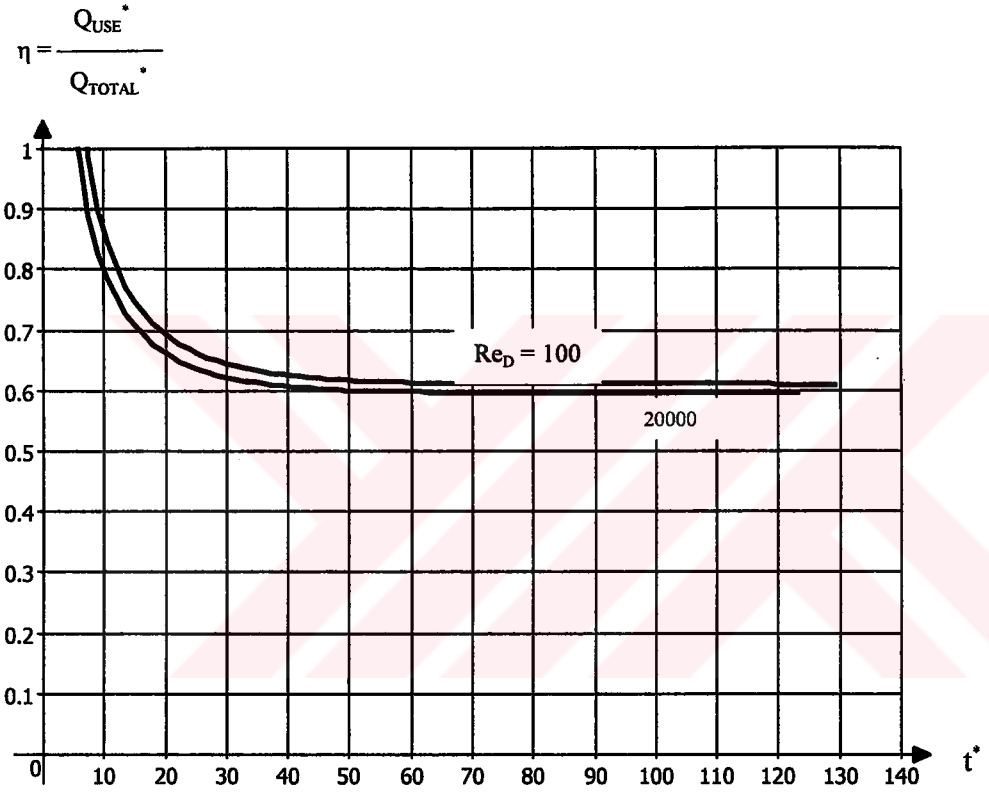

Figure 5.27 Time variation of efficiency for different Reynolds Number (Re_D) values (Objective-2).

5.3.4 PARAMETRIC ANALYSIS FOR DIFFERENT BIOT NUMBERS

This parameter is only used for Objective-2. As it is considered in Chapter 3, one of the important parameter is Biot number defined between solid surface and atmosphere ($Bi_\infty = h_\infty R/k$). It is the combination of combined heat transfer coefficient (h_∞) and thermal conductivity of solid (k). In this section, 0.2, 0.4, 0.6, 0.88, 1, 1.2, 1.5, 2 and 3 are selected.

First parameter is useful heat transfer (Q_{USE}^*) that is shown in Fig. 5.28.

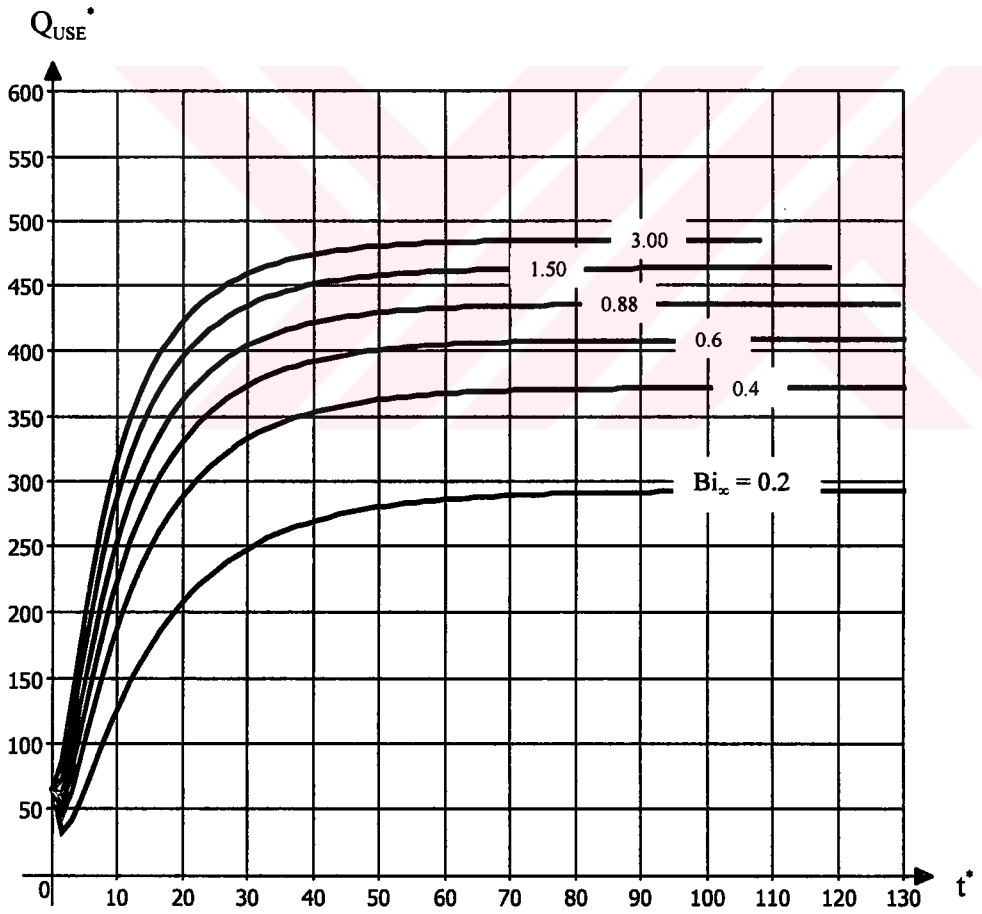

Figure 5.28 Time variation of useful heat transfer for different Biot Number (Bi_∞) values (Objective-2).

As the Biot Number (Bi_∞) increases useful heat transfer (Q_{USE}^*) values increases. But this increase becomes smaller for large Biot Numbers.

Second parameter is critical surface temperature (θ_C) that is shown in Fig. 5.29.

$$\theta_C = \frac{T_C - T_\infty}{T_b - T_\infty}$$

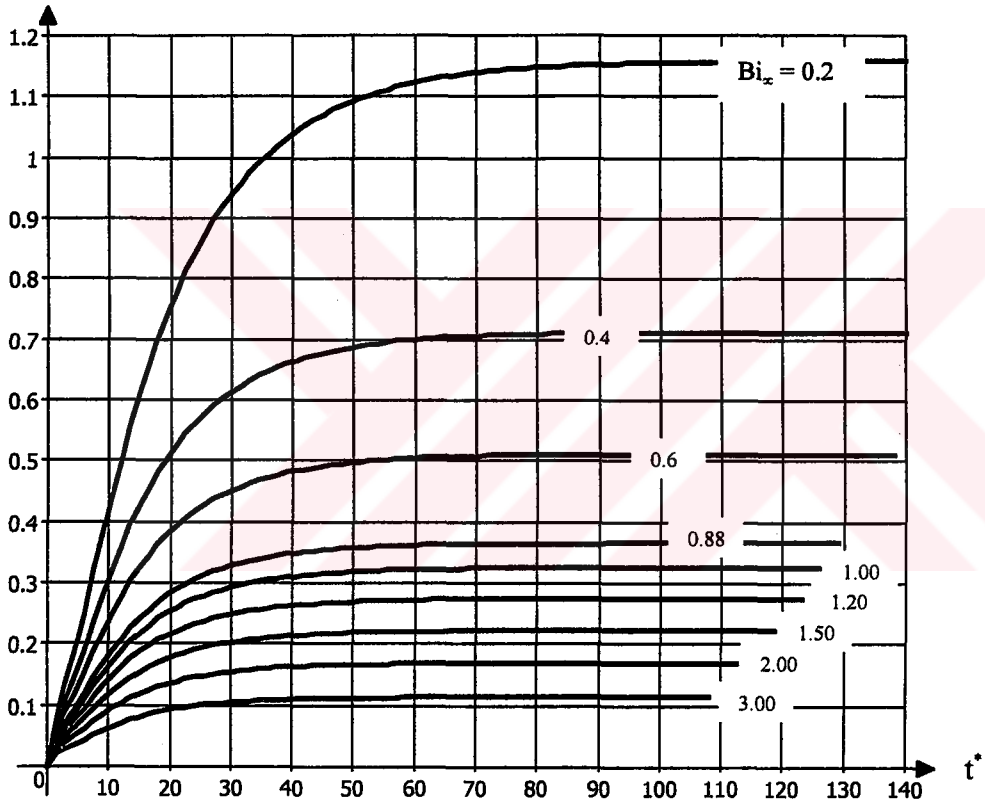

Figure 5.29 Time variation of critical surface temperature for different Biot Number (Bi_∞) values (Objective-2).

In contrast to Fig. 5.28, as the Biot Number (Bi_∞) values increases critical surface temperature (θ_C) decreases. When the values are compared with Table 5.3, Biot number values up to 0.4 can protect the system at a minimum outside temperature of –6°C, with respect to other reference values listed in Appendix A.

Third parameter is efficiency (η) that is shown in Figure 5.30

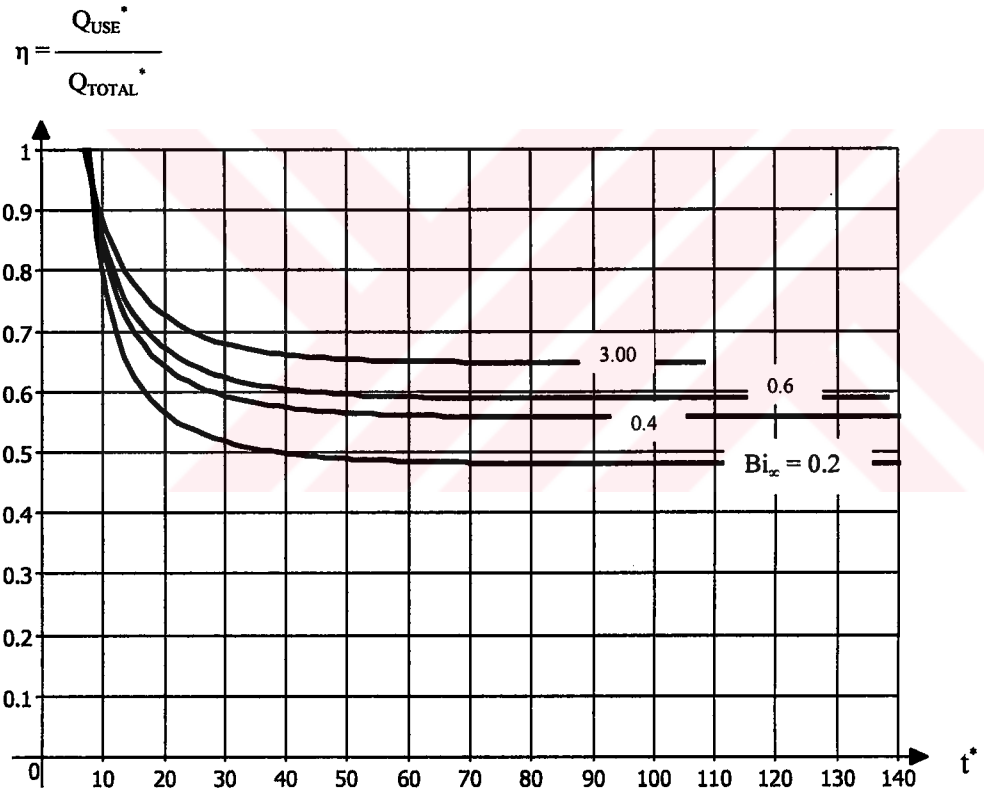

Figure 5.30 Time variation of efficiency for different Biot Number (Bi_∞) values (Objective-2).

5.3.5 PARAMETRIC ANALYSIS FOR DIFFERENT PIPE BURIAL DEPTHS

In Figures 5.30 – 5.32, time variation of useful heat transfer, critical surface temperature and efficiency values were plotted. For this section reference value of the distance c (Fig. 3.4a) is taken as 30 instead of 13.

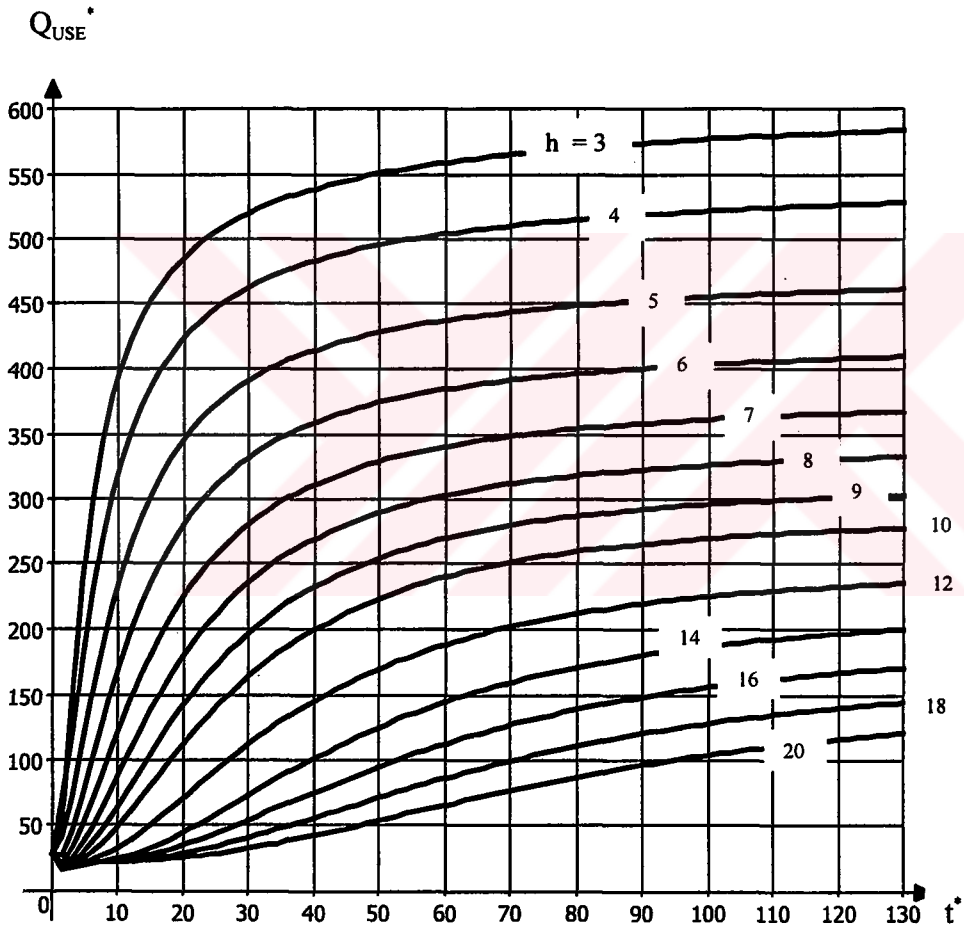

Figure 5.31 Time variation of useful heat transfer for different pipe burial depth (h) values (Objective-2).

In Fig. 5.31, useful heat transfer (Q_{USE}^{*}) decreases as the pipe burial depth increases.

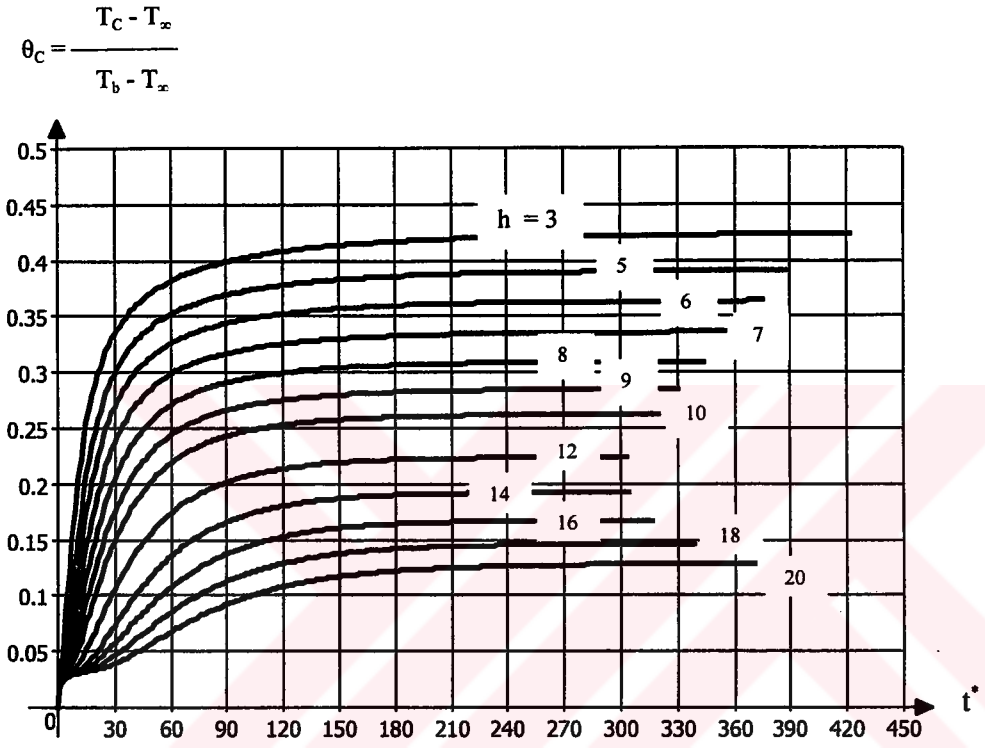

Figure 5.32 Time variation of critical surface temperature for different pipe burial depth (h) values (Objective-2).

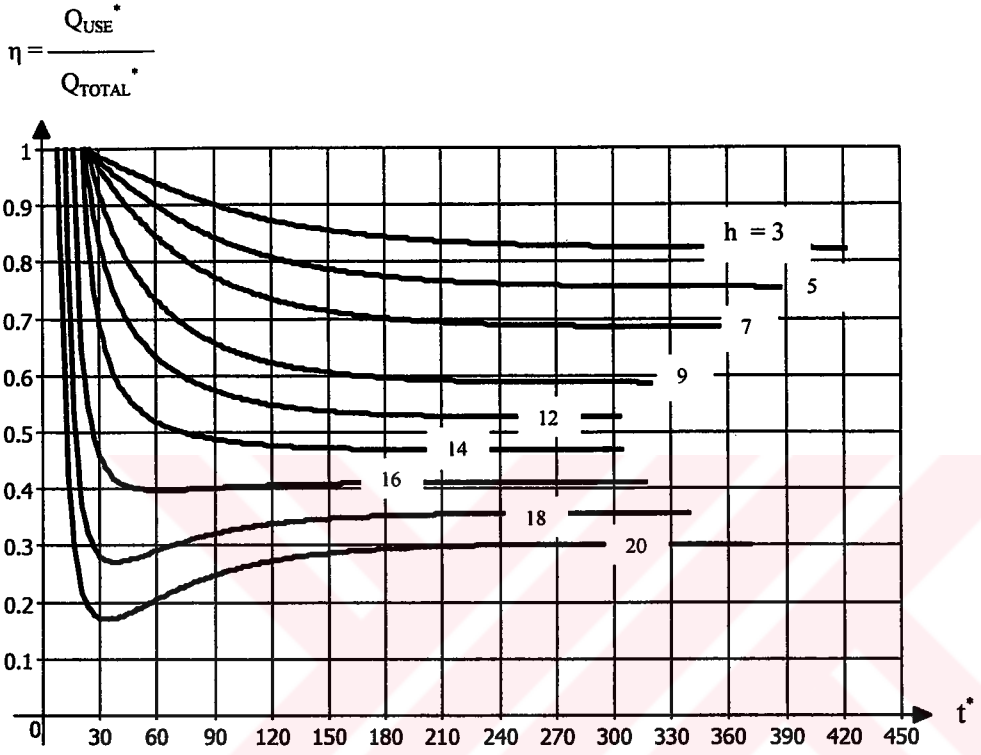

Figure 5.33 Time variation of efficiency for different pipe burial depth (h) values (Objective-2).

Similar behavior is observed as Fig. 5.15 (Objective-1).

CHAPTER 6

CONCLUSION

One of the major effecting parameter on the system is the pipe burial depth (h). To obtain good performance, it is necessary to keep the burial depth as low as possible. But, due to the effect of plane wheel load, pipe should be buried below a certain depth that should be identified as a result of strength calculations. Unfortunately there is no literature found giving directly the minimum burial depth of pipe. A complex analysis should be performed on wheel load effects on the buried pipe and mechanics of pavement material. The effect of pipe material and pipe thickness should also be investigated. As the pipe thickness is increased it can be possible to bury the pipes at a smaller depth. Moreover stress distribution in the solid may also be determined as the temperature distribution found in Chapter 3 of this thesis. Therefore "determination of minimum pipe burial depth for underground heating of airport aprons and runways" can be another thesis subject.

In this thesis, three-dimensional transient temperature distribution was obtained by creating a computer code using Finite Difference [7] technique in Visual Basic 6.0. For reference geometry there are 8918 unknown non-dimensional temperature values. Obtaining steady-state temperature distribution takes about 10 minutes. In that code no coefficient matrix is used. As a result, lower computer memory is occupied and high calculation speed is obtained. For Objective-1, system reaches steady state at timestep of 81 that corresponds to non-dimensional time (t^*) of 121.5. With respect to

the reference values in Appendix A, this value corresponds to approximately 71 hours. In actual fact, system does not reach steady state because, effective parameters such as the atmospheric temperature, Biot number (for Objective-2), heating load (for Objective -1) are time dependent. Also solid properties depends upon moisture content that is time dependent.

After obtaining temperature distributions, heat transfer values defined and evaluated according to principals stated in Chapter 4 where efficiency and melted snow thickness (for Objective-1) are defined. From Eqn. 4.39 non-dimensional melted snow thickness are also effected by solid density (ρ) besides snow density (ρ_s).

In Chapter 5, parameter variations for both objectives are considered separately. Fortunately, the transient response of the system is considered throughout this chapter. For example in Fig. 5.5 and Table 5.1, 50 cm snow is melted far before system reaches steady state.

For Objective-1, performance indicator of the system is efficiency (η) and melted snow thickness (t_{SM}^*). Atmospheric temperature (T_∞) is just a reference value. Due to melting process, surface temperature (T_S) is kept constant . Therefore atmospheric temperature has no physical effect on temperature distribution and heat transfer values. But to convert non-dimensional temperature values to dimensional temperature (according to Eqn. 3.4b) atmospheric temperature value is used.

From Section 5.2.1 it can be concluded that increasing of pipe spacing (l) grater than 10 is not so beneficial from heat transfer point of view.

For Objective-2, performance indicator of the system is efficiency and critical surface temperature. From the information of temperature distribution surface temperature at the beginning of Solid-2 at the midpoint of x^* direction is critical. In other words once the surface temperature at that point is satisfied, temperature requirement of all

other nodes on the surface is satisfied. Table 5.3 is very important for appreciation of obtained critical surface temperature values. Precautions must be taken when the atmospheric temperature (T_∞) suddenly drops and high wind (this cause increase in heat transfer coefficient (h_∞) and Biot Number (Bi_∞)). In such a case, higher supply fluid temperatures (θ_i) should be applied according to the requirements of Objective-2. This means that water with antifreeze solution is not enough as working fluid. Instead, high pressure steam or high temperature oil can be used. If high temperature oil is preferred, due to viscosity effect, higher pumping power should be supplied.

Consequently, this thesis is modeling and analysis of an underground heating of airport aprons and runways using 1st Law of Thermodynamics. As it is stated in Chapter 1, this analysis can be applied to any kind of floors open to atmosphere. This thesis can be a basic study for application of 2nd Law of Thermodynamics to underground heating systems for surfaces open to atmosphere. But, to obtain optimum system parameters such as pipe spacing (l), pipe diameter (D), type of working fluid and supply fluid temperature (θ_i), an economic analysis should also be performed with 2nd Law analysis.

APPENDIX A

LIST OF SYMBOLS WITH REFERENCE VALUES

Table A.1

Symbol	Description	Variable Name	Reference Value	Unit
A^*	First non-dimensional coefficient, Eqn. (3.24)	A	-	-
$A_{SOLID-2}$	Outer surface area of solid above the pipe (Lz_2 L)	-	-	m^2
$A_{SOLID-2}^*$	Non-dimensional outer surface area of solid above the pipe (lz_2 l)	No special variable name, (lz2*l) is used	840	-
B^*	Second non-dimensional coefficient , Eqn. (3.24)	B	-	-
Bi_∞	Biot number for atmosphere (h_∞ R/k)	Bio	0.88	-
Bi_m	Biot number for pipe (h_m R/k)	Bim	2.29	
C	Distance where the temperature reaches to the ground temperature T_b	-	-	m
c	Non-dimensional value of C (C/R)	c	13 and 30	-
C^*	Third non-dimensional coefficient , Eqn. (4.20)	-	-	-
c_p	Specific heat of solid	-	1840	J/kg K
c_{pw}	Specific heat of fluid	-	3728	J/kg K
D	Pipe diameter	-	0.034	m
dx	Value of increment in x^*	dx	1	-
dy	Value of increment in y^*	dy	1	-
dz	Value of increment in z^*	dz	1	-

Table A.1 (cont.)

Symbol	Description	Variable Name	Reference Value	Unit
Fo	Incremental Fourier Number based on solid parameters ($\alpha \Delta t/R^2$)	Fo	1.5	-
Fo_w	Incremental Fourier Number based on fluid parameters ($\alpha_w \Delta t/R^2$)	Fo_w	1.057 Fo	-
h	Non-dimensional burial depth of pipe (H/R)	h	5	-
H	Burial depth of pipe	-	-	m
h_∞	Combined heat transfer coefficient	hcomb	27	W/m^2K
h_m	Heat transfer coefficient for pipe	hfluid	70	W/m^2K
I_L	Latent heat for melting of snow	-	349000	J/kg
I_L^*	Non-dimensional latent heat for melting of snow, Eqn. (4.37)	LatentHeat	11.16	-
k	Thermal conductivity of solid	ksolid	0.52	W/mK
K_i	Nodal coefficient for entering fluid for first node in the pipe, Section 3.4.3, Eqn. (3.32)	Ki	-	-
k_w	Thermal conductivity of fluid	kfluid	0.546	W/mK
K_{xm1}	Nodal coefficient for neighboring node at $-x^*$ direction , Eqn. (3.12)	Kxm1	-	-
K_{xp1}	Nodal coefficient for neighboring node at $+x^*$ direction , Eqn. (3.12)	Kxp1	-	-
K_{ym1}	Nodal coefficient for neighboring node at $-y^*$ direction , Eqn. (3.12)	Kym1	-	-
K_{yp1}	Nodal coefficient for neighboring node at $+y^*$ direction , Eqn. (3.12)	Kyp1	-	-
K_{zm1}	Nodal coefficient for neighboring node at $-z^*$ direction , Eqn. (3.12)	Kzm1	-	-

Table A.1 (cont.)

Symbol	Description	Variable Name	Reference Value	Unit
K_{zp1}	Nodal coefficient for neighboring node at $+z^*$ direction , Eqn. (3.12)	Kzp1	-	-
L	Pipe spacing	-	-	m
l	Non-dimensional pipe spacing (L/R)	l	12	-
Lz_1	Length of Solid-1 in z direction	-	-	m
lz_1	Length of Solid-1 in z^* direction	lz1	10	-
Lz_2	Length of Solid-2 in z direction	-	-	m
lz_2	Length of Solid-2 in z^* direction	lz2	30 and 70	-
m	Mass flow rate in the pipe	-	-	kg/s
m_S	Mass of snow	-	-	kg
Nu_R	Nusselt Number (h_m R/k_w)	NuR	2.29	-
nx	Total number of nodes in x^* direction	nx	13	-
ny	Total number of nodes in y^* direction	ny	14	-
nz_1	Number of nodes in z^* direction of Solid-1	nz1	11	-
nz_2	Number of nodes in z^* direction of Solid-2	nz2	39	-
nztotal	Total number of nodes in z^* direction	nztotal	51	-
Pr	Prandtl Number	Pr	12	
Q_{DOWN}	Heat transfer rate to ground for any node at base plane	-	-	W
Q_{DOWN}^*	Non-dimensional value of Q_{DOWN}, Eqn. (4.11)	downderv	-	-
$Q_{DOWNSUM}^*$	Total non-dimensional heat transfer rate to ground , Eqn. (4.12)	DownHeat	-	-
Q_{LOAD}	Heating load	-	-	J
Q_{LOAD}^*	Non-dimensional heating load, Eqn (4.37)	HeatLoad	12182	-
Q_{LOSS}^*	Heat loss rate (Section 4.3)	LossHeat	-	-

Table A.1 (cont.)

Symbol	Description	Variable Name	Reference Value	Unit
Q_{SIDES}	Heat transfer rate to first side plane for any node at first side plane	-	-	W
Q_{SIDES}^*	Non-dimensional value of Q_{SIDES} , Eqn. (4.15)	sidederv	-	-
$Q_{SIDESSUM}^*$	Total non-dimensional heat transfer rate to atmosphere , Eqn. (4.16)	SideHeat	-	-
Q_{TOTAL}^*	Total heat transfer rate , Eqn. (4.24)	TotalHeat	-	-
Q_{UP}	Heat transfer rate to atmosphere for any node at outer surface	-	-	W
Q_{UP}^*	Non-dimensional value of Q_{UP} , Eqn. (4.7)	upderv	-	-
Q_{UPSUM}^*	Total non-dimensional heat transfer rate to atmosphere, Eqn. (4.8)	UpHeat	-	-
Q_{USE}^*	Useful heat transfer rate (Section 4.3)	UpHeatUsed	-	
Q_{USECUM}	Cumulative heat transfer , Eqn.(4.26)	-	-	J
Q_{USECUM}^*	Non-dimensional form of cumulative heat transfer, Eqn.(4.34).			
R	Pipe Radius	R	0.017	m
r	Radial direction defined from point of origin (x and y coordinates are zero)	-	-	m
r`	Radial direction defined from point with x coordinate is L and y coordinate is zero)	-	-	m
r`*	Non-dimensional value of r` (r'/R)	-	-	-
r^*	Non-dimensional value of r (r/R)	-	-	-
Re_D	Reynolds Number ($4\ m/\pi D\mu$)	ReD	100	
S_m	Sum of nodal coefficients , Eqn. (3.14))	Sm	-	-

Table A.1 (cont.)

Symbol	Description	Variable Name	Reference Value	Unit
S_{xm1}	Shape factor for neighboring node at -x direction	-	-	m or m^2
S_{xm1}^*	Non-dimensional shape factor for neighboring node at $-x^*$ direction	Sxm1	-	-
S_{xp1}	Shape factor for neighboring node at +x direction	-	-	m or m^2
S_{xp1}^*	Non-dimensional shape factor for neighboring node at $+x^*$ direction	Sxp1	-	-
S_{ym1}	Shape factor for neighboring node at -y direction	-	-	m or m^2
S_{ym1}^*	Non-dimensional shape factor for neighboring node at $-y^*$ direction	Sym1	-	-
S_{yp1}	Shape factor for neighboring node at +y direction	-	-	m or m^2
S_{yp1}^*	Non-dimensional shape factor for neighboring node at $+y^*$ direction	Syp1	-	-
S_{zm1}	Shape factor for neighboring node at -z direction	-	-	m or m^2
S_{zm1}^*	Non-dimensional shape factors for neighboring node at $-z^*$ direction	Szm1	-	-
S_{zp1}	Shape factor for neighboring node at +z direction	-	-	m or m^2
S_{zp1}^*	Non-dimensional shape factor for neighboring node at $+z^*$ direction	Szp1	-	-
t	Time	-	-	s
T_∞	Atmospheric temperature	-	-12	°C
t^*	Non-dimensional time ($\alpha t/R^2$)	Elapsedtime	-	-
T_b	Ground temperature	-	5	°C
T_C	Critical surface temperature, Section 5.3.1	-	-	°C
T_{CL}	Limit of critical surface temperature	-	2	°C
Timestep	Number of increment in t^*	Timestep	-	-
T_m	Fluid temperature	-	-	°C

Table A.1 (cont.)

Symbol	Description	Variable Name	Reference Value	Unit
T_{mi}	Supply fluid temperature	-	-	°C
T_{mo}	Fluid temperature at the exit of the pipe	-	-	°C
T_S	Surface temperature considered for Objective-1	-	0	°C
t_S^*	Thickness of snow or ice on $A_{SOLID-2}^*$	-	-	-
t_{SR}^*	Reference snow or ice thickness on $A_{SOLID-2}^*$	RefSnowThickness	30	-
t_{SM}	Melted snow thickness	-	-	m
t_{SM}^*	Dimensionless melted snow thickness (t_{SM}/R)	SnowThickness	-	-
$T_{X+1,y,z}^{P+1}$	Temperature value of neighboring node at +x direction at t+Δt	-	-	°C
$T_{x,Y+1,z}^{P+1}$	Temperature value of neighboring node at +y direction at t+Δt	-	-	°C
$T_{x,y,Z+1}^{P+1}$	Temperature value of neighboring node at +z direction at t+Δt	-	-	°C
$T_{x,y,Z-1}^{P+1}$	Temperature value of neighboring node at -z direction at t+Δt	-	-	°C
$T_{x,y,z}^{P}$	Temperature for pointer node (or center node) of any prismatic nodal element at any time t	-	-	°C
$T_{x,y,z}^{P+1}$	Temperature for pointer node (or center node) of any prismatic nodal element at any time t+Δt	-	-	°C
$T_{x,Y-1,z}^{P+1}$	Temperature value of neighboring node at -y direction at t+Δt	-	-	°C
$T_{X-1,y,z}^{P+1}$	Temperature value of neighboring node at -x direction at t+Δt	-	-	°C
V^*	Nodal volume, Eqn. (3.11)	V	-	-

Table A.1 (cont.)

Symbol	Description	Variable Name	Reference Value	Unit
x	Coordinate index value along x^* coordinate direction (Section 3.4.3)	x	-	-
x^*	Non-dimensional coordinate value	xx	-	-
y	Coordinate index value along y^* coordinate direction (Section 3.4.3)	y	-	-
y^*	Non-dimensional coordinate value	yy	-	-
z	Coordinate index value along z^* coordinate direction (Section 3.4.3)	z	-	-
z^*	Non-dimensional coordinate value	zz	-	-
σ	Stefan-Boltzman Constant	-	$5.669\ 10^{-8}$	W/m^2K^4
ϵ	Emissivity, Eqn. (3.1)	-	1	-
θ	Non-dimensional temperature $((T-T_\infty)/(T_b-T_\infty))$	Tp	-	-
α	Thermal diffusivity of solid	-	$1.378\ 10^{-7}$	m^2/s
η	Efficiency , Eqn. (4.26)	Efficiency	-	-
μ	Dynamic viscosity of fluid	-	$9.82\ 10^{-4}$	Pa s
ρ	Density of solid	solidden	2050	kg/m^3
ρ_S	Density of snow	snowden	88.8	kg/m^3
θ_∞	Dimensionless atmospheric temperature	-	0 (Const.)	-
θ_b	Non-dimensional base temperature	Tb	1 (Const.)	-
θ_C	Critical surface temperature, Section 5.3.1	Csurftemp	-	-
θ_{CL}	Limit of critical surface temperature	-	0.823	-
θ_i	Supply fluid temperature	Tmi	5.41	-
θ_{mo}	Non-dimensional exit fluid temperature	Texit	-	-
θ_S	Non-dimensional surface temperature	Tsurf	0.70588	-
ρ_S	Density of snow	snowden	88.8	kg/m^3
Δt	Time increment	-	-	s

Table A.1 (cont.)

Symbol	Description	Variable Name	Reference Value	Unit
α_w	Thermal diffusivity of fluid	-	$1.457\ 10^{-7}$	m^2/s
ρ_w	Density of fluid	-	1005	kg/m^3
$\theta_{x,y,Z+1}^{P+1}$	Non-dimensional temperature value of neighboring node at $+z^*$ direction at t^*+Fo	-	-	-
$\theta_{x,y,z}^{P}$	Non-dimensional temperature for pointer node (or center node) of any prismatic nodal element at any time t^*	-	-	-
$\theta_{x,y,z}^{P+1}$	Non-dimensional temperature for pointer node (or center node) of any prismatic nodal element at any time t^*+Fo	-	-	-
$\theta_{x,Y+1,z}^{P+1}$	Non-dimensional temperature value of neighboring node at $+y^*$ direction at t^*+Fo	-	-	-
$\theta_{X+1,y,z}^{P+1}$	Non-dimensional temperature value of neighboring node at $+x^*$ direction at t^*+Fo	-	-	-
$\theta_{x,y,Z-1}^{P+1}$	Non-dimensional temperature value of neighboring node at $-z^*$ direction at t^*+Fo	-	-	-
$\theta_{x,Y-1,z}^{P+1}$	Non-dimensional temperature value of neighboring node at $-y^*$ direction at t^*+Fo	-	-	-
$\theta_{X-1,y,z}^{P+1}$	Non-dimensional temperature value of neighboring node at $-x^*$ direction at t^*+Fo	-	-	-

APPENDIX B

ANALYSIS OF SOME NUMERICAL DIFFERENTIATION METHODS

In Chapter 4 heat transfer values have to be evaluated using the numerical differentiation methods for first partial derivatives. It is necessary to evaluate numerical derivatives at boundaries. Therefore, forward difference or backward difference [7] technique has to be used. Before evaluation of derivatives, it is necessary to consider curve fitting techniques for numerical values of non-dimensional temperature.

B.1 SOME NUMERICAL DIFFERENTIATION METHODS

In this appendix four curve fitting techniques will be used and compared.

1) First Order Lagrange Interpolating Polynomial (Line fitting, two points are necessary).
2) Second Order Lagrange Interpolating Polynomial (Three points are necessary).
3) Third Order Lagrange Interpolating Polynomial (Four points are necessary).
4) Cubic Spline Interpolation (Four points are used).

Although the above techniques does not require equally spaced data points, in this thesis the data points are equally spaced in x^*, y^* and z^* directions. As it is stated

before data spacings are dx, dy and dz respectively for x^*, y^* and z^* directions. In this appendix, dx will be used to denote data spacing.

B.1.1 FIRST ORDER LAGRANGE INTERPOLATING POLYNOMIAL

This polynomial is actually a line between two given non-dimensional temperature values. First Order Lagrange Interpolating polynomial can be written as:

$$L_1(x^*) = \frac{x^* - x_1}{x_0 - x_1} y_0 + \frac{x^* - x_0}{x_1 - x_0} y_1 \qquad \text{(B.1)}$$

where

x_0 : Independent variable (x^*) coordinate of first point

x_1 : Independent variable (x^*) coordinate of second point

y_0 : Dependent variable (θ) coordinate of first point

y_1 : Dependent variable (θ) coordinate of second point

The above coordinate values are placed in Figure B.1 for both forward difference and backward difference approximation. From Figure B.1,

$$x_0 - x_1 = -dx \qquad x_1 - x_0 = dx \qquad \text{(B.2)}$$

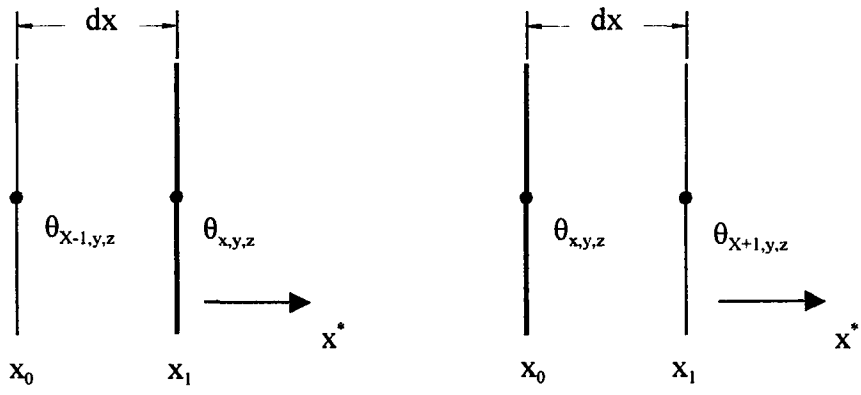

a) Backward difference b) Forward difference

Figure B.1. Forward and backward difference approx. of 1st Order Lagrange Interpolating Polynomial

Combining Equations (B.1) and (B.2) gives the following result.

$$L_1(x^*) = \frac{x^* - x_1}{-dx} y_0 + \frac{x^* - x_0}{dx} y_1 \qquad \text{(B.3)}$$

First derivative of Eqn. (B.1) with respect to x^* becomes:

$$\frac{d}{dx^*} L_1(x^*) = \frac{y_1 - y_0}{dx} \qquad \text{(B.4)}$$

This derivative value is constant at both points x_0 and x_1. From Figure B.1 for forward difference (derivative at point x_0) following equation can be written.

$$\frac{\partial\theta}{\partial x^*} = \frac{\theta_{X+1,y,z} - \theta_{x,y,z}}{dx} \qquad \text{(B.4)}$$

For backward difference (derivative at point x_1),

$$\frac{\partial\theta}{\partial x^*} = \frac{\theta_{x,y,z} - \theta_{X-1,y,z}}{dx} \qquad \text{(B.5)}$$

B.1.2 SECOND ORDER LAGRANGE INTERPOLATING POLYNOMIAL

Second Order Lagrange Interpolating polynomial can be written as:

$$L_2(x^*) = \frac{(x^* - x_1)(x^* - x_2)}{(x_0 - x_1)(x_0 - x_2)} y_0 + \frac{(x^* - x_0)(x^* - x_2)}{(x_1 - x_0)(x_1 - x_2)} y_1 + \frac{(x^* - x_0)(x^* - x_1)}{(x_2 - x_0)(x_2 - x_1)} y_2 \qquad \text{(B.6)}$$

where

x_0 : Independent variable (x^*) coordinate of first point

x_1 : Independent variable (x^*) coordinate of second point

x_2 : Independent variable (x^*) coordinate of third point

y_0 : Dependent variable (θ) coordinate of first point

y_1 : Dependent variable (θ) coordinate of second point

y_2 : Dependent variable (θ) coordinate of third point

Since the points are equally spaced with value dx, following equations can be written according to Figures B.2 and B.3.

$$x_0 - x_1 = -dx \qquad x_0 - x_2 = -2\,dx \qquad x_1 - x_0 = dx$$
$$x_1 - x_2 = -dx \qquad x_2 - x_0 = 2\,dx \qquad x_2 - x_1 = dx \qquad \text{(B.7)}$$

Combining Equations (B.6) and (B.7) gives the following result.

$$L_2(x^*) = \frac{(x^* - x_1)(x^* - x_2)}{2\,dx^2} y_0 + \frac{(x^* - x_0)(x^* - x_2)}{-dx^2} y_1 + \frac{(x^* - x_0)(x^* - x_1)}{2\,dx^2} y_2 \qquad \text{(B.8)}$$

First derivative of Eqn. (B.8) with respect to x^* becomes:

$$\frac{d}{dx^*} L_2(x^*) = \frac{0.5\,(x^* - x_2)}{dx^2} y_0 + \frac{0.5\,(x^* - x_1)}{dx^2} y_0 - \frac{(x^* - x_2)}{dx^2} y_1 - \frac{(x^* - x_0)}{dx^2} y_1$$
$$+ \frac{0.5\,(x^* - x_1)}{dx^2} y_2 + \frac{0.5\,(x^* - x_0)}{dx^2} y_2 \qquad \text{(B.9)}$$

In contrast to Section B.1.1, this derivative depends on position x^*. For forward difference approximation, x^* is replaced by x_0. So, Eqn. (B.9) is reduced to following equation.

$$\frac{d}{dx^*} L_2(x_0) = \frac{1}{2\,dx}(-3\,y_0 + 4\,y_1 - y_2) \qquad \text{(B.10)}$$

Partial derivative of θ with respect to x^* at point x_0 (forward difference approximation) according to Fig. B.2, can be written as:

$$\frac{\partial \theta}{\partial x^*} = \frac{1}{2\,dx}(-3\,\theta_{x,y,z} + 4\,\theta_{X+1,y,z} - \theta_{X+2,y,z}) \qquad \text{(B.11)}$$

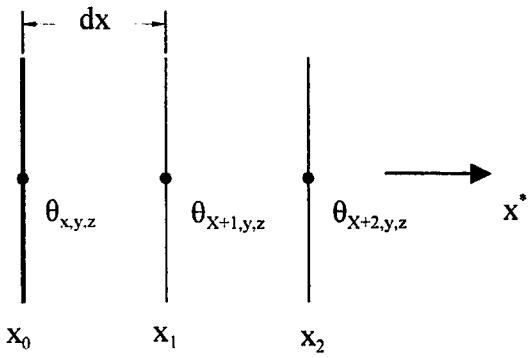

Figure B.2. Forward difference approx. of 2nd Order Lagrange Interpolating Polynomial

For backward difference approximation, x^* is replaced by x_2. So, Eqn. (B.9) reduced to following equation.

$$\frac{d}{dx^*} L_2(x_2) = \frac{1}{2\,dx}(y_0 - 4\,y_1 + 3\,y_2) \qquad \text{(B.12)}$$

Partial derivative of θ with respect to x^* at point x_2 (backward difference approximation) according to Fig. B.3 can be written as:

$$\frac{\partial\theta}{\partial x^*} = \frac{1}{2\,dx}(3\,\theta_{x,y,z} - 4\,\theta_{X-1,y,z} + \theta_{X-2,y,z}) \qquad \text{(B.13)}$$

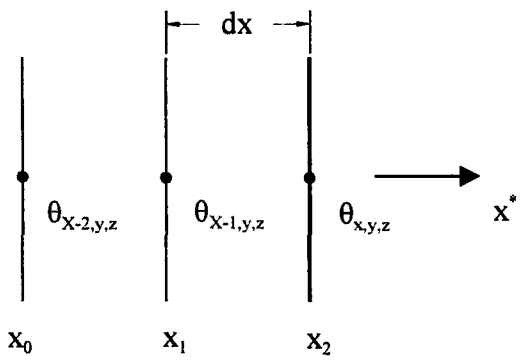

Figure B.3. Backward difference approx. of 2nd Order Lagrange Interpolating Polynomial

B.1.3 THIRD ORDER LAGRANGE INTERPOLATING POLYNOMIAL

Third Order Lagrange Interpolating polynomial can be written as:

$$L_3(x^*) = \frac{(x^* - x_1)(x^* - x_2)(x^* - x_3)}{(x_0 - x_1)(x_0 - x_2)(x_0 - x_3)} y_0 + \frac{(x^* - x_0)(x^* - x_2)(x^* - x_3)}{(x_1 - x_0)(x_1 - x_2)(x_1 - x_3)} y_1 +$$

$$+ \frac{(x^* - x_0)(x^* - x_1)(x^* - x_3)}{(x_2 - x_0)(x_2 - x_1)(x_2 - x_3)} y_2 + \frac{(x^* - x_0)(x^* - x_1)(x^* - x_2)}{(x_3 - x_0)(x_3 - x_1)(x_3 - x_2)} y_3 \quad \text{(B.14)}$$

where

x_0 : Independent variable (x^*) coordinate of first point

x_1 : Independent variable (x^*) coordinate of second point

x_2 : Independent variable (x^*) coordinate of third point

x_3 : Independent variable (x^*) coordinate of fourth point

y_0 : Dependent variable (θ) coordinate of first point

y_1 : Dependent variable (θ) coordinate of second point

y_2 : Dependent variable (θ) coordinate of third point

y_3 : Dependent variable (θ) coordinate of fourth point

Similar derivation procedure is followed for first derivative at point x_0 (forward difference approximation) and first derivative at point x_3 (backward difference approximation). As a result, for forward difference:

$$\frac{d}{dx^*} L_3(x_0) = \frac{1}{3\,dx}(-5.5\,y_0 + 9\,y_1 - 4.5\,y_2 + y_3) \qquad \text{(B.15)}$$

Partial derivative of θ with respect to x^* at point x_0 (forward difference approximation) according to Fig. B.4 can be written as:

$$\frac{\partial \theta}{\partial x^*} = \frac{1}{3\,dx}(-5.5\,\theta_{x,y,z} + 9\,\theta_{X+1,y,z} - 4.5\,\theta_{X+2,y,z} + \theta_{X+3,y,z}) \qquad \text{(B.16)}$$

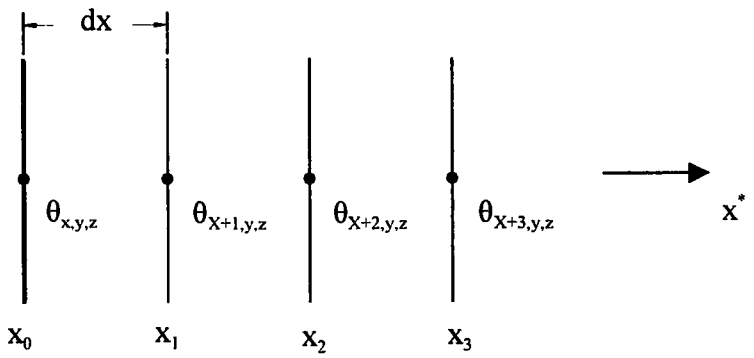

Figure B.4. Forward difference approx. of 3rd Order Lagrange Interpolating Polynomial

For backward difference,

$$\frac{d}{dx^*} L_3(x_3) = \frac{1}{3\,dx}(-y_0 + 4.5\,y_1 - 9\,y_2 + 5.5\,y_3) \qquad \text{(B.17)}$$

Partial derivative of θ with respect to x^* at point x_3 (backward difference approximation) according to Fig. B.5 can be written as:

$$\frac{\partial\theta}{\partial x^*} = \frac{1}{3\,dx}(5.5\,\theta_{x,y,z} - 9\,\theta_{X-1,y,z} + 4.5\,\theta_{X-2,y,z} - \theta_{X-3,y,z}) \qquad \text{(B.18)}$$

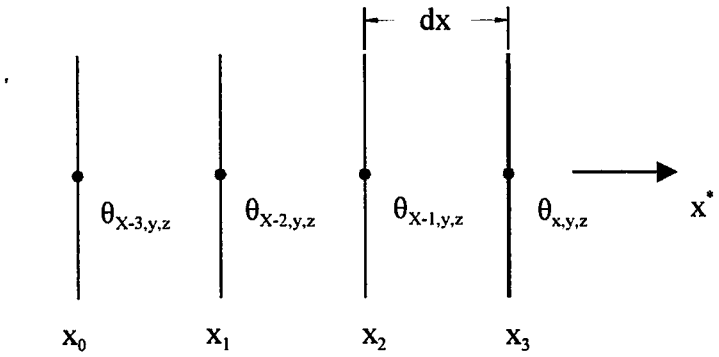

Figure B.5. Backward difference approx. of 3rd Order Lagrange Interpolating Polynomial

B.1.4 CUBIC SPLINE INTERPOLATION

Similar to 3rd Order Lagrange Interpolating Polynomial, for Cubic Spline [7] interpolation four data points are used. Figures B.4 and B.5 can also be used to describe the derivation procedure for numerical derivative using Cubic Spline. By definition, second derivatives at first (x_0) and last points (x_3) are zero. Unknown second derivatives at x_1 (Sd_1) and at x_2 (Sd_2) can be found from the simultaneous solution of following two equations.

$$4\,dx\,Sd_1 + dx\,Sd_2 = \frac{6}{dx}(y_2 - y_1) + \frac{6}{dx}(y_0 - y_1) \qquad \text{(B.19)}$$

$$dx\,Sd_1 + 4\,dx\,Sd_2 = \frac{6}{dx}(y_3 - y_2) + \frac{6}{dx}(y_1 - y_2) \qquad \text{(B.20)}$$

Unknown values are obtained as:

$$Sd_1 = \frac{2}{5\,dx^2}(4\,y_0 - 9\,y_1 + 6\,y_2 - y_3) \qquad \text{(B.21)}$$

$$Sd_2 = \frac{2}{5\,dx^2}(-\,y_0 + 6\,y_1 - 9\,y_2 + 4\,y_3) \qquad \text{(B.22)}$$

In Cubic Spline, there are three intervals each having different interpolation equations. For forward difference approximation, the equation of first interval is differentiated at x_0. Similarly for backward difference approximation, the equation of last interval is differentiated at x_3. So, the equation of first interval is:

$$f_1(x^*) = \frac{Sd_1}{6\,dx}(x^* - x_0)^3 + \frac{y_0}{dx}(x_1 - x^*) + \left(\frac{y_1}{dx} - \frac{1}{6}Sd_1\,dx\right)(x^* - x_0) \qquad \text{(B.23)}$$

First order differentiation with respect to x^* at x_0 gives the following result.

$$\frac{d}{dx^*}f_1(x_0) = \frac{y_1}{dx} - \frac{1}{6}Sd_1\,dx - \frac{y_0}{dx} \qquad \text{(B.24)}$$

Substitution of Eqn. (B.21) into Eqn. (B.24) and rearranging the terms, results in following equation.

$$\frac{d}{dx^*}f_1(x_0) = \frac{1}{15\,dx}(-19\,y_0 + 24\,y_1 - 6\,y_2 + y_3) \qquad \text{(B.25)}$$

Partial derivative of θ with respect to x^* at point x_0 (forward difference approximation) according to Fig. B.4 can be written as:

$$\frac{\partial\theta}{\partial x^*} = \frac{1}{15\,dx}(-19\,\theta_{x,y,z} + 24\,\theta_{X+1,y,z} - 6\,\theta_{X+2,y,z} + \theta_{X+3,y,z}) \qquad \text{(B.26)}$$

To evaluate backward difference approximation, Cubic Spline Interpolation equation of last interval is written as:

$$f_1(x^*) = \frac{Sd_2}{6\,dx}(x_3 - x^*)^3 + \left(\frac{y_2}{dx} - \frac{1}{6}Sd_2\,dx\right)(x_3 - x^*) + \frac{y_3}{dx}(x^* - x_3) \qquad \text{(B.27)}$$

First order differentiation with respect to x^* at x_3 gives the following result.

$$\frac{d}{dx^*}f_3(x_3) = -\frac{y_2}{dx} + \frac{1}{6}Sd_2\,dx + \frac{y_3}{dx} \qquad \text{(B.28)}$$

Partial derivative of θ with respect to x^* at point x_3 (backward difference approximation) according to Fig. B.5 can be written as:

$$\frac{\partial\theta}{\partial x^*} = \frac{1}{15\,dx}(19\,\theta_{x,y,z} - 24\,\theta_{X-1,y,z} + 6\,\theta_{X-2,y,z} - \theta_{X-3,y,z}) \qquad \text{(B.29)}$$

Up to this point four numerical differentiation method for evaluation of first partial derivatives were summarized. Next step is comparison of their accuracy and selection

of the best method for numerical differentiation that will be used to calculate heat transfer.

B.2 COMPARISON OF NUMERICAL DIFFERENTIATION METHODS

To compare the performance of these numerical methods, the values of partial derivatives must be known at the related boundary. In Chapter 3 boundary conditions were considered in detail. From the first boundary condition (BC-1) following relation is valid at y = h:

$$\frac{\partial\theta}{\partial y^*} + Bi_\infty\theta = 0 \qquad (B.30)$$

where Bi_∞ is Biot number defined between solid surface and atmosphere. So,

$$\frac{\partial\theta}{\partial y^*} = -Bi_\infty\theta \qquad (B.31)$$

Once the non-dimensional temperature distribution is obtained at any timestep at any point on this boundary, partial derivative of θ with respect to y^* can be determined from the Biot Number and non-dimensional temperature value of this point. So that this value can be compared with the partial derivative of θ with respect to y^* obtained using the methods in previous section. This comparison is actually a comparison of two numerically obtained values. Therefore, this type of comparison is called as *relative comparison.*

From BC-2, BC-4, BC-6 and BC-8 following condition can be written:

$$\frac{\partial \theta}{\partial x^*} = 0 \qquad \text{(B.32)}$$

At these boundaries the value of partial derivative of θ with respect to x^* is absolutely zero. Therefore, this type of comparison is called as *absolute comparison.*

B.3 COMPARISON RESULT

Using the base data values of Fig. 3.16 according to relative comparison, first order numerical differentiation with cubic spline in Equations (B.26) and (B.29) gave the best result. However according to absolute comparison, first order numerical differentiation with third order Lagrange Interpolating polynomials in Equations (B.16) and (B.18) gave the best result.

Consequently for the numerical differentiation in Chapter 4, differentiation of Third Order Lagrange Interpolating Polynomial as in Equations (B.16) and (B.18) was used.

APPENDIX C

LIST OF COMPUTER PROGRAM FOR SOLUTION OF FINITE DIFFERENCE EQUATIONS (SAMPLE FOR OBJECTIVE-1)

```
Private Sub cmdTS3D4b_Click()

  l = 12
  h = 5!
   c = 13!
       lz1 = 10!
          lz2 = 70!


dx = 1!
 dy = 1!
  dz = 1!


   hcomb = 27
   R = 0.017
   ksolid = 0.52
   kfluid = 0.546
    Pr = 12
    ReD = 100

  solidden = 2050 'kg/cubicmeter
  snowden = 88.8  'kg/cubicmeter

  LatentHeat = 11.16
  RefSnowThickness = 30
```

```
If ReD < 2300 Then
  NuR = 2.18
Else
  NuR = 0.5 * 0.023 * (ReD ^ 0.8) * (Pr ^ 0.33)
End If


  Bio = hcomb * R / ksolid

hfluid = NuR * kfluid / R

  Bim = hfluid * R / ksolid

    Tb = 1!
     Tsurf = 0.70588

     Tmi = 5.41

     Tbase = 278
      Tinfinity = 261


nx = CInt(l / dx) + 1
ny = CInt(c / dy) + 1
  nz1 = CInt(lz1 / dz) + 1
    nz2 = CInt(lz2 / dz) - 1

 nztotal = 2 * nz1 + nz2

     nxm = Fix((nx + 1) / 2)
      nzm = Fix((nztotal + 1) / 2)

ybase = -(c - h)
  ytop = h
   xleft = 0!
    xright = l

'w: Relaxation factor
w = 1.7

ReDim Tin(nx, ny, nztotal)

  ReDim T(nx, ny, nztotal)
```

```
ReDim Tp(nx, ny, nztotal)


'GENERATION OF INITIAL CONDITIONS AND BOUNDARY CONDITIONS

zz = -dz

zcount = 0

nxx = nx


  Do
   zz = zz + dz
    zcount = zcount + 1

      yy = ybase - dy
       ycount = 0

   If zcount >= nz1 Then
        xxm = (1 / (nz2 + 1)) * (nz1 + nz2 - zz / dz)

         nxx = Fix(xxm / dx) + 1
   End If
     Do
       yy = yy + dy
        ycount = ycount + 1

        xx = xleft - dx
         xcount = 0

       Do
          xx = xx + dx
           xcount = xcount + 1



   Tinitial = (Tb - Tsurf) * (h - yy) / c + Tsurf

   Tin(xcount, ycount, zcount) = Tinitial

   T(xcount, ycount, zcount) = Tinitial
```

```
    Tp(xcount, ycount, zcount) = Tinitial



        Loop Until xcount = nxx
      Loop Until ycount = ny
    Loop Until zcount = nz1 + nz2 + 1

'Close #1

'GENERATION OF EQUATIONS

ElapsedTime = 0

Timestep = 0

UpHeatCum = 0
Iternum = 0

Fo = 1.5

    Fow = 1.057 * Fo

     A = ReD * Pr * Fow * (1 / (2 * dz))
      B = NuR * Fow


 ToutputFormatting2
Do

Timestep = Timestep + 1


ElapsedTime = ElapsedTime + Fo

iterstep = 0

            For k = 1 To nz1 + nz2 + 1

              For j = 1 To ny - 1

                For i = 1 To nx
```

```
            Tin(i, j, k) = Tp(i, j, k)

              Next i

             Next j

            Next k


Do

  iterstep = iterstep + 1
nxx = nx
zz = 0!
z = 1

            For k = 1 To nz1 + nz2 + 1

             For j = 1 To ny - 1

              For i = 1 To nx

    T(i, j, k) = w * Tp(i, j, k) + (1 - w) * T(i, j, k)

              Next i

             Next j

            Next k


  Do
    zz = zz + dz
     z = z + 1

       yy = ybase
        y = 1


   If z >= nz1 Then
        xxm = (1 / (nz2 + 1)) * (nz1 + nz2 - zz / dz)
```

```
        nxx = Fix(xxm / dx) + 1
    End If

      Do
        yy = yy + dy
        y = y + 1

        xx = xleft - dx
        x = 0

        Do
          xx = xx + dx
          x = x + 1

SysGeometry


    Loop Until x = nxx
     Loop Until y = ny - 1
      Loop Until z = nz1 + nz2 + 1

Loop Until Abs(Tp(nxm, ny - 3, nz1 + 1) - T(nxm, ny - 3, nz1 + 1)) < 0.0000005

Iternum = Iternum + iterstep


ToutputFormatting2



 SScheck = (Abs(Tp(nxm, ny - 3, nz1 + 1) - Tin(nxm, ny - 3, nz1 + 1) < 0.000005))

 Loop Until SScheck

txtOutletTemp.Text = Tp(nx, ny - CInt(h / dy), nz1 + 1)

txtL.Text = l



End Sub
```

```
Private Sub SysGeometry()


'IMPORTANT REGION SEPERATORS


 Solid13z = (z < nz1)

  Solid2z = (z >= nz1)

    Solid2xy1 = (xx * xx + yy * yy > 2 + EOR)

      Solid2xy2 = ((xx - l) ^ 2 + yy * yy > 2 + EOR)

        Solid2xy = (Solid2xy1 And Solid2xy2)

        LR = (x = 1 Or x = nx)

         Inside = (Not LR)

     Solid13LR = (Solid13z And LR)

       Solid2LR = (Solid2z And LR And Solid2xy)

  S13inside = (Solid13z And Inside)

    S2inside = (Solid2z And Inside And Solid2xy)


'THE GEOMETRIC COEFFICIENTS

  'LEFT AND RIGHT BOUNDARIES


     If Solid13LR Or Solid2LR Then

       Sym1 = dx * dz / (2 * dy)
```

```
    Sxp1 = dy * dz / dx
     Syp1 = dx * dz / (2 * dy)
      Sxm1 = dy * dz / dx
       Szp1 = dx * dy / (2 * dz)
        Szm1 = dx * dy / (2 * dz)
          V = 0.5 * dx * dy * dz
    If y = ny Then
     Sxp1 = dy * dz / (2 * dx)
      Syp1 = 0.5 * dx * dz * Bio
       Sxm1 = dy * dz / (2 * dx)
        Szp1 = dx * dy / (4 * dz)
         Szm1 = dx * dy / (4 * dz)
           V = 0.25 * dx * dy * dz
     End If
    If x = nx Then Sxp1 = 0
      If x = 1 Then Sxm1 = 0
End If

'INSIDE
  If S13inside Or S2inside Then
    Sym1 = dx * dz / dy
     Sxp1 = dy * dz / dx
      Syp1 = dx * dz / dy
```

```
        Sxm1 = dy * dz / dx

        Szp1 = dx * dy / dz

        Szm1 = dx * dy / dz

          V = dx * dy * dz

      If y = ny Then

       Sxp1 = dy * dz / (2 * dx)

        Syp1 = dx * dz * Bio

        Sxm1 = dy * dz / (2 * dx)

        Szp1 = dx * dy / (2 * dz)

        Szm1 = dx * dy / (2 * dz)

          V = 0.5 * dx * dy * dz

      End If


   End If

'NODE N1

zzz = (z = nz1 Or z = nz1 + nz2 + 1)
  xyN1 = (xx = 0 And yy = 0)

  xyN1a = (xx = 1 And yy = 0)

    If zzz And (xyN1 Or xyN1a) Then

      Sym1 = 0.25 * dz

      If xyN1 Then

        Sxp1 = 0.5 * dz

        Sxm1 = 0
      End If
```

```
If xyN1a Then
  Sxp1 = 0
  Sxm1 = 0.5 * dz
End If
   Syp1 = 0.25 * dz

  If z = nz1 Then
    Szp1 = 0.5 * pi * Bim
    Szm1 = 0.5 / dz
  Else
    Szp1 = 0.5 / dz
    Szm1 = 0.5 * pi * Bim
  End If
   V = 0.25 * dz
End If

'NODE N2
xyN2 = (xx = 0 And yy = 1)
xyN2a = (xx = 1 And yy = 1)
  If zzz And (xyN2 Or xyN2a) Then
    Sym1 = 0.25 * dz
    If xyN2 Then
     Sxp1 = 0.817 * dz
```

```
        Sxm1 = 0
       End If

       If xyN2a Then

        Sxp1 = 0

        Sxm1 = 0.817 * dz
       End If

         Syp1 = 0.5 * dz


        If z = nz1 Then

         Szp1 = 0.272 / dz

         Szm1 = 0.5 / dz

        Else

         Szp1 = 0.5 / dz

         Szm1 = 0.272 / dz

        End If

         V = 0.386 * dz

   End If


'NODE N3
 xyN3 = (xx = 0 And yy = -1)

  xyN3a = (xx = 1 And yy = -1)


    If zzz And (xyN3 Or xyN3a) Then

      Sym1 = 0.5 * dz

      If xyN3 Then
```

```
        Sxp1 = 0.817 * dz

        Sxm1 = 0
      End If

      If xyN3a Then

        Sxp1 = 0
        Sxm1 = 0.817 * dz
      End If

         Syp1 = 0.25 * dz


       If z = nz1 Then

        Szp1 = 0.272 / dz

        Szm1 = 0.5 / dz

       Else

        Szp1 = 0.5 / dz

        Szm1 = 0.272 / dz

       End If

        V = 0.386 * dz

   End If

'NODE N4
 xyN4 = (xx = 1 And yy = 0)

  xyN4a = (xx = 1 - dx And yy = 0)


   If zzz And (xyN4 Or xyN4a) Then

    Sym1 = 0.817 * dz

    If xyN4 Then
      Sxp1 = dz
```

```
      Sxm1 = 0.5 * dz
    End If

    If xyN4a Then
      Sxp1 = 0.5 * dz

      Sxm1 = dz
    End If

       Syp1 = 0.817 * dz


      If z = nz1 Then

       Szp1 = 0.544 / dz

       Szm1 = 1 / dz

      Else

       Szp1 = 1 / dz

       Szm1 = 0.544 / dz

      End If

       V = 0.772 * dz

  End If
'NODE N5

xyN5 = (xx = 1 And yy = 1)

 xyN5a = (xx = 1 - dx And yy = 1)


  If zzz And (xyN5 Or xyN5a) Then

    Sym1 = 0.817 * dz

    If xyN5 Then
      Sxp1 = dz
```

```
    Sxm1 = 0.817 * dz
  End If

  If xyN5a Then
    Sxp1 = 0.817 * dz

    Sxm1 = dz
  End If

    Syp1 = dz

   If z = nz1 Then

    Szp1 = 0.92 / dz

    Szm1 = 1 / dz

   Else

    Szp1 = 1 / dz

    Szm1 = 0.92 / dz

   End If

    V = 0.96 * dz


 End If

'NODE N6
xyN6 = (xx = 1 And yy = -1)

 xyN6a = (xx = 1 - dx And yy = -1)


 If zzz And (xyN6 Or xyN6a) Then

   Sym1 = dz

   If xyN6 Then
    Sxp1 = dz

    Sxm1 = 0.817 * dz
```

```
    End If

    If xyN6a Then
      Sxp1 = 0.817 * dz

      Sxm1 = dz
    End If

       Syp1 = 0.817 * dz

     If z = nz1 Then

       Szp1 = 0.92 / dz

       Szm1 = 1 / dz

     Else

       Szp1 = 1 / dz

       Szm1 = 0.92 / dz

     End If

       V = 0.96 * dz

  End If

'NODE SP1

  vvv = (z > nz1 And z < nz1 + nz2 + 1)


  If vvv And xx = 0 And yy = -1 Then

    Sym1 = 0.5 * dz

      Sxp1 = 0.634 * dz

        Syp1 = 0.25 * pi * dz * Bim

          Sxm1 = 0
```

```
            Szp1 = 0.272 / dz

             Szm1 = 0.272 / dz

               V = 0.272 * dz
  End If

'NODE SP2
  xySP2 = (xx = 1 And yy = -1)

   xySP2a = (xx = l - dx And yy = -1)

   If vvv And (xySP2 Or xySP2a) Then

      Sym1 = dz

     If xySP2 Then
      Sxp1 = dz

      Sxm1 = 0.634 * dz
     End If

     If xySP2a Then
      Sxp1 = 0.634 * dz

      Sxm1 = dz
     End If
         Syp1 = 0.634 * dz

           Szp1 = 0.92 / dz

             Szm1 = 0.92 / dz

               V = 0.92 * dz
   End If

'NODE SP3
  xySP3 = (xx = 1 And yy = 0)

   xySP3a = (xx = l - dx And yy = 0)

   If vvv And (xySP3 Or xySP3a) Then

      Sym1 = 0.634 * dz
```

```
    If xySP3 Then
      Sxp1 = dz

      Sxm1 = 0.5 * pi * dz * Bim
    End If

    If xySP3a Then
      Sxp1 = 0.5 * pi * dz * Bim

      Sxm1 = dz
    End If

       Syp1 = 0.634 * dz

          Szp1 = 0.544 / dz

             Szm1 = 0.544 / dz

                V = 0.544 * dz
  End If

'NODE SP4
  xySP4 = (xx = 1 And yy = 1)

   xySP4a = (xx = 1 - dx And yy = 1)

   If vvv And (xySP4 Or xySP4a) Then

      Sym1 = 0.634 * dz

      If xySP4 Then
        Sxp1 = dz

        Sxm1 = 0.634 * dz
      End If

      If xySP4a Then
        Sxp1 = 0.634 * dz

        Sxm1 = dz
      End If

         Syp1 = dz
```

```
            Szp1 = 0.92 / dz

            Szm1 = 0.92 / dz

               V = 0.92 * dz
    End If


'NODE SP5
    If vvv And xx = 0 And yy = 1 Then

        Sym1 = 0.25 * pi * dz * Bim

        Sxp1 = 0.634 * dz

        Syp1 = 0.5 * dz

        Sxm1 = 0

        Szp1 = 0.272 / dz

        Szm1 = 0.272 / dz

           V = 0.272 * dz
    End If


'NODAL COEFFICIENTS FOR THE NODES IN SOLIDS 1, 2 & 3

    Kym1 = (Sym1 / V) * Fo

    Kxp1 = (Sxp1 / V) * Fo

    Kyp1 = (Syp1 / V) * Fo

    Kxm1 = (Sxm1 / V) * Fo

    Kzp1 = (Szp1 / V) * Fo

    Kzm1 = (Szm1 / V) * Fo
```

```
        Ki = 0
'NODAL COEFFICIENTS FOR THE NODES IN THE PIPE

If vvv And xx = 0 And yy = 0 Then
   Sxm1 = 0
    Sxp1 = B
     Kym1 = 0.5 * B
      Kxp1 = B
       Kyp1 = 0.5 * B
        Kxm1 = 0
         If z = nz1 + nz2 Then Kzp1 = (1 / dz) * B Else Kzp1 = 0
         If z = nz1 + 1 Then
            Kzm1 = (1 / dz) * B
             Ki = A
         Else
            Kzm1 = A
             Ki = 0
         End If
End If
  Sm = Ki + Kym1 + Kxp1 + Kyp1 + Kxm1 + Kzp1 + Kzm1

'TEMPERATURE ELEMENTS
    Tii = Ki * Tmi
      Tym1 = Kym1 * Tp(x, y - 1, z)
```

```
        If z > nz1 And x = nxx Then
          Txp1 = Tp(nx - x, y, nztotal + 1 - z)
        Else

  If Sxp1 = 0 Then Txp1 = 0 Else Txp1 = Tp(x + 1, y, z)

        End If

          Txp1 = Kxp1 * Txp1

If y = ny Then Typ1 = 0 Else Typ1 = Kyp1 * Tp(x, y + 1, z)

  If Sxm1 = 0 Then Txm1 = 0 Else Txm1 = Kxm1 * Tp(x - 1, y, z)

           zzp = zz + dz

       zzpmax = (nz1 + nz2 - ((nz2 + 1) / l) * xx) * dz

          If zzp > zzpmax + EOR Then

           Tzp1 = Kzp1 * Tp(nx + 1 - x, y, nztotal - z)
          Else
             Tzp1 = Kzp1 * Tp(x, y, z + 1)
          End If
               Tzm1 = Kzm1 * Tp(x, y, z - 1)

                Tn = Tin(x, y, z)

'THE GENERAL FORM OF EQUATIONS

Tp(x, y, z) = (1 / (1 + Sm)) * (Tii + Tym1 + Txp1 + Typ1 + Txm1 + Tzp1 + Tzm1 +
Tn)



End Sub


Private Sub ToutputFormatting2()

'TRANSIENT OUTPUT FORMATTING2

Dim upderv As Single
```

```
Dim downderv As Single
Dim sidederv As Single
Dim SurfArea As Single

UpHeatLoss = 0
UpHeatUsed = 0
DownHeat = 0
SideHeat = 0
LossHeat = 0
TotalHeat = 0

nxx = nx
zz = -dz
   For z = 1 To nztotal

     zz = zz + dz

      yy = ybase - dy

        For y = 1 To ny

          xx = xleft - dx

          yy = yy + dy

          For x = 1 To nx

            xx = xx + dx

     zzmax = (nz1 + nz2 - ((nz2 + 1) / l) * xx) * dz

      If z > nz1 And zz > zzmax + EOR Then

         Tp(x, y, z) = Tp(nx + 1 - x, y, nztotal + 1 - z)

      End If


           Next x
         Next y
       Next z
```

```
For z = 1 To nztotal
  zz = zz + dz
  yy = ybase - dy
    For y = 1 To ny
      xx = xleft - dx
      yy = yy + dy
      For x = 1 To nx
        xx = xx + dx

'HEAT TRANSFER TO ATMOSPHERE
If y = ny Then

upderv = (1 / (3 * dy)) * (5.5 * Tp(x, y, z) - 9 * Tp(x, y - 1, z) + 4.5 * Tp(x, y - 2, z) -
Tp(x, y - 3, z))

' upderv = (1 / (15 * dy)) * (19 * Tp(x, y, z) - 24 * Tp(x, y - 1, z) + 6 * Tp(x, y - 2, z) -
Tp(x, y - 3, z))

    If x = 1 Or x = nx Then
      If z = 1 Or z = nztotal Then
        SurfArea = 0.25 * dx * dz
      Else
        SurfArea = 0.5 * dx * dz
      End If
    Else
      If z = 1 Or z = nztotal Then
        SurfArea = 0.5 * dx * dz
      Else
        SurfArea = dx * dz
      End If
    End If

  If z < nz1 Or z > nz1 + nz2 + 1 Then
```

```
    UpHeatLoss = UpHeatLoss + (-1) * upderv * SurfArea
  Else
    UpHeatUsed = UpHeatUsed + (-1) * upderv * SurfArea
  End If
End If
'HEAT LOSS TO DOWNWARDS
If y = 1 Then
downderv = (1 / (3 * dy)) * (-5.5 * Tp(x, y, z) + 9 * Tp(x, y + 1, z) - 4.5 * Tp(x, y + 2,
z) + Tp(x, y + 3, z))
'downderv = (1 / (15 * dy)) * (-19 * Tp(x, y, z) + 24 * Tp(x, y + 1, z) - 6 * Tp(x, y +
2, z) + Tp(x, y + 3, z))
    If x = 1 Or x = nx Then
      If z = 1 Or z = nztotal Then
        SurfArea = 0.25 * dx * dz
      Else
        SurfArea = 0.5 * dx * dz
      End If
    Else
      If z = 1 Or z = nztotal Then
        SurfArea = 0.5 * dx * dz
      Else
        SurfArea = dx * dz
      End If
    End If

DownHeat = DownHeat + SurfArea * downderv
End If
'HEAT LOSS TO THE SIDES
If z = 1 Then
```

```
sidederv = (1 / (3 * dz)) * (-5.5 * Tp(x, y, z) + 9 * Tp(x, y, z + 1) - 4.5 * Tp(x, y, z +
2) + Tp(x, y, z + 3))

'sidederv = (1 / (15 * dz)) * (-19 * Tp(x, y, z) + 24 * Tp(x, y, z + 1) - 6 * Tp(x, y, z +
2) + Tp(x, y, z + 3))


    If x = 1 Or x = nx Then
      If y = 1 Or y = ny Then
        SurfArea = 0.25 * dx * dy
      Else
        SurfArea = 0.5 * dx * dy
      End If
    Else
      If y = 1 Or y = ny Then
        SurfArea = 0.5 * dx * dy
      Else
        SurfArea = dx * dy
      End If
    End If


SideHeat = SideHeat + SurfArea * sidederv

End If


          Next x
        Next y
      Next z



LossHeat = DownHeat + 2 * SideHeat + UpHeatLoss
TotalHeat = UpHeatUsed + LossHeat

If Timestep > 0 Then

Efficiency = UpHeatUsed / TotalHeat
```

```
End If

If Timestep = 0 Then

IntegralIncrement = 0
f1 = UpHeatUsed

Else
f0 = f1
f1 = UpHeatUsed
   IntegralIncrement = (Fo / 2) * (f0 + f1)
End If


 UpHeatCum = UpHeatCum + IntegralIncrement


'HEATING LOAD

HeatLoad = (snowden / solidden) * l * lz2 * LatentHeat _
* RefSnowThickness

Melted = (UpHeatCum > HeatLoad)

'MELTED SNOW THICKNESS

SnowThickness = UpHeatCum / ((snowden / solidden) _
* l * lz2 * LatentHeat)



UpHeatUsed = Format$(UpHeatUsed, " ####.######")

UpHeatLoss = Format$(UpHeatLoss, " ####.000000")

LossHeat = Format$(LossHeat, " ####.######")

TotalHeat = Format$(TotalHeat, " ####.000000")

Csurftemp = Format$(Tp(nxm, ny, nz1 + 1), " ##.000000")

Efficiency = Format$(Efficiency, "##.000000")

UpHeatCum = Format$(UpHeatCum, " #######.0000")
```

```
IntegralIncrement = Format$(IntegralIncrement, " ####.00000")

SnowThickness = Format$(SnowThickness, " ####.00000")

HeatLoad = Format$(HeatLoad, " #####.00000")

'SideHeat = Format$(2 * SideHeat, "####.000000")


grdTmp.Row = 0

Newrow = Str$(ElapsedTime) & vbTab & UpHeatUsed & vbTab & _
TotalHeat & vbTab & Efficiency & vbTab & UpHeatCum _
& vbTab & HeatLoad & vbTab & SnowThickness

grdTmp.AddItem Newrow



OutputFileCreator1



'Print #1, ElapsedTime; Efficiency
'Close #1


End Sub
```

REFERENCES

1. Adlam, Napier T , *Snow Melting* , 1950, The Industrial Press , New York

2. Holman, J. P, 1983 *Heat Transfer* , 1983, Mc Graw- Hill Book, New York

3. Kiev Institute of Civil Aviation, 1989, *Classification & General Characteristics of Aerodrome Pavement*

4. ICAO, Doc. 9137 - AN / 898, 1984, *Airport Services Manual Part-9 Airport Maintenance Practices*

5. R. Mataracı, *An Investigation Of Floor Panel Heating By Conductive Sheet Anology,* Ms. Thesis In Mechanical Engineering Department Of METU 1988

6. Kakaç, Sadık & Yener, Yaman *Heat Conduction, 1979,* Kelaynak Publication & Print Co.

7. Chapra, Steven, *Numerical Methods For Engineers*, 1988, Mc. Graw – Hill Publishing Company

8. M. Chung, R. Hangel *Semi-Analytical Solution For Heat Transfer From A Buried Pipe With Convection On The Exposed Surface,* International Journal Of Heat And Mass Transfer 1999, Vol. 42, pp 3771 - 3786

9. G.P. Zhang, S. Weinbaum, *An Approximae Three Dimensional Solution For Melting Or Freezing Around A Buried Pipe Beneath A Free Surface,* Transactions of ASME 1986, Vol. 108, pp 900-906

10. G.P. Zhang, S. Weinbaum, *An Approximae Three Dimensional Solution For Melting Or Freezing Around A Buried Pipe In A Semi-Infinite Medium,* Journal of Heat Tranfer 1985, Vol. 107, pp 245-247

11.A. Negiz, A. Hastaoglu, A. Heidemann. *Three-Dimensional Transient Heat Transfer From A Buried Pipe: Solidification Of A Stationary Fluid,* Numerical Heat Transfer, Part-A 1995, Vol. 28 pp 175-193

12.Facas. N, *Natural Convection From A Buried Pipe With External Baffles*, Numerical Heat Transfer, Part-A 1995, Vol. 28 pp 595-609

13.Ali M, Latif M, S. Weinbaum, *Boundary Integral Equation Technique With Application To Freezing Around A Buried Pipe*, International Journal Of Heat And Mass Transfer 1987, Vol. 30, pp 223 - 232

14.Dayan A, H. Herbaum, *Temperature Distributions Around A Buried Pipe Networks In Soil With A Temperature Dependent Thermal Cunductivity,* International Journal Of Heat And Mass Transfer 1984, Vol. 27, pp 409 - 417

15.Haim H. Bau, *Heat Losses From A Fluid Flowing In A Buried Pipe,* International Journal Of Heat And Mass Transfer 1982, Vol. 25, No. 11, pp 1621 – 1629

16.Haim H. Bau, *Convective Heat Losses From A Buried Pipe In A Semi-infinite Porous Medium,* International Journal Of Heat And Mass Transfer 1984, Vol. 27, No. 11, pp 2047 – 2056

17.R.E.S. Moya, A.T. Prata, J.A.B. Neto, *Experimentel Analysis Of Unsteady Heat And Moisture Transfer Around A Heated Cylinder Buried Into A Porous Medium*

18.C. Gauthier, M. Lacroix, *Numerical Solution Of Soil Heat Exchanger-Storage Systems For Greenhouses,* Solar Energy 1997, Vol. 60. No. 6, pp 333-346

19.V.C. Mei, *Heat Trasnsfer Of Buried Pipe For Heat Pump Application*, Journal Of Solar Energy engineering 1991, Vol. 113, pp 51 – 55

20.A. Negiz, M.A. Hastaoglu, *Three-Dimensional Transient Heat Transfer From A Buried Pipe*, Chemical Engineering Science 1993, Vol. 48, No.20, pp 3507 – 3517

21.W. Yoshikoshi, *Vertical Earth Pressure On A Pipe In Ground,* Soils And Foundations 1976, Vol. 16, No.2, pp 31 – 38

22.D. V. Ramsamooj, G. S. Lin, *Stresses At Joints And Cracks In Highway And Airport Pavements,* Engineering Fracture Mechanics 1998, Vol. 60 No. 5-6, pp 507-518

23.O.O.R. Famiyesin, T. G. Davies, A.H.C. Chan, *Numerical Modeling Of Cyclic Loading On Reinforced Unbound Pavements,* Computers And Structures 1998, Vol. 68